

Elevated gastrin secretion by *in vivo* gene electroporation in skeletal muscle

AKIHIRO YASUI¹, KOJI ODA², HIROTOSHI USUNOMIYA³, KENICHI KAKUDO³, TAKAYUKI SUZUKI⁴, TOYONOBU YOSHIDA⁴, HYI-MAN PARK⁴, KAZUTERU FUKAZAWA⁴ and TATSUO MURAMATSU⁴

¹Department of Surgery, Chubu National Hospital, Ohbu 474-8511; ²Department of Surgery, Nagoya University Graduate School of Medicine, Nagoya 466-8550; ³Second Department of Pathology, Wakayama Medical College, Wakayama 640-8155; ⁴Department of Applied Molecular Biosciences, Graduate School of Bioagricultural Sciences, Nagoya University, Nagoya 464-8601, Japan

Received June 26, 2001; Accepted July 25, 2001

Abstract. Whether or not *in vivo* gene transfer of gastrin gene into skeletal muscle by electroporation could modify gastrin secretion was examined. The expression plasmid vector, either pMEPrGaspA encoding the rat gastrin gene or pEGFP-N1 encoding the GFP reporter gene was injected into *M. rectus abdominis* of rats or *M. biceps formis* of mice. Subsequently, square electric pulses of direct current were applied six times at 25 V with a loading period of 100 msec per pulse. Clear foreign gene expression in the skeletal muscle was demonstrated by both GFP fluorescence and immunostaining of rat gastrin. Time course changes in plasma gastrin levels after transfection revealed that in rats, gastrin gene transfer significantly increased the plasma gastrin level for 4 weeks post-transfection ($P < 0.05$), but the difference diminished at the end of the 10-week period. In mice, plasma gastrin level elevated similarly for 3 weeks, and pH of gastric contents decreased in the gastrin gene transfected group compared with the control counterpart ($P < 0.05$). These findings suggest that localized *in vivo* gene transfer by electroporation allows skeletal muscle to become an artificial endocrine tissue for hormonal manipulation of animals.

Introduction

Tissues in which foreign genes are transferred *in vivo* could be used as a production site for physiologically active proteins such as hormones, cytokines, and antibodies. The concept of such genetically engineered organs designated as an artificial

endocrine tissue has progressed rapidly in the last decade. In principle, any organ within the body can be the target of the genetically engineered artificial endocrine tissue. However, skeletal muscle may be the most preferable and promising tissue with which a number of *in vivo* gene transfer studies have been conducted, starting from the expression of reporter genes (1), to the production of hormones (2,3), and neurotrophic factors (4). The reasons for using skeletal muscle may lie in its characteristics that: a) it makes up about 40% of adult body mass; b) it is easily accessible to most of the gene delivery methods; c) there is no significant cell replacement (5), and; d) the introduced genes are not constantly lost following mitosis. Particularly the last factor is of considerable importance because it may result in durable foreign gene expression in this tissue (6). Indeed, in the mouse skeletal muscle the *in vivo* transferred gene was expressed as long as 15 months (3). In contrast to skeletal muscle, foreign gene expression lasted from only several days to 4 weeks in other tissues including testis, liver, and oviduct (7,8).

The use of skeletal muscle as an artificial endocrine tissue (9) may have considerable impact on gene therapy of disorders associated with hyposecretion of digestive hormones. As a representative of digestive hormones to be manipulated, we have chosen gastrin, a physiological regulator of gastric acid secretion and at the same time an important promoter of gastric mucosal cell proliferation. The reduction in gastrin production and secretion from antral G cells may result in reduced gastric acid secretion.

Since there are a number of clinical observations related to hypo- or hyper-secretory disorders of gastrin and gastric acids, manipulations of this hormone in the blood circulation by using genetically engineered skeletal muscle as an artificial endocrine tissue may be of crucial importance from a clinical point of view.

The present study was conducted to examine whether *in vivo* transfer of gastrin gene into skeletal muscle could modify gastrin secretion. For this purpose, *in vivo* gene electroporation (EP) was employed, because it was more powerful and convenient than any other nonviral method (7). Indeed, in terms of the intensity of transgene expression, our findings

Correspondence to: Dr Tatsuo Muramatsu, Department of Applied Molecular Biosciences, Graduate School of Bioagricultural Sciences, Nagoya University, Nagoya 464-8601, Japan
E-mail: tatsumu@agr.nagoya-u.ac.jp

Key words: skeletal muscle, *in vivo* electroporation, gastrin secretion, GFP expression

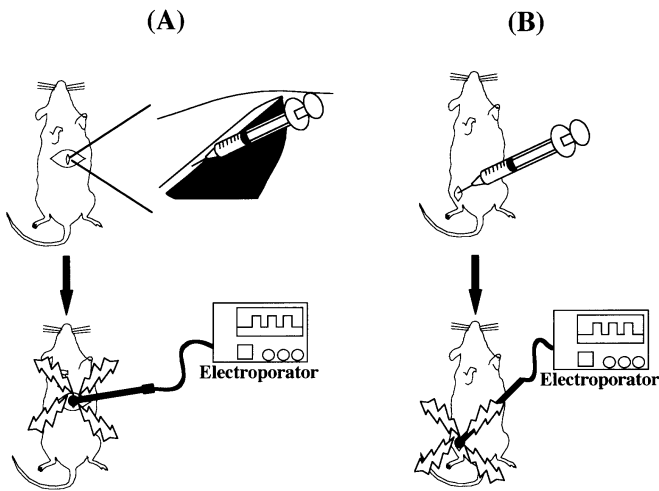


Figure 1. Outline of *in vivo* gene electroporation in skeletal muscle of rats (A) and mice (B). DNA solution was injected into *M. rectus abdominis* of rats or *M. biceps formis* of mice. *In vivo* electroporation was done by applying six square pulses of direct current at 25 V with a loading period of 100 msec per pulse. The entire operation procedures were done under anesthesia.

and those of others demonstrated the superiority of *in vivo* gene EP to any other nonviral *in vivo* method in the chicken embryo (10), the mouse testis (11-13), the mouse skeletal muscle (14), and the oviduct of laying hens (15).

Materials and methods

Animals. Male Wistar strain rats at 12 weeks of age or ICR strain mice at 9 weeks of age were used. At first, rats were used as an experimental animal to manipulate plasma gastrin levels. However, to elucidate the acid-secretory function of genetically produced rat gastrin, mice were used instead to save the amount of DNA to be transfected per animal. The rats and mice were cared for under the Guideline of Animal Experimentation, laid down by the Committee of Experimental Animal Care, Nagoya University, Nagoya, Japan. Throughout the experimental period of 10 weeks for rats and 3 weeks for mice, the animals were allowed free access to a commercial diet (MR Stock, Nihon Nosan Kogyo Co. Ltd., Tokyo, Japan) and water except for overnight fasting prior to the blood sampling day.

DNA constructs. The plasmid DNAs transfected were pMEPrGas9pA, pMEPpA, pEGFP-N1 and pAdVantage. The plasmid vector, pMEPrGas9pA was made by inserting the rat gastrin gene excised from pGas9-pCDNA3, which was generously gifted from Dr R. Dimaline, Physiological Laboratory, University of Liverpool, Liverpool, UK, into the *Bam*HI and *Sal*I sites of pMEP9pA, an empty vector that was served as a negative control. The MEP9pA was constructed with the miw promoter excised from pmiwZ (16), and substituted for the RSV promoter of a commercially available plasmid, pREP9 (Invitrogen, CA, USA). The pEGFP-N1 and pAdVantage were obtained commercially from Clontech (Palo Alto, CA, USA) and Promega (Madison, WI, USA), respectively.

***In vivo* gene EP.** *In vivo* gene transfer was performed by EP as described previously (11,12), and the outline of procedures is shown in Fig. 1 (A, for rats, and B, for mice). Rats and mice were operated under deep anesthesia attained by intraperitoneal injection of pentobarbital at 25 mg/kg body weight. In rats, the skin was cut approximately 2 cm, and an incision was made along the median plane in *M. rectus abdominis* located beneath, while in mice, the skin around *M. biceps formis* was cut approximately 1 cm, and no incision was made in the muscle. Into the incision of the abdominal muscle of rats or the biceps muscle of mice, designated doses of plasmids were injected with a 1 ml syringe fitted with a 29 gauge needle. DNA amounts given per injection site were: for the rat experiment, pMEPrGas9pA at 50 μ g, pMEPpA at 50 μ g, pEGFP-N1 at 50 μ g, pAdVantage at 10 μ g, and; for the mouse experiment, pMEPrGas9pA at 200 μ g, pMEPpA at 200 μ g, pEGFP-N1 at 20 μ g, and pAdVantage at 20 μ g. For the immuno-staining experiment, pMEPrGas9pA, and for the plasma gastrin manipulation experiment either pMEPrGas9pA or pMEPpA was dissolved together with pAdVantage in 100 μ l of TE buffer (10 mM Tris, and 1 mM EDTA, pH adjusted to 7.5). The co-transfection with pAdVantage vector was done to enhance gene expression according to the manufacturer of this plasmid (Promega, Madison, WI, USA). For GFP imaging experiment, the GFP reporter plasmid, pEGFP-N1 was similarly dissolved in 100 μ l of the TE buffer. Immediately after the injection, six square electric pulses of direct current were applied at 25 V with a pulse length of 100 msec per pulse with an Electro-Square Porator (CUY21, NEPA Gene, Ichikawa, Japan) in combination with pincette-type electrodes (CUY641, Tokiwa Science, Tsukushino, Japan) as described previously (3). The electrodes had one circular gold-plated steel of 10 mm in diameter on each end of forceps with separate electrical connection to the above electro-square porator. The mean resistance value with SEM for the rat abdominal muscle was 0.46 ± 0.03 k Ω /cm, and mouse biceps muscle, 0.50 ± 0.15 k Ω /cm. After *in vivo* EP, the skin was stitched immediately with No. 3 silk suture.

At the designated period of time, the skin around the injection site was cut under deep anesthesia attained by intraperitoneal injection of pentobarbital at an excessive dose of 100 mg/kg body weight. For GFP detection, specific green fluorescence was observed *in vivo* with a fluorescence microscope. Subsequently, the GFP positive sample blocks were removed quickly for preparing cross sections for detailed microscopic observation. For immuno-staining, the muscle sample block was immediately removed for preparing cross sections. For measuring plasma gastrin levels, the animals were fasted overnight, and in the following morning, blood was collected from tail vein at 1, 4 and 10 weeks post-transfection. For gastric pH determination, stomach was excised from the euthanized mice, and then flashed with 2 ml of physiological saline. The solution containing gastric contents was centrifuged at 1000 g x 10 min, and supernatant was used for pH determination.

Chemical analysis. For GFP imaging of muscle samples, green fluorescence was detected with a reflected light fluorescence microscope (SZX-RFL2 for *in vivo* observations, Olympus, Tokyo, Japan, and MRC-1024 confocal imaging system for

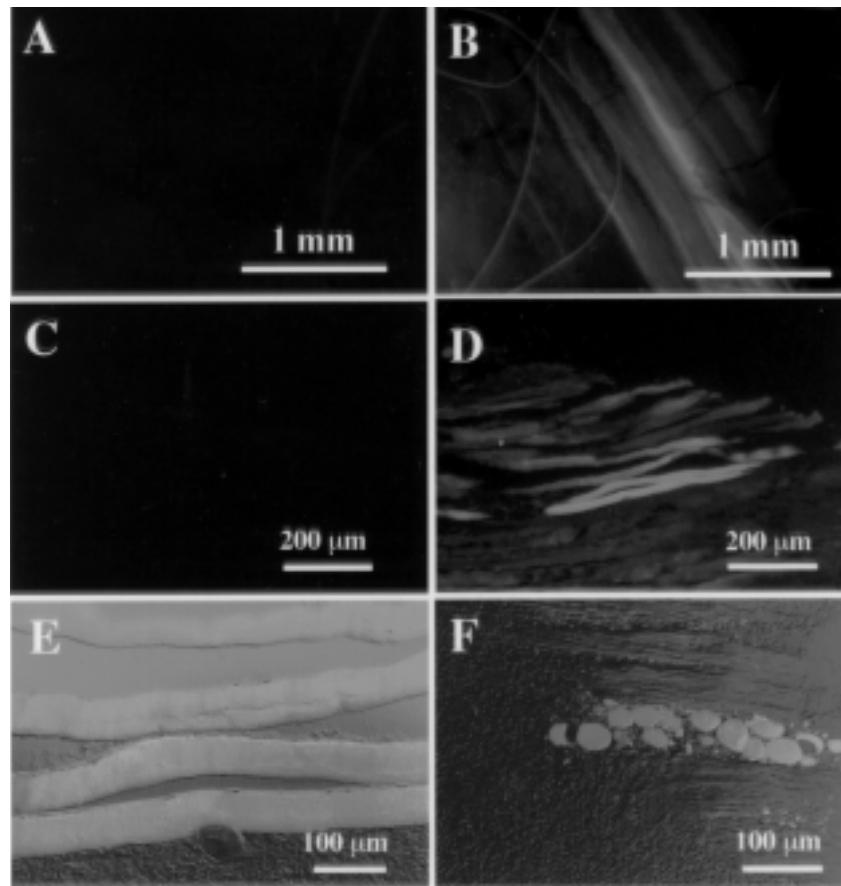


Figure 2. Green fluorescent protein (GFP) expression in the rat abdominal muscle, *M. rectus abdominis*, following *in vivo* gene electroporation. A GFP gene encoding plasmid, pEGFP-N1, was injected at a dose of 50 μ g per site, and six square pulses of direct current were applied at 25 V with a loading period of 100 msec per pulse. The GFP expression was detected at 24 h post-transfection with a reflected light fluorescence microscope: A and B (*in vivo*); C, D, and E, sections along the muscle fiber, and; F, section across the muscle fiber. A and C, control muscle; B, D, E and F, GFP gene transferred muscle. The scale bar is shown at the lower right corner of each photo.

section observations, Nippon Bio-Rad Laboratories, Japan) at excitation and emission wave lengths of 460 and 490 nm, respectively. Immuno-staining of the muscle samples was done with rabbit antiserum raised against the C-terminus of amidated rat gastrin, L425, which was a generous gift from Dr R. Dimaline, Physiological Laboratory, University of Liverpool, Liverpool, UK. The antiserum was specific for the C-terminus of amidated gastrin (Dimaline, personal communication). Plasma samples separated from the collected blood by centrifuging blood at 8000 \times g for 10 min, and circulating gastrin levels were determined by using a radio-immuno assay kit (RIA2 kit, Dainabot, Tokyo, Japan). The pH of the gastric solution was determined with a pH meter (type F-8, Horiba Ltd., Kyoto, Japan).

Statistical analysis. Analysis of variance was done on the data, and significance of differences between means was inspected by a protected least significant difference test by using a commercially available statistical package (SAS ver. 5, SAS Institute Inc, Cary, NC, USA).

Results

GFP reporter expression. GFP expression at 24 h post-transfection in rats is shown in Fig. 2. The expression was

detected either *in vivo* in muscle of living animals (Fig. 2A and B) or in the muscle sections (Fig. 2C-F). In comparison with the negative control (Fig. 2A and C) in which only phosphate buffered saline was injected followed by electroporation, clear GFP signals were observed in the pEGFP-N1 transferred muscle (Fig. 2B and D). This was further confirmed by detailed examination of sections along the muscle fibers (Fig. 2E) and across the fiber (Fig. 2F) of the transfected area. Signals of GFP expression were mostly confined to muscle fibers, and little expression was detected in the extracellular spaces.

Immuno-staining of gastrin positive skeletal muscle cells.

Fig. 3 represents the results of immuno-staining of the muscle sections from the rat abdominal muscle with the specific antiserum against the C-terminus of amidated rat gastrin. No clear signals were found in negative control sections (Fig. 3A), while positively stained, scattered dark spots were observed primarily in the fibers of the pMEPrGaspA-transferred muscle with some scattered spots in the extracellular space (Fig. 3B). This pattern of expression signals was a mirror image of GFP expression, and therefore was in good agreement with the reporter gene expression in the abdominal muscle. As a positive control, antral mucosal sections were also stained. Among the cells lined to form mucosal gland, dark brown spots were

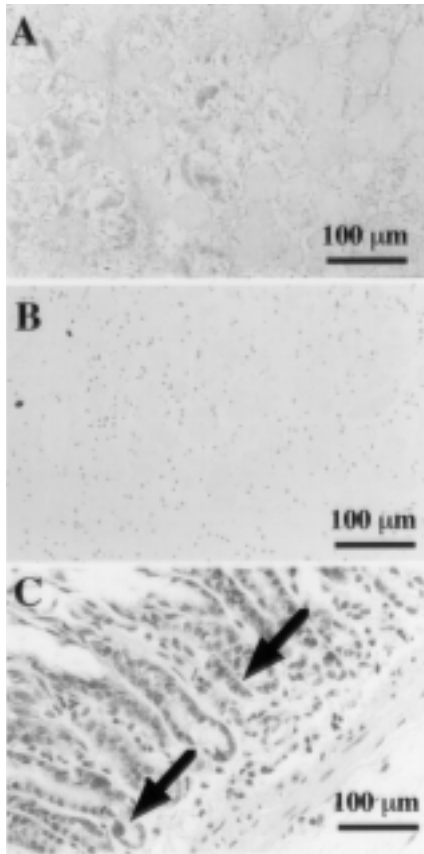


Figure 3. Immuno-staining of rat skeletal muscle to which an expression plasmid encoding the rat gastrin gene was transferred by *in vivo* gene electroporation. The plasmid, pMEPrGaspA, was injected at a dose of 50 µg per site, and six square pulses of direct current were applied at 25 V with a loading period of 100 msec per pulse. The amidated rat gastrin expression was detected at 24 h later. The scale bar is shown at the lower right corner of each photo. A, control muscle; B, the rat gastrin gene transferred muscle, and; C, rat antral mucosa served as a positive control. Arrows indicate the immunoreactive, putative antral G cells.

found only in some cells that were assumed to be antral G cells (Fig. 3C), suggesting that the specific antiserum against physiologically active gastrin functioned well.

Time course of plasma gastrin levels. Plasma gastrin levels of rats over 10 weeks post-transfection are shown in Fig. 4. The overall means of the gastrin level was significantly increased by the gastrin gene transfer compared with the empty vector transfer ($P < 0.05$). Time course changes in the plasma gastrin levels indicated that for the first 4 weeks post-transfection, plasma gastrin levels tended to be higher in the gastrin gene transfected than in the empty vector transfected groups, and significant difference was found at 4 weeks post-transfection ($P < 0.05$). However, the difference diminished, and no significant difference was found at the end of the 10-week experimental period.

Whether or not the same expression plasmid encoding the rat gastrin gene could function in mice was tested. As shown in Fig. 5A, gastrin gene transfer also resulted in essentially similar increases in plasma gastrin levels over the 3-week period in mice when compared with the empty vector transfer ($P < 0.05$).

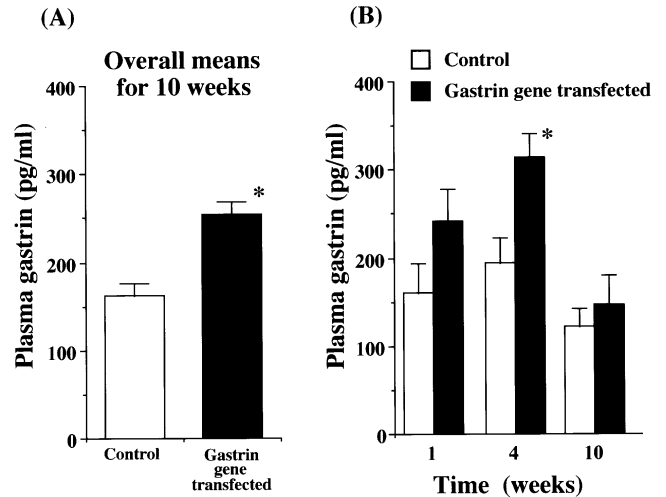


Figure 4. Changes in plasma gastrin levels of rats following *in vivo* electroporation of the rat gastrin gene into skeletal muscle during the 10-week experimental period (A, overall means; B, time course). The plasmid, pMEPrGaspA, was injected at a dose of 50 µg per site together with 10 µg of pAdVantage per site, and six square pulses of direct current were applied at 25 V with a loading period of 100 msec per pulse. Plasma rat gastrin concentration was determined at designated time period over the 10-week experimental period. Vertical bars represent mean \pm SEM. *Significantly different from the corresponding control value at $P < 0.05$.

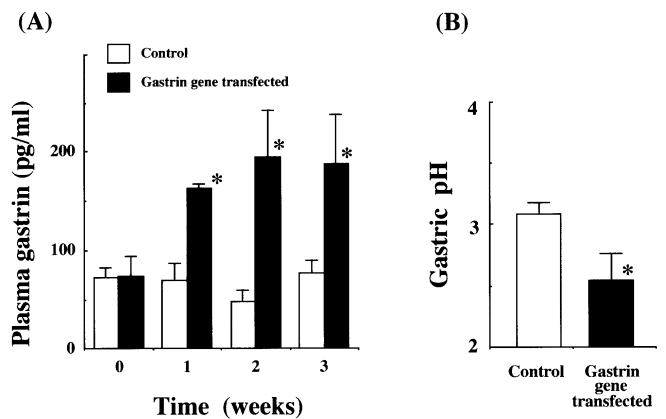


Figure 5. Changes in plasma gastrin levels of mice following *in vivo* electroporation of the rat gastrin gene into skeletal muscle during the 3-week experimental period (A) and in pH of gastric solution at 3 weeks post-transfection (B). The plasmid, pMEPrGaspA, was injected at a dose of 200 µg per site together with 20 µg of pAdVantage per site, and six square pulses of direct current were applied at 25 V with a loading period of 100 msec per pulse. Vertical bars represent mean \pm SEM. *Significantly different from the corresponding control value at $P < 0.05$.

Changes in gastric content pH. Fig. 5B represents pH of mouse gastric content at 3 weeks after *in vivo* gene electroporation with the rat gastrin gene. A significantly lower value for the pH was detected in the gastrin gene transferred mice than in the control counterparts, implicating that even in mice, the rat gene expression product may not only elevate plasma gastrin level but also appear to function normally.

Discussion

In the present study, we have demonstrated successful manipulation of gastrin homeostasis, not depending upon food, and its component such as certain amino acids, ingestion, but solely upon the expression of exogenous gastrin gene transferred *in vivo* into skeletal muscle. At the same time, the rat gastrin gene transcript not only increased plasma gastrin levels but also appeared to function normally for enhancing gastric acid secretion, leading to lowered gastric pH. This finding may provide a basis of gene therapy for innate or acquired gastrin deficiency through genetically engineered skeletal muscle as an artificial endocrine tissue. The perspectives and general aspects of the artificial endocrine tissue have been reviewed elsewhere (9).

Before the concept of artificial endocrine tissues is brought into practice, a number of questions should be addressed. First of all, the limit of foreign gene expression would have to be clarified. Admittedly, skeletal muscle is one of the most appropriate tissues that allow durable foreign gene expression (7). However, the duration appears to depend, at least partly if not entirely, on the type of recombinant proteins expressed. Previously, we found that in mouse skeletal muscle, GFP expression lasted only several months whereas mouse EPO protein was expressed as long as 15 months (3). This may suggest that if the expressed recombinant product were a non-natural protein to animals and humans, the removal of such proteins from the body in general would be accelerated by activated host immune system. When the rat gastrin gene was transferred *in vivo* into mice, plasma gastrin levels increased for at least 3 weeks so that the rejection of the non-natural protein by the host immune system should take longer time period than 3 weeks under the present experimental conditions. Homology of the non-natural protein to the inherent one might be one of the determinant of expected duration of recombinant protein expression in different animal species. Whether or not the above hypothesis is true remains to be investigated.

The second question concerns with post-translational modifications that are frequently of critical importance *in vivo*. As reviewed in detail (17), post-translational processing of gastrin involves several cleavage steps and C-terminal amidation of phenylalanine, the latter of which is essential for the production of biologically active gastrin. An enzyme, peptidyl-glycine- α -amidating enzyme, catalyzes this amidation step. Two forms of gastrin-amidating enzyme have been identified in antral mucosa and pituitary extracts (18). The question is then whether or not skeletal muscle has such enzymatic activities to complete the C-terminal amidation reaction. The antiserum used for the immuno-histochemistry in the present study specifically recognizes the C-terminus of amidated gastrin (Dimaline, personal communication). Therefore, at least, gastrin positive muscle cells processed recombinant progastrin to form and secrete amidated, physiologically active gastrin. This was further supported by the observation that the *in vivo* transferred and expressed gastrin gene in skeletal muscle appeared to promote mouse gastric acid secretion, a most important index of gastrin function (Fig. 5B).

The third question relates to the regulation of foreign gene expression. For the correction of disturbed hormonal homeostasis through artificial endocrine system, hormones

must be synthesized and secreted into blood circulation at the right amount and right time. Such strictly controlled gene expression is obviously insufficient at present, although some regulated expression of *in vivo* transferred genes have been reported (19-22). In this sense, the use of daily nutrient supply as physiological stimuli is an attractive approach as demonstrated by the regulation of foreign gene expression driven by the phosphoenolpyruvate carboxykinase promoter (8) and the pyruvate kinase promoter (23). Further refinement of DNA constructs including promoters may bring about promising applications of controllable foreign gene expression to clinical studies.

Finally, more improvements should be made on the *in vivo* EP procedures per se. At present, the state of the art of *in vivo* gene EP is far from satisfactory for clinical trials. Even if only one parameter of EP conditions such as voltage is considered, the reported results in the literature are not consistent. We have been routinely using the voltage at 25 V or lower for skeletal muscle, whereas another group found that 100 V was the most efficient (14). Moreover, it has recently been claimed that 900 V would be more suitable when a longer gene expression was desired (24). The disagreement may lie in the effective area of electrodes used. Depending upon the shape of electrodes, the area hence the resistance differs substantially, and thereby leading to wide range of heat generated in the target site. Within a certain range, this heat generation may parallel to the intensity of foreign gene expression at a fixed time point after *in vivo* gene transfer (7). Thus, with almost infinite number of electrode shapes, the only and the most comprehensive term to describe the efficacy of *in vivo* gene EP would be the applied energy which can be simply calculated by the product of squares of voltage and sum of loading period divided by the resistance (25). By assuming that the average resistance is 0.45 k Ω /cm (26), and the gap between electrodes is 5 mm, the recalculation of the published results indicates that the recent work using 900 V (24) would have generated the energy at 1.4 J, whereas the EP condition employed by others using 100 V (14) at 21 J, and that of the present study at 1.3 J for the target site. This suggests that electric energy in any target site of skeletal muscle having an electrode distance of 5 mm or so should be limited to less than 2 J, and that hyper-generation of electricity would cause irreversible heat damage to the muscle tissue. No doubt that there is plenty of room for EP condition optimization in other parameters such as amperage, loading period, the ratio of loading to unloading period, number of pulses, temperature of target site, and ionic strength of DNA solution.

Acknowledgements

The authors are grateful to Dr R. Dimaline, Physiological Laboratory, University of Liverpool, Liverpool, UK for generously providing us with the pGas9-pCDNA3 plasmid and rabbit antiserum raised against the C-terminus of amidated rat gastrin, L425.

References

1. Wolff JA, Malon RW, Williams P, Chong W, Acsadi G, Jani A and Felgner PL: Direct-gene transfer into mouse muscle *in vivo*. *Science* 247: 1465-1468, 1990.

2. Tripathy SK, Svensson EC, Black HB, Goldwasser E, Margalith M, Hobart PM and Leiden JM: Long-term expression of erythropoietin in the systemic circulation of mice after intramuscular injection of a plasmid DNA vector. *Proc Natl Acad Sci USA* 93: 10876-10880, 1996.
3. Muramatsu T, Arakawa S, Fukazawa K, Fujiwara Y, Yoshida T, Sasaki R, Masuda S and Park H-M: *In vivo* gene electroporation in skeletal muscle with special reference to the duration of gene expression. *Int J Mol Med* 7: 37-41, 2001.
4. Haase G, Kennel P, Vigne E, Akli S, Revah F, Schmalbruch H and Kahn A: Gene therapy of murine motor neuron disease using adenoviral vectors for neurotrophic factors. *Nat Med* 3: 429-436, 1996.
5. Fischman D: Development of striated muscle. In: *The Structure and Function of Muscle*. Boume GH (ed). 2nd edition. Academic Press, New York, NY, pp75-142, 1972.
6. Bohl D, Naffakh N and Heard JM: Long-term control of erythropoietin secretion by doxycycline in mice transplanted with engineered primary myoblasts. *Nat Med* 3: 299-305, 1997.
7. Muramatsu T, Nakamura A and Park H-M: *In vivo* electroporation: a powerful and convenient means of nonviral gene transfer to tissues of living animals. *Int J Mol Med* 1: 55-62, 1998.
8. Muramatsu T, Ito N, Tamaoki N, Oda H and Park H-M: *In vivo* gene electroporation confers nutritionally-regulated foreign gene expression in the liver. *Int J Mol Med* 7: 61-66, 2001.
9. MacColl GS, Goldspink G and Bouloux PMG: Using skeletal muscle as an artificial endocrine tissue. *J Endocrinol* 162: 1-9, 1999.
10. Muramatsu T, Mizutani Y, Ohmori Y and Okumura J: Comparison of three nonviral transfection methods for foreign gene expression in early chicken embryos *in ovo*. *Biochem Biophys Res Commun* 230: 376-380, 1997.
11. Muramatsu T, Shibata O, Ohmori Y and Okumura J: *In vivo* electroporation: a convenient method for gene transfer to testicular cells in mice. *Anim Sci Technol (Jpn)* 67: 975-982, 1996.
12. Muramatsu T, Shibata O, Ryoki S, Ohmori Y and Okumura J: Foreign gene expression in the mouse testis by localized *in vivo* gene transfer. *Biochem Biophys Res Commun* 233: 45-49, 1997.
13. Yamazaki Y, Fujimoto H, Ando H, Ohyama T, Hirota Y and Noce T: *In vivo* gene transfer to mouse spermatogenic cells by deoxyribonucleic acid injection into seminiferous tubules and subsequent electroporation. *Biol Reprod* 59: 1439-1444, 1998.
14. Aihara H and Miyazaki J: Gene transfer into muscle by electroporation *in vivo*. *Nat Biotechnol* 16: 867-870, 1998.
15. Ochiai H, Park H-M, Nakamura A, Sasaki R, Okumura J and Muramatsu T: Synthesis of human erythropoietin *in vivo* in the oviduct of laying hens by localized *in vivo* gene transfer using electroporation. *Poult Sci* 77: 299-302, 1998.
16. Suemori H, Kadokawa Y, Goto K, Araki I, Kondoh H and Nakatsuji N: A mouse embryonic stem cell line showing pluripotency of differentiation in early embryos and ubiquitous β -galactosidase expression. *Cell Differ Dev* 29: 181-186, 1990.
17. Walsh JH: Chapter 1. Gastrointestinal hormones. In: *Physiology of the Gastrointestinal Tract*. Johnson LR, Alpers DH, Christensen J, Jacobson ED and Walsh JH (eds). 3rd edition. Raven Press, New York, NY, pp1-128, 1994.
18. Dickinson CJ and Yamada T: Gastrin-amidating enzyme in the porcine pituitary and antrum. Characterization of molecular forms and substrate specificity. *J Biol Chem* 266: 334-338, 1991.
19. Mayo KE, Warren R and Palmiter RD: The mouse metallothionein-I gene is transcriptionally regulated by cadmium following transfection into human or mouse cells. *Cell* 29: 99-108, 1982.
20. Staeheli P, Danielson P, Haller O and Sutcliffe JG: Transcriptional activation of the mouse Mx gene by type I interferon. *Mol Cell Biol* 6: 4770-4774, 1986.
21. Mader S and White JS: A steroid-inducible promoter for the controlled overexpression of cloned genes in eukaryotic cells. *Proc Natl Acad Sci USA* 90: 5603-5607, 1993.
22. Park H-M and Muramatsu T: *In vivo* manipulation of foreign gene expression by steroid administration in the oviduct of laying hens. *J Reprod* 163: 173-179, 1999.
23. Lee HC, Kim S-J, Kim K-S, Shin H-C and Yoon J-W: Remission in models of type 1 diabetes by gene therapy using a single-chain insulin analogue. *Nature* 408: 483-488, 2000.
24. Vicat JM, Boisseau S, Jourdes P, Laine M, Wion D, Bouali-Benazzouz R, Benabid AL and Berger F: Muscle transfection by electroporation with high-voltage and short-pulse currents provides high-level and long-lasting gene expression. *Hum Gene Ther* 11: 909-916, 2000.
25. Hofmann GA: Instrumentation. In: *Methods in Molecular Biology. Electroporation Protocols for Microorganisms*. Vol. 47. Nickoloff JA (ed). Humana Press Inc., Totowa, NJ, pp27-45, 1995.
26. Semrov D and Miklavcic D: Numerical modeling for *in vivo* electroporation. In: *Electrochemotherapy, Electrotherapy, and Transdermal Drug Delivery: Electrically Mediated Delivery of Molecules to Cells*. Jaroszeski M, Heller R and Gilbert R (eds). Humana Press Inc., Totowa, NJ, pp63-81, 2000.



Anti-monocyte chemoattractant protein-1 gene therapy attenuates pulmonary hypertension in rats

Yasuhiro Ikeda, Yoshikazu Yonemitsu, Chu Kataoka, Shiro Kitamoto, Terutoshi Yamaoka, Ken-Ichi Nishida, Akira Takeshita, Kensuke Egashira and Katsuo Sueishi

AJP - Heart 283:2021-2028, 2002. First published Jun 20, 2002; doi:10.1152/ajpheart.00919.2001

You might find this additional information useful...

This article cites 27 articles, 12 of which you can access free at:

<http://ajpheart.physiology.org/cgi/content/full/283/5/H2021#BIBL>

This article has been cited by 3 other HighWire hosted articles:

Hypoxia, leukocytes, and the pulmonary circulation

K. R. Stenmark, N. J. Davie, J. T. Reeves and M. G. Frid

J Appl Physiol, February 1, 2005; 98 (2): 715-721.

[Abstract] [Full Text] [PDF]

Specific inhibition of p38 mitogen-activated protein kinase with FR167653 attenuates vascular proliferation in monocrotaline-induced pulmonary hypertension in rats

J. Lu, H. Shimpō, A. Shimamoto, A. J. Chong, C. R. Hampton, D. J. Spring, M. Yada, M.

Takao, K. Onoda, I. Yada, T. H. Pohlman and E. D. Verrier

J. Thorac. Cardiovasc. Surg., December 1, 2004; 128 (6): 850-859.

[Abstract] [Full Text] [PDF]

Anti-Monocyte Chemoattractant Protein-1 Gene Therapy Attenuates Renal Injury Induced by Protein-Overload Proteinuria

H. Shimizu, S. Maruyama, Y. Yuzawa, T. Kato, Y. Miki, S. Suzuki, W. Sato, Y. Morita, H.

Maruyama, K. Egashira and S. Matsuo

J. Am. Soc. Nephrol., June 1, 2003; 14 (6): 1496-1505.

[Abstract] [Full Text] [PDF]

Updated information and services including high-resolution figures, can be found at:

<http://ajpheart.physiology.org/cgi/content/full/283/5/H2021>

Additional material and information about *AJP - Heart and Circulatory Physiology* can be found at:

<http://www.the-aps.org/publications/ajpheart>

This information is current as of March 17, 2005 .



Anti-monocyte chemoattractant protein-1 gene therapy attenuates pulmonary hypertension in rats

YASUHIRO IKEDA,¹ YOSHIKAZU YONEMITSU,^{1,2} CHU KATAOKA,² SHIRO KITAMOTO,² TERUTOSHI YAMAOKA,³ KEN-ICHI NISHIDA,⁴ AKIRA TAKESHITA,² KENSUKE EGASHIRA,² AND KATSUO SUEISHI¹

¹*Division of Pathophysiological and Experimental Pathology, Department of Pathology,*

²*Department of Cardiovascular Medicine, and* ³*Department of Surgery and Science, Graduate School of Medical Sciences, Kyushu University, Fukuoka 812-8582; and*

⁴*Tokyo R&D Center, Daiichi Pharmaceutical Company, Tokyo 103-8234, Japan*

Received 1 November 2001; accepted in final form 18 June 2002

Ikeda, Yasuhiro, Yoshikazu Yonemitsu, Chu Kataoka, Shiro Kitamoto, Terutoshi Yamaoka, Ken-Ichi Nishida, Akira Takeshita, Kensuke Egashira, and Katsuo Sueishi. Anti-monocyte chemoattractant protein-1 gene therapy attenuates pulmonary hypertension in rats. *Am J Physiol Heart Circ Physiol* 283: H2021–H2028, 2002. First published June 20, 2002; 10.1152/ajpheart.00919.2001.— Monocyte/macrophage chemoattractant protein-1 (MCP-1), a potent chemoattractant chemokine and an activator for mononuclear cells, may play a role in the initiation and/or progression of pulmonary hypertension (PH). To determine whether blockade of a systemic MCP-1 signal pathway in vivo may prevent PH, we intramuscularly transduced a naked plasmid encoding a 7-NH₂ terminus-deleted dominant negative inhibitor of the MCP-1 (7ND MCP-1) gene in monocrotaline-induced PH. We also simultaneously gave a duplicate transfection at 2-wk intervals or skeletal muscle-directed in vivo electroporation (EP) to evaluate whether a longer or higher expression might be more effective. The intramuscular reporter gene expression was enhanced 10 times over that by EP than by simple injection, and a significant 7ND MCP-1 protein in plasma was detected only in the EP group. 7ND MCP-1 gene transfer significantly inhibited the progression of MCT-induced PH as evaluated by right ventricular systolic pressure, right ventricular hypertrophy, medial hypertrophy of pulmonary arterioles, and mononuclear cell infiltration into the lung. Differential effects of longer or higher transgene expression were not apparent. Although the in vivo kinetics of 7ND MCP-1 gene therapy should be studied further, these encouraging results suggest that an anti-inflammatory strategy via blockade of the MCP-1 signal pathway may be an alternative approach to treat subjects with PH.

MCP-1; monocrotaline; electroporation

PULMONARY HYPERTENSION (PH) is an intractable disease with sustained elevations of pulmonary arterial pressure (mean pressure >25 mmHg at rest) affecting about one to two cases of primary PH (PPH) in a million persons of the

general population (1, 15, 17). Because the prognosis of PH is poor, many efforts have been extensively conducted in clinic. Recent promising clinical studies using epoprostenol (prostacyclin) have demonstrated a significant improvement in survival time for patients with PH (3, 8, 9); however, it seems still distant from curative treatment. Furthermore, although cardiopulmonary transplantation has been effective for PH, related complications including bronchiolitis obliterans occur and retransplantation is needed (19). More effective and less invasive therapy based on the pathophysiology of PH should thus be developed.

Current limitations to treat PPH, however, include less knowledge of the exact mechanisms in the initiation and progression of the disease. For instance, although the pathological changes in PH include intimal thickening and/or medial and intimal hypertrophy of arteries, luminal thrombosis, and plexogenic pulmonary arteriopathy (PPA) (4–6, 15), no precise evidence is now available as to whether these untoward events lead to the disease or may be the result of the disease. No relevant animal model of PPH is available.

Although monocrotaline (MCT)-induced PH has been well accepted as an experimental model of PH (4–6), for instance, only medial hypertrophy of pulmonary arteries is noted, not other important findings, such as PPA lesions, suggesting some questions regarding the relevancy of this model.

Some common histological findings between humans and animals, on the other hand, have also been suggested. An exclusive perivascular inflammatory cell infiltrate, including monocyte/macrophages, was found in the PPA of PH patients (11, 22, 23) as well as in a rat model of MCT-induced PH (20, 21). Evidence shows that transient elevation of plasma levels of monocyte chemoattractant protein-1 (MCP-1) are associated in the early phase; therefore, this may play a role not only in the inflammatory response of MCT-induced PH (10) but also of human PPH. Although the role of MCP-1-

Address for reprint requests and other correspondence: Y. Yonemitsu, Div. of Pathophysiology and Experimental Pathology, Dept. of Pathology, Graduate School of Medical Sciences, Kyushu Univ., 3-1-1 Maidashi, Higashi-ku, Fukuoka 812-8582, Japan (E-mail: yonemitsu@pathol1.med.kyushu-u.ac.jp).

The costs of publication of this article were defrayed in part by the payment of page charges. The article must therefore be hereby marked "advertisement" in accordance with 18 U.S.C. Section 1734 solely to indicate this fact.

mediated inflammatory reaction in human PPH is still controversial, it is likely to be significant to clarify the role of inflammatory processes in the initiation and/or progression of the disease.

MCP-1, a member of the C-C chemokine family, has a potent chemotactic molecule for monocytes (12, 16, 18) and activates the receptor CCR2 as a dimer (12). Our recent study has demonstrated that a 7-NH₂ terminus-deleted mutant gene, namely 7ND MCP-1, is a potent dominant negative inhibitor for MCP-1 (26, 27). We reported that the intramuscular gene delivery of 7ND MCP-1 prevented vascular remodeling in rats with a chronic blockade of nitric oxide production (7), as well as atherosclerotic plaque formation of apolipoprotein E-deficient mice *in vivo* (13), which suggests that this approach might be effective in treating subjects with PH.

In the present study, we determined whether the intramuscular injection of a naked plasmid DNA encoding 7ND MCP-1 might prevent the disease progression of MCT-induced PH in a rat model. To evaluate the kinetics of this strategy, we examined three different intramuscular gene therapy protocols: 1) simple naked DNA injection; 2) duplicate injection to prolong transgene expression; and 3) simple injection with electronic pulses, which is well known as an effective technique to markedly increase intramuscular transgene expression (2).

METHODS

Plasmid DNA

Plasmid pCMV-luciferase was prepared as described previously (25). Human 7ND MCP-1 cDNA with a FLAG epitope was constructed as previously described (7). These plasmids, purified by equilibrium centrifugation in CsCl-ethidium bromide gradients were suspended in Tris-EDTA buffer (10 mM Tris·HCl and 1 mM EDTA; pH 8.0) at a concentration of 1.0 mg/ml.

Animals and Experimental Protocol

Adult male Sprague-Dawley rats (6–8 wk old, 250–350 g) were separated into six groups as follows: 1) buffer-injected control (C group, $n = 8$); 2) MCT injection without gene transfer (MCT group, $n = 34$); 3) MCT + gene transfer of luciferase once (Lucif group, $n = 9$); 4) MCT + gene transfer of 7ND MCP-1 once (7ND group, $n = 34$); 5) MCT + 7ND MCP-1 twice at 2-wk intervals (7ND×2 group, $n = 21$); and 6) MCT + *in vivo* electroporation once (EP group, $n = 27$). The experimental protocol is summarized in Fig. 1. Seventy-two thigh muscles were used for direct comparison study of pCMV-luciferase gene transfer, and luciferase activity was measured as previously described (25). The following animal experiments were reviewed by the Committee of Ethics on Animal Experiments in the Faculty of Medicine, Kyushu University. The National Institutes of Health *Guide for the Care and Use of Laboratory Animals* (NIH Publication No. 80-23, Revised 1985) was also followed.

Intraperitoneal injections of pentobarbital were given during the following procedures. The rats were given a single subcutaneous injection of MCT (60 mg/kg, Wako; Osaka, Japan). Rats were maintained under the humanized conditions throughout. Right ventricular (RV) hypertrophy and

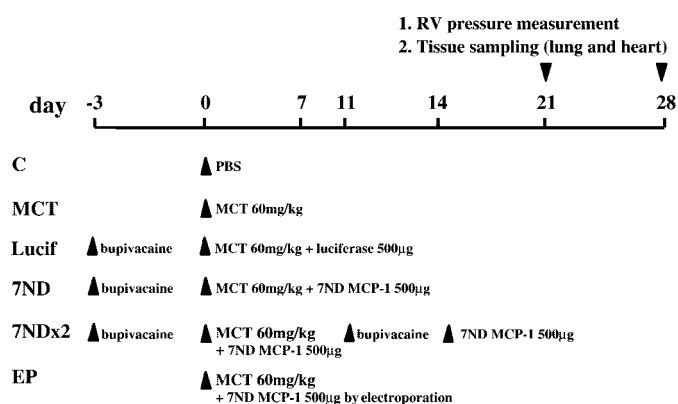


Fig. 1. Experimental protocols. The rats not in the control (C) group were given a single subcutaneous injection of monocrotaline (MCT; 60 mg/kg) at day 0. Three days before intramuscular plasmid DNA injection (Lucif group and 7ND group at day -3; 7ND×2 group at days -3 and 11), 0.25% bupivacaine was injected into bilateral thigh muscles using a 26-gauge needle. Six independent experiments were performed. 7ND MCP-1, 7 NH₂ terminus-deleted mutant gene of monocyte/macrophage chemoattractant protein; RV, right ventricle.

the percent wall thickness of pulmonary arterioles were assessed as previously described (10): percent wall thickness = $2 \times$ wall thickness (in μm)/external diameter (in μm) \times 100. RV systolic pressure was measured using a clinically available electric pressure meter (NEC; Tokyo, Japan) via direct puncture.

Intramuscular Gene Transfer

Direct injection. Three days before gene transfer, 500 μl of 0.25% bupivacaine were injected into both thigh muscles, and a total 500 μl solution of plasmid DNA (total 500 μg) was subsequently injected at the same sites (24).

Electroporation. Electronic pulses were delivered using a standard square-wave electroporator (CUY21, BEX; Tokyo, Japan) at 100 V, 50-ms pulse length and six pulses, soon after plasmid DNA injection (total 500 μg) (2). The steel electrode, a pair of 2.5 \times 0.5-cm parallel plates, was brought into contact with the muscle in parallel orientation with respect to the muscle fibers.

Western Blot Analysis

Cytoplasmic fraction was subjected to Western blot analysis using a primary monoclonal mouse anti-FLAG antibody (dilution 1:200, Stratagene; La Jolla, CA) and visualized by fluorescence using the HNPP-Fast Red TR System (Takara; Tokyo, Japan).

Enzyme-Linked Immunosorbent Assay

Commercially available ELISA systems (Bio Source; Camarillo, CA) were used to detect human MCP-1 and rat MCP-1 according to the manufacturer's instructions. Cross-reactivity of each species was determined as $<3\%$ (data not shown).

Immunohistochemistry

Immunohistochemistry for monocyte/macrophage labeling was done using a primary monoclonal mouse anti-rat ED1 IgG antibody (Serotec; Raleigh, NC) diluted 1:500, and signals were then developed using an avidin-biotinylated peroxidase complex method. For quantification, two blinded observers counted the number of ED1-positive cells on the same nine high-power fields ($\times 400$) in the lung of each animal.

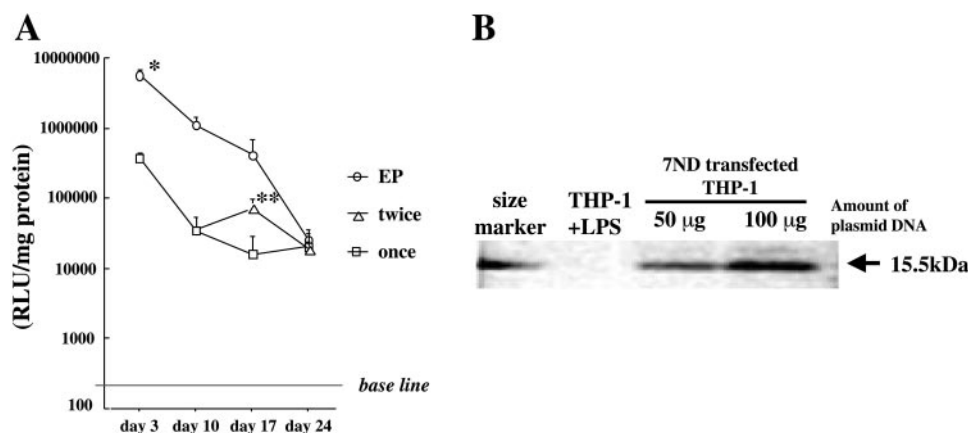


Fig. 2. Evaluations of transgene expression via gene transfer techniques. **A:** intramuscular gene expression efficiency via injection of pCMV-luciferase plasmid DNA with or without electronic pulse in vivo. Muscles were subjected to luciferase assay at 3, 10, 17, and 24 days after gene transfer. Electric pulse-mediated intramuscular gene transfer showed an ~ 15 -fold greater gene expression compared with the direct injection once on *day 3*. RLU, relative light units. $*P < 0.01$ vs. direct injection once; $**P < 0.05$ vs. direct injection once. **B:** Western blot analysis of 7ND MCP-1 protein expression using a FLAG-specific antibody in vitro. A dose-dependent increase of 7ND MCP-1 protein with FLAG sequence was observed (*lanes 2 and 3*) in cytoplasmic fractions of THP-1 cells subjected to lipid-mediated gene transfer. Cytoplasmic protein of THP-1 cells, which strongly express endogenous MCP-1 under LPS stimulation, showed negative results (*lane 1*), thereby indicating a transfected cDNA-specific gene product in *lanes 2 and 3*.

Statistical Analyses

All values are expressed as means \pm SD. Data were analyzed using one-way ANOVA, and, where appropriate, Student's *t*-test with Scheffé's adjustment for multiple comparisons was used.

The survival rate, determined by Kaplan-Meier's method, was calculated on *day 28*. The statistical significance of the survival experiments was determined using the log rank test.

RESULTS

Transgene Expression Via Intramuscular Injection With or Without Electric Pulses

We first determined intramuscular gene transfer efficiency of direct injection or in vivo electroporation using pCMV-luciferase plasmid DNA. These muscles were subjected to luciferase assay at 3, 10, 17, and 24 days after the gene transfer. Electric pulse-mediated intramuscular gene transfer showed an ~ 15 -fold greater gene expression compared with the direct injection of plasmid DNA once on *day 3* [Fig. 2A; direct injection: 3.8×10^5 relative light units (RLU)/mg protein ($n = 10$) and electroporation: 5.8×10^6 RLU/mg

protein ($n = 8$), respectively, $P < 0.001$]. Transgene expressions using both techniques were gradually decreased and showed almost equal levels with an apparent significant expression on *day 24*. Gene transfer of luciferase done twice showed an increase in intramuscular gene expression on *day 17* that was approximately fivefold greater than the direct injection once [once: 1.6×10^4 RLU/mg protein ($n = 10$) and twice: 7.5×10^4 RLU/mg protein ($n = 8$), respectively, $P < 0.05$] on *day 17*; however, even at that time, the level was still lower than that seen with electroporation.

To determine whether our construct of the 7ND MCP-1 gene could be translated in mammalian cells efficiently, in vitro lipid-mediated 7ND MCP-1 gene transfer was done. We used an anti-FLAG antibody to exclude 7ND MCP-1 from endogenous expression of wild MCP-1 protein. Western blot analysis using the cytoplasmic protein of THP-1 cells, which strongly expressed endogenous MCP-1 under LPS stimulation, showed no expression of MCP-1 with the FLAG (Fig. 2B), whereas a dose-dependent increase in 7ND MCP-1 protein was observed in Western blot analysis using

Table 1. Expression and time course of human-derived 7ND MCP-1 protein

Group	Plasma, pg/ml			Muscle, ng/g protein (Day 5)
	Day 3	Day 10	Day 17	
Lucif	<20 (5)	<20 (6)	<20 (6)	<0.01 (2)
7ND	<20 (8)	<20 (6)	<20 (6)	6.2 ± 2.0 (4)
7ND \times 2			<20 (6)	
EP	482.73 ± 366.21 (7)*	64.16 ± 72.56 (8)*	<20 (5)	105.9 ± 34.2 (5)*

Values are means \pm SD. Numbers in parentheses are the numbers of animals. 7ND MCP-1; 7-NH₂ terminus-deleted mutant gene (7ND) of monocyte/macrophage chemoattractant protein-1 (MCP-1). The following groups are shown: monocrotaline (MCT) + gene transfer of luciferase (Lucif); MCT + gene transfer of 7ND MCP-1 once (7ND); MCT + gene transfer of 7ND MCP-1 twice at 2-wk intervals (7ND \times 2); and MCT + in vivo electroporation (EP). $*P < 0.01$ vs. the 7ND group.

cytoplasmic proteins of THP-1 with lipid-mediated gene transfer of 7ND plasmid (Fig. 2B, lanes 2 and 3).

We reported that the intramuscular injection of 7ND plasmid efficiently prevented recombinant MCP-1-mediated intradermal infiltration of monocytes, thus indicating that the 7ND transgene products functioned well (7). However, little information is available regarding the required transgene expression level of 7ND MCP-1 compared with endogenous wild (rat) MCP-1 expression [untreated control plasma: $83.3 \pm$

19.9 pg/ml ($n = 2$)]. At various time points after gene transfer, we assessed the protein expression level of 7ND MCP-1 in plasma (days 3, 10, and 17) and muscles (day 5) in rats given an intramuscular gene transfer using human MCP-1-specific ELISA systems (Table 1). In plasma samples of all experimental groups, however, human sequence-specific 7ND MCP-1 protein was significantly detected only in the EP group on days 3 and 10 ($P < 0.01$). More than 18-fold higher 7ND MCP-1 protein was also obtained in the muscular tis-

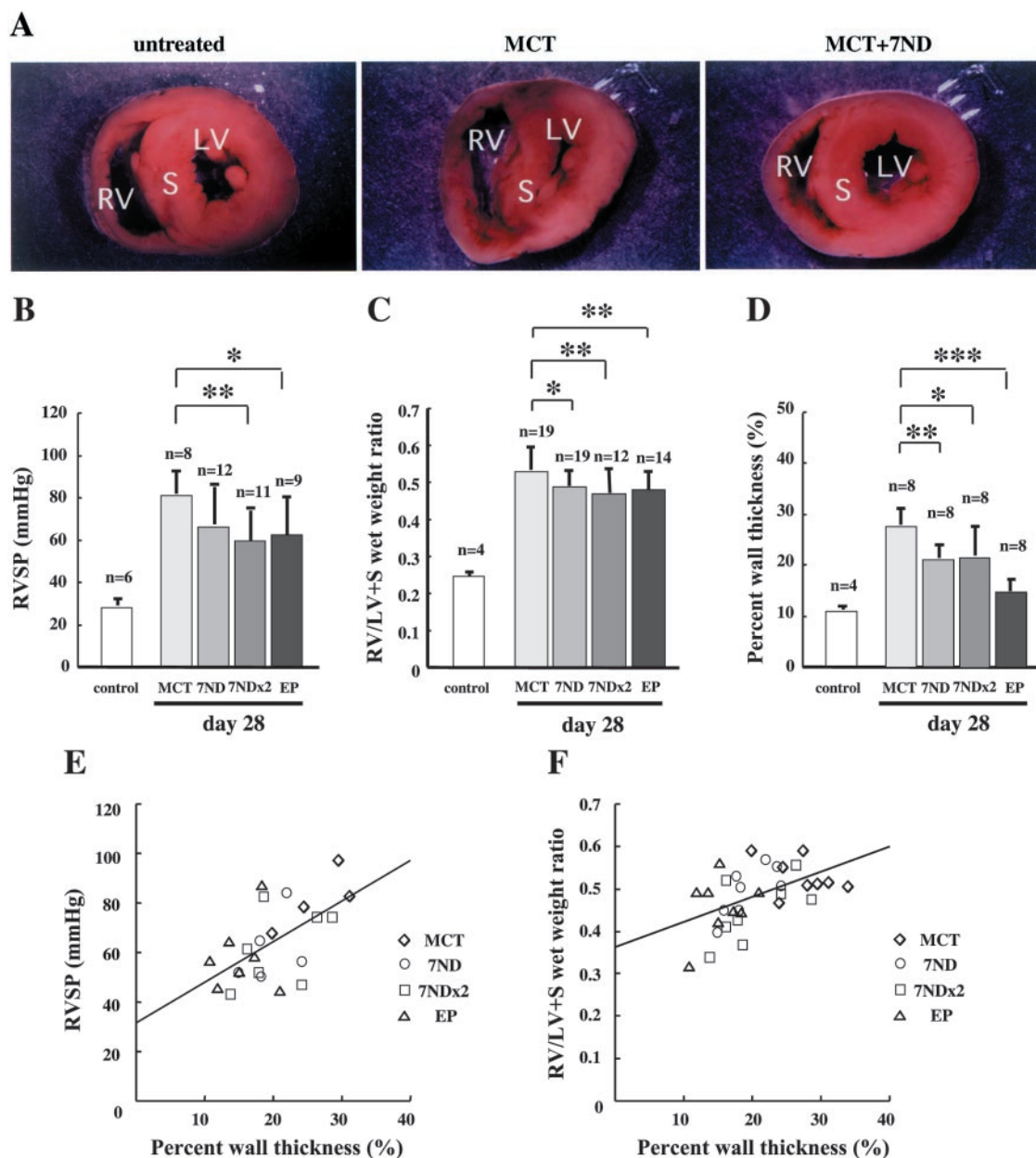


Fig. 3. A: typical macroscopic view of a ventricular cross section of the rat heart. An enlarged RV and shifted septum (S) to the left ventricle (LV) in the heart of the MCT-injected rat (middle) are apparent. Note that these are not obvious in the heart treated with 7ND (right), similar to findings in the untreated control heart (left). B–D: measurements of RV systolic pressure (RVSP; B), the wet weight RV-to-LV + S ratio (RV/LV+S; C), and the percent wall thickness of pulmonary arterioles (D). Data were analyzed by one-way ANOVA. * $P < 0.05$ vs. the MCT group; ** $P < 0.01$ vs. the MCT group; *** $P < 0.001$ vs. the MCT group. E and F: scattered plot analyses to determine the relationships between RVSP vs. the percent wall thickness of pulmonary arterioles (E) or RV/LV + S vs. the percent wall thickness of pulmonary arterioles (F). Both graphs indicate significant relationships among these parameters.

sue in case of electroporation than that with naked DNA injection ($P < 0.01$). These findings suggested that *in vivo* electroporation enhanced not only transgene expression in skeletal muscle but also plasma levels of 7ND MCP-1 protein.

Therapeutic Effects of 7ND MCP-1 Gene Transfer

We then assessed the therapeutic effects of 7ND MCP-1 gene transfer by assessing RV systolic pressure (RVSP) via direct needle puncture connected to a clinically available pressure meter. The hearts were harvested, and the wet weight was recorded [RV-to-left ventricle + septum (LV + S) ratio]. The lung was

histopathologically and immunohistochemically examined for macrophage infiltration.

7ND MCP-1 gene transfer prevents pulmonary arterial pressure, RV hypertrophy, and vascular remodeling of pulmonary arterioles. On day 21, a marked elevation of RVSP was observed in the MCT group [day 21: 47.8 ± 11.4 mmHg ($n = 9$) and day 28: 82.5 ± 10.6 mmHg ($n = 7$)]. At that time, the elevation of RVSP was significantly prevented in the EP group [38.4 ± 2.3 ($n = 6$), $P < 0.05$] on day 21 but not in other groups on day 21 [7ND: 42.2 ± 4.6 mmHg ($n = 8$), $P = 0.154$]. On day 28, elevation of RVSP in the MCT group [80.64 ± 11.07 mmHg ($n = 8$)] was significantly prevented in the 7ND \times 2 and EP groups

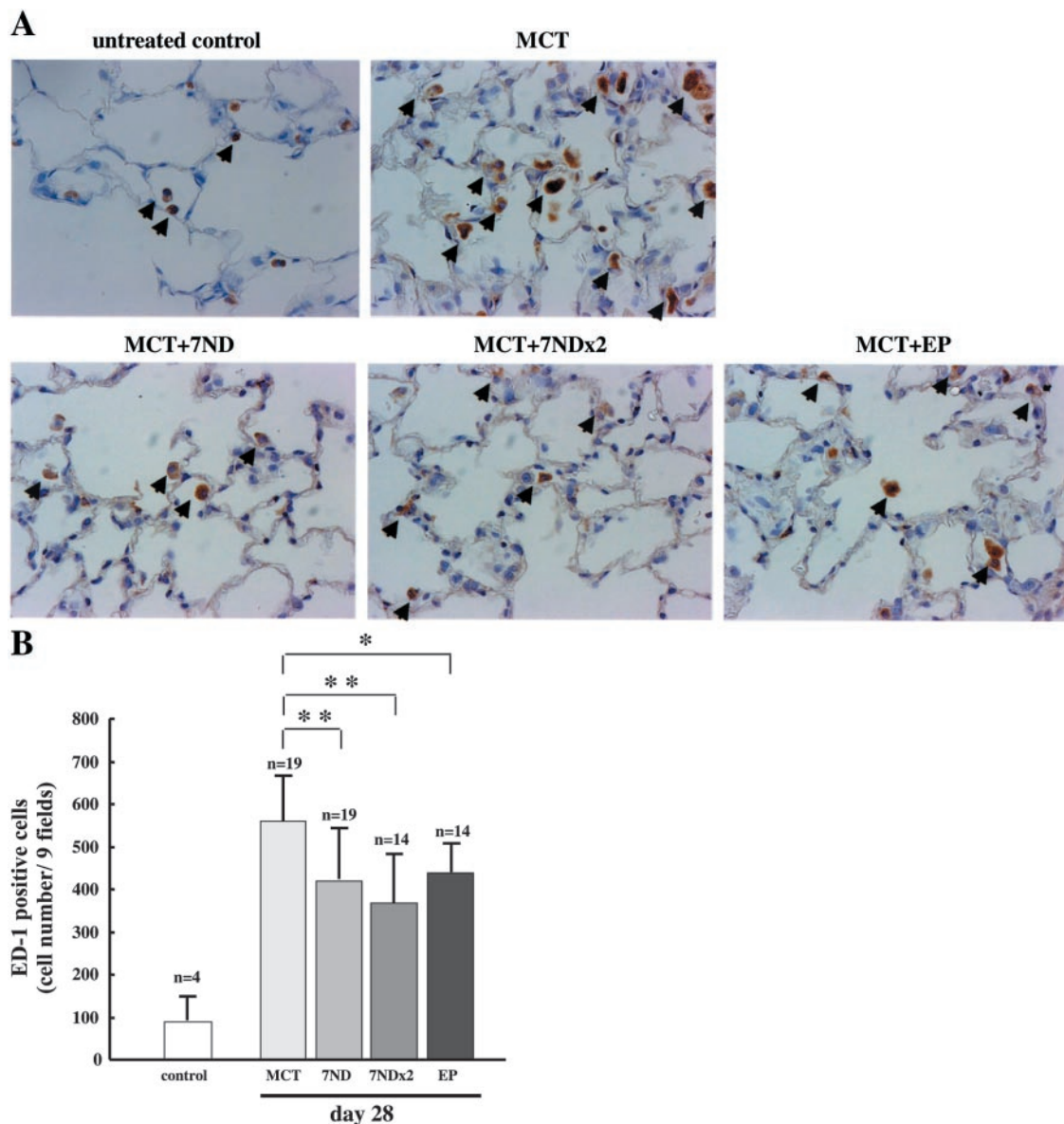


Fig. 4. Immunohistochemical findings indicating monocyte/macrophage infiltration in the lung using ED1 antibody (A) and quantification of a positive cell number (B). A: typical immunohistochemical findings of ED1-positive cells on day 28. The ED1-positive cells (brown-labeled cytoplasm, arrows), indicating macrophages and monocytes, infiltrated into the alveolar spaces (original magnification $\times 400$). B: ED1-positive cells were counted at the same nine high-power fields ($\times 400$) in the lung of each animal, and the total cell number was expressed. Data were analyzed using one-way ANOVA. * $P < 0.05$ vs. the MCT group; ** $P < 0.01$ vs. the MCT group.

[7ND×2: 60.4 ± 14.5 mmHg ($n = 11$), $P < 0.01$; EP: 63.6 ± 17.4 mmHg ($n = 9$), $P < 0.05$; Fig. 3B].

The degree of RV hypertrophy was determined by assessing the wet weight RV-to-LV + S ratio (Fig. 3, A and C). On *day 21*, no significant difference was observed among groups tested [C: 0.39 ± 0.06 ($n = 8$); 7ND: 0.38 ± 0.06 ($n = 7$), $P = 0.801$; EP: 0.34 ± 0.05 ($n = 6$), $P = 0.073$]. On *day 28*, the RV-to-LV + S ratios of the all 7ND-treated groups were significantly decreased [7ND: 0.49 ± 0.06 ($n = 19$), $P < 0.05$; 7ND×2: 0.47 ± 0.07 ($n = 12$), $P < 0.01$; EP: 0.48 ± 0.07 ($n = 14$), $P < 0.01$] compared with findings in the MCT group [0.54 ± 0.05 ($n = 19$); Fig. 3C].

On *day 28*, medial hypertrophy of pulmonary arterioles was significantly reduced in all 7ND-treated groups [7ND: $19.2 \pm 3.5\%$ ($n = 8$), $P < 0.01$; 7ND×2: $20.2 \pm 5.5\%$ ($n = 8$), $P < 0.05$; EP: $15.4 \pm 3.4\%$ ($n = 8$), $P < 0.001$] compared with findings in the MCT group [$27.3 \pm 4.5\%$ ($n = 8$); Fig. 3D]. To confirm the physiological significance and relationships among these parameters, we made scattered plot analyses. As shown in Fig. 3, E and F, medial hypertrophy of pulmonary arterioles significantly correlated to the RVSP and RV-to-LV + S ratio ($P < 0.01$, respectively).

7ND MCP-1 gene transfer prevents monocyte/macrophage recruitment in the lung. To determine the effects of 7ND MCP-1 gene transfer regarding mononuclear cell recruitment in the lung, immunohistochemical analyses for rat ED1-positive cells, indicating macrophages and monocytes, were made. On *day 21*, an increased number of ED1-positive cells was present in the lung of the MCT group (452.4 ± 95.0 cells/9 fields). At that time, ED1-positive cell infiltration in the EP group (337.5 ± 64.0 cells/9 fields, $n = 6$) was significantly prevented, compared with findings in the MCT group ($P < 0.05$). On *day 28*, MCT-mediated mononuclear cell infiltration (527.4 ± 124.5 cells/9 fields, $n = 19$) was also significantly prevented in all treatment groups [7ND: 430.8 ± 112.2 cells/9 fields ($n = 19$), $P < 0.01$; 7ND×2: 386.4 ± 122.4 cells/9 fields ($n = 14$), $P < 0.01$; EP: 446.9 ± 58.6 cells/9 fields ($n = 14$), $P < 0.05$; Fig. 4, A and B].

7ND MCP-1 improves the mortality rate of MCT-induced PH rats. As shown in Fig. 5, 10 of 25 rats in the

MCT group were dead by *day 21* ($n = 1$) and *day 28* ($n = 9$) spontaneously (overall survival rate on *day 28*: $15/25 = 60.00\%$), and 5 rats in the Lucif group were also dead by *day 21* ($n = 1$) and *day 28* ($n = 3$; overall survival rate on *day 28*: $5/9 = 55.56\%$). Meanwhile, in the three 7ND-treated groups, eight rats died spontaneously by *day 28* (7ND: $n = 4$; 7ND×2: $n = 2$; EP: $n = 2$). Survival analyses for each group showed that 7ND-treated groups had a significantly improved survival rate (overall survival rate on *day 28*: 7ND, $22/26 = 84.62\%$, $P < 0.05$ vs. the MCT group; 7ND×2, $19/21 = 90.48\%$, $P < 0.05$ vs. the MCT or Lucif group; EP, $19/21 = 90.48\%$, $P < 0.05$ vs. the MCT or Lucif group; Fig. 5).

DISCUSSION

Monocyte/macrophage recruitment to inflammatory foci releases various cytokines, growth factors, and chemokines, including MCP-1, resulting in the initiation and/or progression of various diseases via the autocrine/paracrine loop. Recent studies have suggested that recruitment of monocyte/macrophage plays a role not only for MCT-induced PH in rats (10, 20, 21) but also for various human diseases, including primary PH (23). Therefore, we tested a skeletal muscle-directed gene transfer approach, which was shown to be effective in preventing systemic MCP-1 activity (7), to determine whether it would be applicable in a rat model of MCT-induced PH.

We found that in all 7ND-treated groups, disease progression was significantly suppressed and survival rates improved, and thus we concluded that this approach is likely to be a strategy to treat diseases related to inflammatory consequences associated with MCP-1 activity. Furthermore, to address the therapeutic effect of this strategy more precisely, we used two additional groups, including duplicate DNA injection to prolong transgene expression and electroporation-mediated muscular gene transfer to enhance transgene expression. No significant differences were observed among these 7ND-treated groups, suggesting that the neutralizing effect of 7ND for endogenous MCP-1 seems not to largely depend on the duration and strength of the transgene expression.

Regarding the level of transgene expression, electroporation showed a constantly higher transgene expression when using the luciferase reporter gene and a higher exogenous gene product level in muscle and plasma than seen in the case of single or duplicate injections (Fig. 2A and Table 1). Regarding the therapeutic outcome, however, no significant differences were found in almost all parameters among these groups when using the same therapeutic gene in vivo (Figs. 3, B and C, and 4B). The exact reason is unclear, but one possible explanation may be that 7ND MCP-1 expression was still too low, even in the EP group, to prevent disease progression completely. To assess this more confidentially, we also did another set of experiments to achieve a higher level of 7ND MCP-1 gene transfer to the respiratory tract using a more efficient

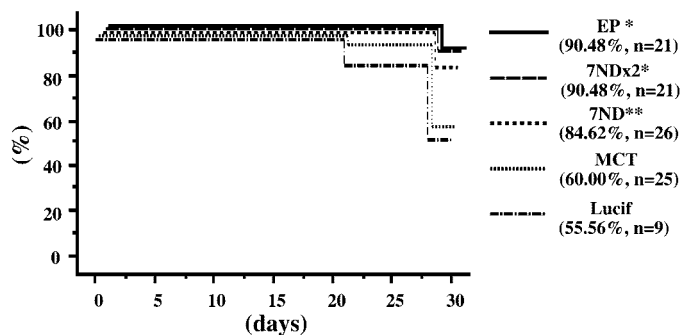


Fig. 5. Survival curve evaluated by Kaplan-Meier's method. The statistical significance of the survival experiments was determined using the log rank test. * $P < 0.05$ vs. the MCT or Lucif group; ** $P < 0.05$ vs. each MCT group.



viral vector, including the novel recombinant Sendai virus (25).

This notion is supported by findings indicating the requirement of a >30 times greater molar ratio of 7ND MCP-1 for 50% inhibition of MCP-1 activity in vitro (Ref. 26 and our unpublished observations). However, this seems not to be likely because, if these in vitro findings are comparable in in vivo situations, a 15 times higher therapeutic gene expression should be more effective. Another explanation is that the biological effect of 7ND MCP-1 may be independent of plasma concentrations. C-C chemokines, including MCP-1, are locally stored via binding to glycosaminoglycans in vivo (16), suggesting that the lower transgene expression of 7ND might be sufficient to prevent MCP-1 activity. This was supported by our previous data indicating that intramuscular plasmid-mediated 7ND injection could inhibit >80% of recombinant MCP-1 activity in the skin in vivo (7, 13). These kinetic studies of antagonistic effects of 7ND MCP-1 in vivo should be clarified further in the near future.

One more important question is also raised: Does MCP-1 play a role in the initiation and/or progression during MCT-induced PH disease? Although Cowan et al. (5a) reported that elastase inhibitor treatment could reverse established PH, 7ND gene administration could not do so in case of established PH (data not shown). These results suggest that elastase activity may be important during the whole process of MCT-induced PH, whereas MCP-1 might contribute to early but not to late disease initiation or progression in a rat model of MCT-induced PH. This notion seems reasonable because the endogenous MCP-1 level in the plasma showed a peak level 7 days after the MCT injection and declined within 2 wk (10), suggesting that later blockade of the MCP-1 signal pathway is likely to be without effect. However, suppression of early MCP-1 activity may affect the later disease phenotype, because suppression of ED1-positive cell infiltration in the lung was evident in all 7ND treatment groups. Therefore, early inhibition of MCP-1 signaling may prevent the autocrine/paracrine recruitment of monocytes/macrophages in a diseased lung.

In addition, timing of the gene transfer needs to be reconsidered. We injected the 7ND MCP-1 gene at the same time as MCT administration because, as mentioned above, it was seen that the plasma endogenous MCP-1 level showed a peak level 1 wk later. Because transgene expression via the intramuscular route showed a peak 3–5 days later, this gene transfer protocol might not prevent early MCP-1 activity.

In conclusion, intramuscular gene transfer of 7ND MCP-1 cDNA suppressed disease progression of MCT-induced PH and improved the survival rate. These results showed that monocyte/macrophage recruitment and the systemic MCP-1 signal pathway contribute to progression of this disease. Although kinetic studies including the level and duration of transgene expression as well as the timing of gene transfer are needed, this approach can be considered for use to block the systemic MCP-1 signal pathway and to treat

subjects with PH. Most importantly, more informations regarding that inflammatory process in the initiation and/or progression of human PH subjects should be obtained in the near future.

We thank H. Fujii, Y. Hori, and F. Takase for assistance with experiments.

This work was supported in part by Ministry of Education, Science, Technology, Sports and Culture of Japan Grant-in-Aids 12557020 and 12470057 (to Y. Yonemitsu), 11470059 and 11557020 (to K. Nakagawa), and 10307003 and 11557017 (to K. Sueishi).

REFERENCES

1. **Abenheim L, Moride Y, Brenot F, Rich S, Benichou J, Kurz X, Higenbottam T, Oakley C, Wouters E, Aubier M, Simonneau G, and Begaud B.** Appetite-suppressant drugs and the risk of primary pulmonary hypertension. International Primary Pulmonary Hypertension Study Group. *N Engl J Med* 335: 609–661, 1996.
2. **Aihara H and Miyazaki J.** Gene transfer into muscle by electroporation in vivo. *Nat Biotechnol* 16: 867–870, 1998.
3. **Barst RJ, Rubin LJ, McGoon MD, Caldwell EJ, Long WA, and Levy PS.** Survival in primary pulmonary hypertension with long-term continuous intravenous prostacyclin. *Ann Intern Med* 121: 409–415, 1994.
4. **Bjornsson J and Edwards WD.** Primary pulmonary hypertension: a histopathologic study of 80 cases. *Mayo Clin Proc* 60: 16–25, 1985.
5. **Burke AP, Farb A, and Virmani R.** The pathology of primary pulmonary hypertension. *Mod Pathol* 4: 269–282, 1991.
- 5a. **Cowan KN, Heilbut A, Humpl T, Lam C, Ito S, and Rabinovitch M.** Complete reversal of fatal pulmonary hypertension in rats by a serine elastase inhibitor. *Nat Med* 6: 698–702, 2000.
6. **Edwards WD.** Pathology of pulmonary hypertension. *Cardiol Clin* 18: 321–359, 1988.
7. **Egashira K, Koyanagi K, Kitamoto S, Ni W, Kataoka C, Morishita R, Kaneda Y, Akiyama C, Nishida K, Sueishi K, and Takeshita A.** Anti-monocyte chemoattractant protein-1 gene therapy inhibits vascular remodeling in rats. Blockade of MCP-1 activity following intramuscular transfer of a mutant gene inhibits vascular remodeling induced by chronic blockade of NO synthesis. *FASEB J* 14: 1974–1988, 2000.
8. **Gaine S.** Pulmonary hypertension. *JAMA* 284: 3160–3168, 2000.
9. **Hinderliter AL, Willis 4th PW, Barst RJ, Rich S, Rubin LJ, Badesch DB, Groves BM, McGoon MD, Tapson VF, Bourge RC, Brundage BH, Koerner SK, Langelen D, Keller CA, Murali S, Uretsky BF, Koch G, Li S, Clayton LM, Jobsis MM, Blackburn SD Jr, Crow JW, and Long WA.** Effects of long-term infusion of prostacyclin (epoprostenol) on echocardiographic measures of right ventricular structure and function in primary pulmonary hypertension. Primary Pulmonary Hypertension Study Group. *Circulation* 95: 1479–1486, 1997.
10. **Kimura H, Kasahara Y, Kurosu K, Sugito K, Takiguchi Y, Terai M, Mikata A, Natsume M, Mukaida N, Matsushima K, and Kuriyama T.** Alleviation of monocrotaline-induced pulmonary hypertension by antibodies to monocyte chemotactic and activating factor/monocyte chemoattractant protein-1. *Lab Invest* 78: 571–581, 1998.
11. **Knighton DR and Fiegel VD.** Macrophage-derived growth factors in wound healing: regulation of growth factor production by the oxygen microenvironment. *Am Rev Respir Dis* 140: 1108–1111, 1989.
12. **Matsushima K, Larsen CG, DuBois GC, and Oppenheim JJ.** Purification and characterization of a novel monocyte chemotactic and activating factor produced by a human myelomonocytic cell line. *J Exp Med* 169: 1485–1490, 1989.
13. **Ni W, Egashira K, Kitamoto S, Kataoka C, Koyanagi M, Inoue S, Imaizumi K, Akiyama C, Nishida K, and Takeshita A.** New anti-monocyte chemoattractant protein-1 gene therapy attenuates atherosclerosis in apolipoprotein E-knockout mice. *Circulation* 103: 2096–2101, 2001.



15. **Rich S, Dantzker DR, Ayres SM, Bergofsky EH, Brundage BH, Detre KM, Fishman AP, Goldring RM, Groves BM, Koerner SK, Levy PS, Reid LM, Vrejn CE, and Williams GW.** Primary pulmonary hypertension. A national prospective study. *Ann Intern Med* 107: 216–223, 1987.
16. **Rollins BJ.** Chemokines. *Blood* 90: 909–928, 1997.
17. **Rubin LJ.** Primary pulmonary hypertension. *Chest* 104: 236–250, 1993.
18. **Schall TJ.** Biology of the RANTES/SIS cytokine family. *Cytokine* 3: 165–183, 1991.
19. **Sundaesan S.** The impact of bronchiolitis obliterans on late morbidity and mortality after single and bilateral lung transplantation for pulmonary hypertension. *Semin Thorac Cardiovasc Surg* 10: 152–159, 1998.
20. **Sugita T, Hyers TM, Dauber IM, Wagner WW, McMurtry IF, and Reeves JT.** Lung vessel leak precedes right ventricular hypertrophy in monocrotaline-treated rats. *J Appl Physiol* 54: 371–374, 1983.
21. **Sugita T, Stenmark KR, Wagner WW, Henson PM, Henson JE, Hyers TM, and Reeves JT.** Abnormal alveolar cells in monocrotaline induced pulmonary hypertension. *Exp Lung Res* 5: 201–215, 1983.
22. **Tancredi RG.** Pulmonary vascular disease: primary pulmonary hypertension. *Cardiol Clin* 22: 113–124, 1992.
23. **Tuder RM, Groves B, Badesch DB, and Voelkel NF.** Exuberant endothelial cell growth and elements of inflammation are present in plexiform lesions of pulmonary hypertension. *Am J Pathol* 144: 275–285, 1994.
24. **Wells DJ.** Improved gene transfer by direct plasmid injection associated with regeneration in mouse skeletal muscle. *FEBS Lett* 332: 179–182, 1993.
25. **Yonemitsu Y, Kitson C, Ferrari S, Griesenbach U, Farley R, Steel R, Scheid P, Judd D, Kato A, Hasan MK, Nagai Y, Fukumura M, Hasegawa M, Geddes DM, and Alton EFWF.** Efficient gene transfer to airway epithelium using recombinant Sendai virus. *Nat Biotechnol* 18: 505–513, 2000.
26. **Zhang Y and Rollins BJ.** A dominant negative inhibitor indicates that monocyte chemoattractant protein 1 functions as a dimer. *Mol Cell Biol* 15: 4851–4855, 1995.
27. **Zhang YJ, Rutledge BJ, and Rollins BJ.** Structure/activity analysis of human monocyte chemoattractant protein-1 (MCP-1) by mutagenesis. Identification of a mutated protein that inhibits MCP-1-mediated monocyte chemotaxis. *J Biol Chem* 269: 15918–15924, 1994.



Gene Therapy for Central Diabetes Insipidus: Effective Antidiuresis by Muscle-Targeted Gene Transfer

MASANORI YOSHIDA, YASUMASA IWASAKI, MASATO ASAI, TAKESHI NIGAWARA, AND YUTAKA OISO

Departments of Medicine (M.Y., M.A., Y.O.) and Clinical Pathophysiology (Y.I., T.N.), Nagoya University Graduate School of Medicine and Hospital, Nagoya 466-8550, Japan

Central diabetes insipidus, characterized by severe polyuria and polydipsia, is a disorder resulting from deficient secretion of the small neuropeptide hormone vasopressin in the neurohypophysis. The standard therapy is daily and life-long administration of vasopressin analog (desmopressin acetate), but gene therapy is potentially alternative to the conventional replacement therapy. To obtain the therapeutic neuropeptide more feasibly, we tried to express vasopressin in nonneuronal tissues using nonviral gene transfer techniques. We found that the unprocessed large precursor form, provasopressin, was predominantly produced in nonendocrine cells transfected with the wild-type vasopressin gene, because of the lack of neuroendocrine cell-specific endopeptidases. In sharp

contrast, appropriately processed bioactive vasopressin can be efficiently produced even in nonendocrine cells with a modified vasopressin gene containing a ubiquitous endoprotease furin cleavage site. We also succeeded in maintaining a long-term antidiuretic effect on vasopressin-deficient (Brattleboro) rats by direct introduction of the furin-processible gene into skeletal muscle by electroporation. Altogether, our data clearly show that skeletal muscle is a useful target tissue for continuous delivery of bioactive neuropeptide. Furthermore, our strategies may be applicable to future gene therapies for central diabetes insipidus and other peptide hormone deficiencies. (*Endocrinology* 145: 261–268, 2004)

A SMALL PEPTIDE hormone arginine vasopressin (vasopressin), also known as antidiuretic hormone, is secreted from the neurohypophysis and plays a pivotal role in osmoregulation and water metabolism (1). Deficient vasopressin secretion results in central diabetes insipidus (CDI) with marked polyuria at an amount of more than 10 liters/d. Gene therapy with sustained expression of vasopressin may achieve long-term remission of this disease and can be used instead of the daily repeated replacement of vasopressin analog.

In contrast to GH or other protein deficiencies (2–5), there are very few reports on gene therapy for CDI. Geddes *et al.* (6, 7) carried out a pioneering work, showing that the direct injection of adenovirus encoding vasopressin cDNA into the supraoptic nuclei of the hypothalamus of Brattleboro rats, an animal model of hereditary CDI, improved polyuria. This strategy, however, cannot be applicable clinically, because, unlike the Brattleboro rat in which vasopressin-secreting neurons are exceptionally preserved (8, 9), the homologous neurons are lost or degenerated in patients with CDI (10, 11). In addition, the induction of viral vectors into the human central nervous system does not appear safe or practical. Our aim of this work is to obtain bioactive vasopressin from nonneuronal tissues using a simpler and more feasible approach. When the vasopressin gene is to be introduced into heterologous cells, on the other hand, we face another obstacle, namely, that the processing of vasopressin peptide is

deficient in nonendocrine cells. Like many other neuropeptide hormones, the bioactive nonapeptide form of vasopressin is generated from a large precursor, provasopressin, at the paired basic amino acid residues (⁻¹¹Lys-⁻¹²Arg-) by specific endopeptidase, such as prohormone convertase (PC) 1/3 or PC2, yielding neurophysin II which is a vasopressin-binding protein, and glycoprotein (12–15) (Fig. 1A). Indeed, the vasopressin precursor protein expressed in nonendocrine cells is not appropriately processed (16), probably because of the lack of a processing enzyme(s).

To overcome these limitations, we developed several strategies for expressing bioactive vasopressin even in heterologous nonendocrine cells. We succeeded in showing that mature-sized bioactive vasopressin can be produced efficiently in nonendocrine cells using mutated vasopressin cDNA, in which the amino acid sequences between vasopressin and neurophysin II were altered to be processed by a ubiquitous endoprotease, furin (17). In addition, we normalized the urine volume of the Brattleboro rats by direct *in vivo* introduction of the furin-processible vasopressin gene using a potent nonviral *in vivo* gene delivery system, electroporation (18–21), because skeletal muscle is an excellent target tissue for transgene expression (22–24). The achievement of constitutive processed neuropeptide secretion by muscle-targeted gene delivery paves the way for clinical application of gene therapies for CDI and various other hormone deficiencies.

Materials and Methods

RT-PCR

Expression of PC1/3, PC2, and furin mRNAs was analyzed by RT-PCR technique. Total RNA was extracted from each cell line using TRIzol reagent (Invitrogen, Carlsbad, CA), and RT-PCR was carried out using a commercially available kit (SuperScript, Invitrogen). The PCR

Abbreviations: AVP/Fur, Furin-processible vasopressin expression vector; CDI, central diabetes insipidus; CRE, cAMP-response element; WT, wild-type.

Endocrinology is published monthly by The Endocrine Society (<http://www.endo-society.org>), the foremost professional society serving the endocrine community.

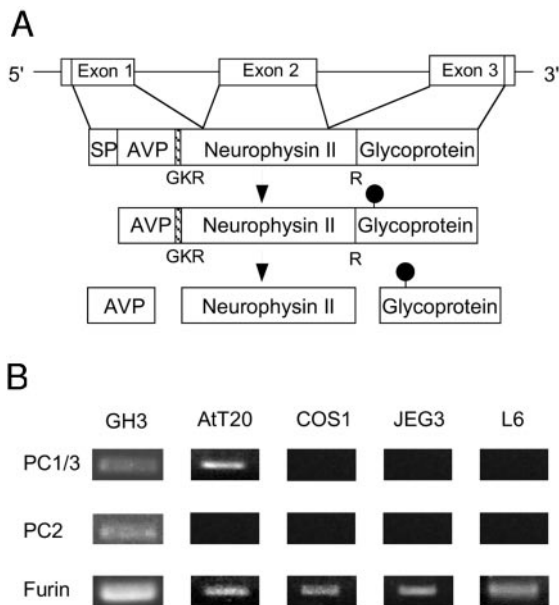


FIG. 1. Processing of vasopressin precursor protein, preprovasopressin, with the associated processing enzymes. **A**, A scheme representing the posttranslational processing of vasopressin (AVP). After removal of a signal peptide (SP), provasopressin is further processed into three small peptides, vasopressin, neurophysin II, and C-terminal glycopeptide. Processing between vasopressin and neurophysin II is known to occur at the paired basic amino acid residues (^{-11}Lys - ^{12}Arg -) by specific endopeptidases, resulting in a bioactive nonapeptide vasopressin. **B**, RT-PCR analyses of the endopeptidases PC1/3, PC2, and furin expression in a variety of cells/tissues used in this study. PC1/3, a neuroendocrine-specific endopeptidase, is expressed in GH₃ and AtT20 but not in other nonendocrine cells/tissues. In contrast, a ubiquitous endopeptidase furin is expressed in all cell lines examined.

primers used were: for mouse AtT20 cells, PC1/3, forward 5'-TTGGCTGAAAGGAAAGAGAT-3', reverse 5'-ACTTCTTTGGTGATTGTTTG-3'; PC2, forward 5'-GATCCTCTTTTTACAAAGCA-3', reverse 5'-AGCACTGTGATGTTGCAT-3'; furin, forward 5'-CCA-GTTTTGACGTGAATGACC-3', reverse 5'-ATGGAGCCCAGCCCTC-CTCG-3'; for rat GH₃ and L6 cells, PC1/3, forward 5'-GTTGGCTGAAAGGAAAGGAT-3', reverse 5'-GAATCTTTGATGATTGCTTTGA-3'; PC2, forward 5'-GATCCTCTTTTTACAAAGCA-3', reverse 5'-AGCACTGTGATGTTGCAT-3'; furin, forward 5'-CCAGCTTTGATGCAATGACC-3', reverse 5'-ATGGAGCCCAGCCCTCCGCG-3'; for COS1 and JEG3 cells, PC1/3, forward 5'-TTGGCTGAAAGAGAACGGAT-3', reverse 5'-ACTTCTTTGGTGATTGCTTTG-3'; PC2, forward 5'-GATCCTCTTTTTACAAAGCA-3', reverse 5'-AGCACAGTCAGATGCTGCAT-3'; furin, forward 5'-AAGTTTCTCAGCAGTGGTA-3', reverse 5'-TTGTCATTACATCTGTGTACC-3'.

Plasmid construction

A wild-type (WT) vasopressin expression vector was constructed by inserting the rat vasopressin cDNA into pRc/RSV expression vector (CLONTECH, Palo Alto, CA). Furin-processible vasopressin expression vector (AVP/Fur) was made from WT by site-directed mutagenesis technique. CAG promoter-driven expression vector (pCAGGS/AVP/Fur) was constructed by inserting the AVP/Fur cDNA into pCAGGS expression vector (kindly provided by Prof. Miyazaki, Osaka University, Osaka, Japan) (25). PC1/3 and PC2 expression vectors were made by inserting the mouse PC1/3 or PC2 cDNA (kindly provided by Dr. Mains, Johns Hopkins University, Baltimore, MD) (26) into a pRc/CMV expression vector (CLONTECH).

Cell culture and transfection

AtT20, GH₃, JEG3, COS1, L6, and LLC-PK1 cells were maintained with standard cell culture techniques. For transient expression, cells

were plated in 35-mm-diameter culture dishes, and each vector was transfected using TransIT reagent (Mirus, Madison, WI). On the next day, the culture medium was changed to serum-free medium, and vasopressin secreted into the medium for 10 h was used for the subsequent analyses. Three separate dishes were used for each experimental condition. In most of the experiments, β -galactosidase expression vector was used as an internal control. For stable transfection, L6 cells were transfected with pCAGGS/AVP/Fur using TransIT reagent. After selection with G418 (Geneticin, Invitrogen), clonal cell lines expressing vasopressin were selected, and the representative cell lines, designated as L6VP, were used for the subsequent experiments.

Gel filtration chromatography

Two milliliters of each culture medium from the transfected cells, or standard vasopressin (Peptide Institute, Osaka, Japan), was loaded and filtrated through a P-10 column (Bio-Rad, Hercules, CA) using a 4% acetic acid solution containing 0.1% BSA as a filtration buffer. Each fraction (8.0 ml each) was vacuum-dried, resuspended with assay buffer, and then applied for vasopressin RIA.

Vasopressin bioassay in vitro

LLC-PK1 cells were plated in 35-mm-diameter dishes and transfected transiently with cAMP response element (CRE \times 5)-luciferase reporter gene using TransIT reagent. After 48 h, the cells were incubated for 5 h with serum-free medium containing standard vasopressin. The vasopressin bioactivity was determined by luciferase assay (27). Three separate dishes were used for each experimental condition. The same protocol was performed when the serum-free culture medium derived from vasopressin-expressing cells containing immunoreactive vasopressin (500 pg/ml, determined by RIA) with or without 1.0 $\mu\text{g}/\text{ml}$ OPC31260 (provided by Otsuka Pharmaceutical Co., Tokyo, Japan) (28, 29), or control serum-free medium incubated with nontransfected cells was used. Each value obtained was normalized by the protein amount of the corresponding cell extract.

Animal experiments

Twenty-week-old male Brattleboro rats (kindly provided by Prof. Yamaoka, Dokkyo University, Tochigi, Japan) were used. All rats were kept under controlled lighting conditions (light, 0900 h; dark, 2100 h) and constant temperature (21 C). Animal surgery and care were in accordance with the Nagoya University institutional guidelines complying with the National Institutes of Health policy. For estimating *in vivo* bioactivity of vasopressin derived from the transfected cells *in vitro*, Brattleboro rats ($n = 4$ in each group) received a sc injection of culture medium (3 ml, 12 h incubation) derived from JEG3 or COS1 cells transiently transfected with AVP/Fur using LipofectAMINE PLUS (Invitrogen), or control medium incubated with nontransfected cells. Each rat was then placed in a metabolic cage for 2 h without water or food, and urine volume was determined by enforced urination every 30 min. For transplantation experiments, Brattleboro rats ($n = 3$ in each group) were sc transplanted with L6VP (1.2×10^8) cells with or without OPC31260. In the OPC-treated group, each rat received an ip injection of OPC31260 (10 mg/kg body weight, 1% in dimethylsulfoxide) on the d 4 or 6 after transplantation. As the control, Brattleboro rats ($n = 3$) transplanted with nontransfected L6 cells (1.2×10^8) were used. During these experiments, each recipient rat was housed in an individual metabolic cage, and daily urine volume and water intake, normalized by body weight, were determined. Food and water were available *ad libitum*. Urine osmolality was measured by OSMOSTAT OM6040 (ARKRAY, Shiga, Japan).

Electric pulse delivery and electrodes

Electric pulses were delivered using an electric pulse generator (Square Electroporator CUY 21 EDIT; NEPA GENE Co. Ltd., Ichikawa, Japan). Brattleboro rats ($n = 3-4$ in each group) were anesthetized with diethylether, and an approximately 5-cm incision was made in the skin of the left hind limb. pCAGGS-AVP/Fur or control vector (pCAGGS) (60

$\mu\text{g}/\text{site}$, 1 mg/ml in saline) was injected into the left anterior tibial and soleal muscles with a 27-gauge needle centered between a pair of stainless electrode needles (5 mm in length and 0.4 mm in diameter, with a fixed distance of 5 mm between them). Total plasmid amount per rat was 5 $\mu\text{g}/\text{g}$ body weight. Immediately after plasmid injection, four pulses of 100 V, 50 msec, followed by four more pulses of the opposite polarity, were administered to each injection site at a rate of 1 pulse/sec. Each rat was then housed in an individual metabolic cage, with food and water available *ad libitum*. Daily urine volume and water intake were determined, and were normalized by body weight. Expression of vasopressin mRNA in injected muscle was analyzed by RT-PCR after deoxyribonuclease treatment. The PCR primers used were: forward 5'-GCCAGGAGGAGAAGTACCTG-3', reverse 5'-ACCAGCCTAAGCAGCAGCTC-3'.

Vasopressin RIA

For the determination of tissue vasopressin, the electroporated muscle was homogenized with 0.1 N HCl and centrifuged, and the supernate was extracted by Sep-Pak C₁₈ column (Waters Associates Inc., Milford, MA) (30). For plasma vasopressin, rats were decapitated and trunk blood was collected in chilled tubes containing EDTA-2K. After immediate centrifugation, plasma was separated and vasopressin was extracted as mentioned above. Vasopressin was determined by a high-sensitive RIA kit (Mitsubishi Chemical Co., Tokyo, Japan) (31). The sensitivity of assay for arginine vasopressin was 0.063 pg/tube, with less than 0.01% cross-reactivity with oxytocin or lysine vasopressin.

Statistical analysis

All of the experiments were carried out more than twice to confirm the reproducibility, and the representative data are presented. Data are expressed as means \pm SEM. Statistical comparison between the groups

was made by one-way ANOVA with Fisher's multiple range test. Differences were considered significant at $P < 0.05$.

Results

Processing profiles of vasopressin expressed in endocrine or nonendocrine cells

First, we found by RT-PCR that the putative enzyme(s) for vasopressin processing, PC 1/3 and/or PC2, are expressed in GH₃ rat somatomammotroph and AtT20 mouse corticotroph cells but not in COS1, JEG3, and L6 cells (Fig. 1B). When WT rat vasopressin cDNA expression vector was introduced, fully processed immunoreactive vasopressin, analyzed by gel filtration chromatography, was released from AtT20 cells (Fig. 2, A and B). In contrast, when WT expression vector was introduced into JEG3 and COS1 cells, vasopressin was not appropriately processed (Fig. 2, C, D, G, and H). In these cell lines, however, when PC1/3 expression vector was coexpressed, the processing profile was dramatically improved and vasopressin was secreted more efficiently (Fig. 2, C, E, G, and I). Coexpression of PC2 was not effective (Fig. 2, C, F, G, and J). Thus, simultaneous expression of peptide hormone and its specific processing enzyme is one of the methods for producing appropriately processed final products. Our data also suggest that PC1/3, but not PC2, is the enzyme re-

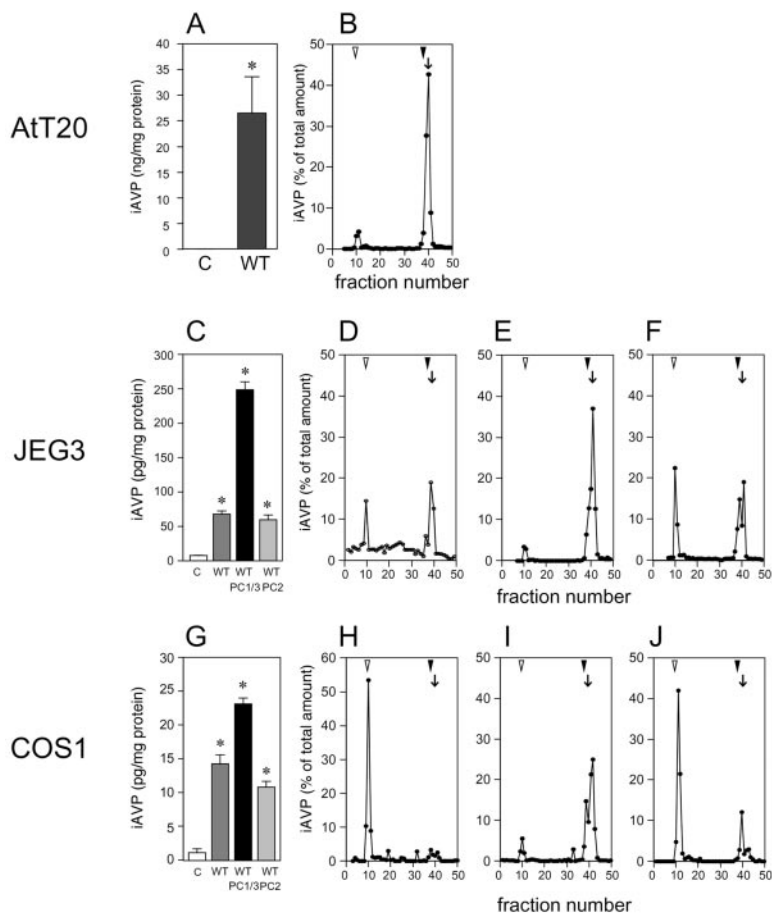


FIG. 2. Processing profiles of vasopressin expressed in endocrine (AtT20) or nonendocrine (JEG3, COS1) cells. A and B, Immunoreactive vasopressin (iAVP) in culture medium obtained from transfected AtT20 cells (A). The molecular size was analyzed by gel filtration chromatography (B). C–F, iAVP in culture medium in JEG3 cells transiently transfected with vehicle, WT alone, WT + PC1/3 coexpression, and WT + PC2 coexpression (C). The molecular size of iAVP in each culture medium is indicated. WT alone (D), WT + PC1/3 (E), and WT + PC2 (F). G–J, A similar experiment in COS1 cells. iAVP in culture medium (G). The molecular size of iAVP in each culture medium is indicated. WT alone (H), WT + PC1/3 (I), and WT + PC2 (J). Data are mean \pm SEM ($n = 3$ in each group). *, $P < 0.05$ vs. control. Open or filled arrowheads represent void or total volume, respectively. Arrows indicate the peak of elution position of standard vasopressin using the same conditions.

sponsible for the processing that occurs between vasopressin and neurophysin II.

Processing profiles of vasopressin transfected with furin-processible provasopressin gene

We also tried an alternative approach using modified provasopressin cDNA, in which the vasopressin and neurophysin II junction was altered to a tetra basic furin cleavage site (Fig. 3A). When the modified expression vector (AVP/Fur) was introduced into JEG3 or COS1 cells that express furin (Fig. 1B), a more efficient vasopressin secretion with a markedly improved processing profile was obtained (Fig. 3, B-E), compared with WT (Fig. 2, D and H).

Assessment of vasopressin bioactivity in vitro and in vivo

The bioactivity of secreted vasopressin in both strategies was confirmed using both *in vitro* and *in vivo* bioassay systems. LLC-PK1, renal epithelial cells known to express V2 vasopressin receptor (32), were treated with culture medium containing expressed vasopressin, and the bioactivity was monitored by cAMP/protein kinase A-stimulated CRE-lu-

ciferase reporter gene expression (Fig. 4A). The efficacy of this system was validated by standard vasopressin peptide (Fig. 4B). Vasopressin derived from WT or AVP/Fur in all cell lines stimulated CRE-luciferase activity, compared with

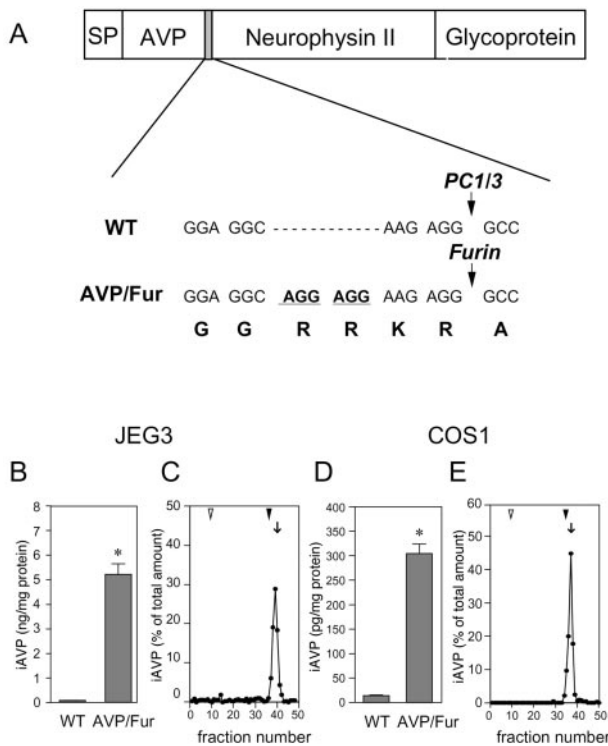


FIG. 3. Processing profiles of vasopressin derived from furin-processible provasopressin precursor protein. A, Scheme of the nucleotide sequences of the vasopressin-neurophysin II connection site in WT, or AVP/Fur vasopressin cDNA with two arginine insertions. B and C, Immunoreactive vasopressin (iAVP) in the culture medium of JEG3 cells transiently transfected with WT or AVP/Fur. The molecular size of iAVP in culture medium of AVP/Fur transfected JEG3 cells (compare with Fig. 2, C and D) is indicated. D and E, A similar experiment in COS1 cells. iAVP in culture medium (D). The molecular size of iAVP in culture medium of AVP/Fur-transfected COS1 cells is indicated (E) (compare with Fig. 2, G and H). Data are mean \pm SEM (n = 3 in each group). *, P < 0.05 vs. WT transfection. Open or filled arrowheads represent void or total volume, respectively. Arrows indicate the peak of elution position of standard vasopressin.

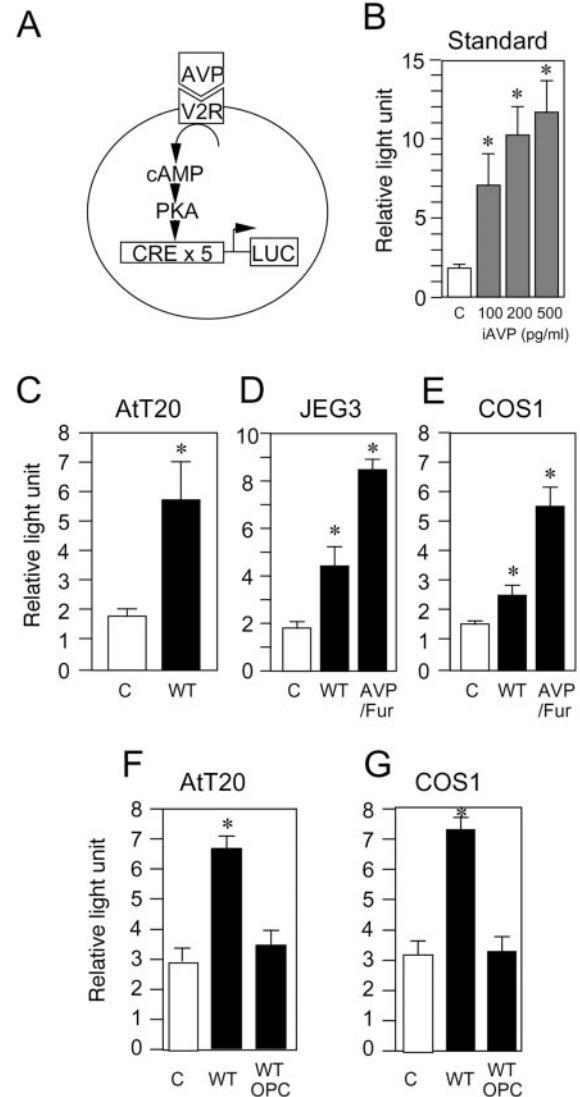


FIG. 4. Assessment of vasopressin bioactivity *in vitro*. A, Scheme of the *in vitro* vasopressin bioassay system using LLC-PK1 cells expressing the intrinsic vasopressin V2 receptor. The degree of receptor stimulation is estimated by the CRE (\times 5)-driven luciferase activity instead of directly measuring cAMP production. B, Dose-response effect of standard vasopressin (100, 200, 500 pg/ml) on the above system. C-E, The bioactivity of vasopressin secreted from the WT or AVP/Fur transfected cells *in vitro*. LLC-PK1 cells transfected with CRE-luciferase reporter gene were treated with the test medium containing 500 pg/ml of immunoreactive vasopressin (iAVP) that were derived from WT or AVP/Fur transfected cells, or control medium (C; medium from nontransfected cells) for 5 h. AtT20 transfected with WT vector (C); JEG3 cells transfected with either WT or AVP/Fur vector (D); COS1 cells transfected with either WT or AVP/Fur vector (E). F and G, The effect of selective V2 receptor antagonist, OPC31260, on the above vasopressin bioassay system. LLC-PK1 cells expressing CRE-luciferase reporter gene were treated with control medium or test medium (containing 500 pg/ml of iAVP derived from JEG3 transfected with AVP/Fur) with or without 1.0 μ g/ml OPC31260 (F). A similar experiment in COS1 cells (G). Data are mean \pm SEM (n = 3 in each group). *, P < 0.05 vs. control.

the nontransfected control medium. Notably, AVP/Fur-derived vasopressin showed higher bioactivity than vasopressin derived from WT in JEG3 or COS1 cells, probably because of the improved processing efficiency (Fig. 4, D and E). We confirmed that these enhancements were completely inhibited after the treatment with the selective V2 receptor antagonist OPC31260 (Fig. 4, F and G), indicating that the secreted vasopressin increased the CRE-luciferase activity via the V2 receptor. Furthermore, when the AVP/Fur-derived culture medium was sc injected into Brattleboro CDI rats, the cumulated urine volume was markedly suppressed (Fig. 5). Collectively, these data indicate that AVP/Fur-derived immunoreactive vasopressin expressed in nonendocrine cells is physiologically bioactive both *in vitro* and *in vivo*.

Antidiuretic effect of vasopressin-expressing L6 myoblasts

We then attempted to express vasopressin in live animals using nonviral *in vivo* gene delivery techniques. We selected skeletal muscle as the target organ to obtain bioactive vasopressin *in vivo*. To achieve higher levels of expression, we constructed a new expression vector, pCAGGS-AVP/Fur, in which AVP/Fur cDNA was driven by a more potent CAG promoter in myocytes (21, 25) (Fig. 6A). We confirmed that the expression vector indeed produced vasopressin more efficiently (>20-fold) than did RSV-AVP/Fur in the L6 rat skeletal muscle cell line (Fig. 6B). When L6VP cells in which pCAGGS-AVP/Fur were stably transfected were sc transplanted into Brattleboro rats, polyuria and polydipsia were significantly improved toward an almost normal range, accompanied with a marked increase of urine osmolality; in contrast, these parameters were not changed in L6 cell-transplanted control rats (Fig. 6, C–E). Moreover, the antidiuretic effect was blocked by the administration of OPC31260 for about 24 h, and this inhibition was reversed on the next day (Fig. 7), suggesting that the V2 receptor is responsible for the antidiuresis of L6VP-derived vasopressin, and the combination of V2 antagonists may prevent the water intoxication. Afterwards, this antidiuretic effect returned to the initial

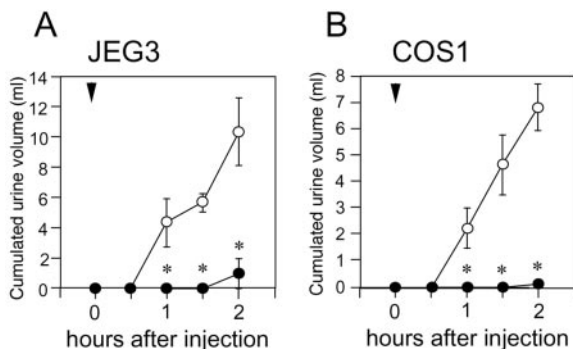


FIG. 5. The bioactivity of vasopressin secreted from the transfected cells *in vivo*. The cumulated urine volume was estimated in Brattleboro rats injected sc with the test medium, derived from the AVP/Fur vector transfected JEG3 (A) or COS1 (B) cells (closed circles), or the control medium (derived from nontransfected JEG3 or COS1 cells) (open circles) ($n = 4$ in each group). The concentration of immunoreactive vasopressin was 8.2 ng/ml (JEG3) and 7.5 ng/ml (COS1). Data are mean \pm SEM. *, $P < 0.05$ vs. control. Arrowheads represent the time of injection.

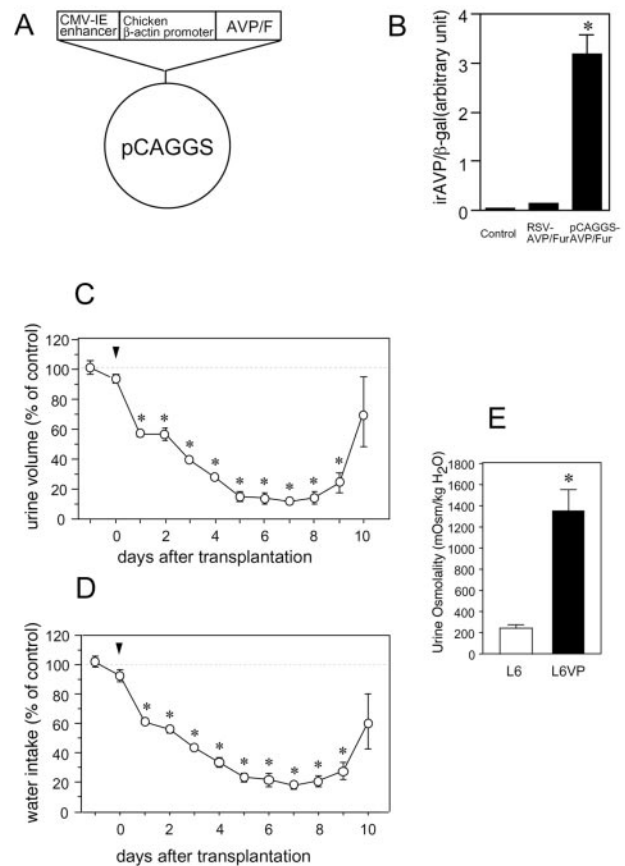


FIG. 6. Antidiuretic effects of L6VP cell transplantation in Brattleboro rats. A, Scheme of pCAGGS-AVP/Fur vector. Furin-processible vasopressin cDNA is driven by CMV-IE enhancer and chicken β -actin promoter. B, Immunoreactive vasopressin (irAVP) in the culture medium of L6 cells transiently transfected with pRSV-AVP/Fur or pCAGGS-AVP/Fur ($n = 3$ in each group). C and D, L6VP or L6 cells transplanted sc into the Brattleboro rats ($n = 3$ in each group). Daily urine volume (C) and water intake (D) were measured in both groups (data are shown as % of control L6-transplanted rats). E, Urine osmolality of Brattleboro rats 6 d after L6 or L6VP cell transplantation ($n = 3$ in each group). Data are mean \pm SEM. *, $P < 0.05$ vs. control. Arrowheads represent the day of transplantation.

level without immunosuppressive drugs. However, these data indicate that myocyte-derived immunoreactive vasopressin exerts a potent antidiuretic effect via the V2 receptor as well as authentic vasopressin.

Antidiuretic effect of vasopressin expressed in the skeletal muscle of Brattleboro rats

Finally, an electroporation technique was applied to deliver the vasopressin expression vector into skeletal muscles *in vivo*. After direct introduction of pCAGGS-AVP/Fur plasmid into unilateral (left) tibial and soleal muscles of Brattleboro rats by electroporation, the daily urine volume and water intake significantly decreased compared with control DI rats, to which control vector (pCAGGS) was introduced with electroporation (Fig. 8, A and B). Urine osmolality increased by up to 3-fold, compared with that of control (pCAGGS) rats. The antidiuretic effect was maintained for approximately 3 wk, and returned to the preinjection level on

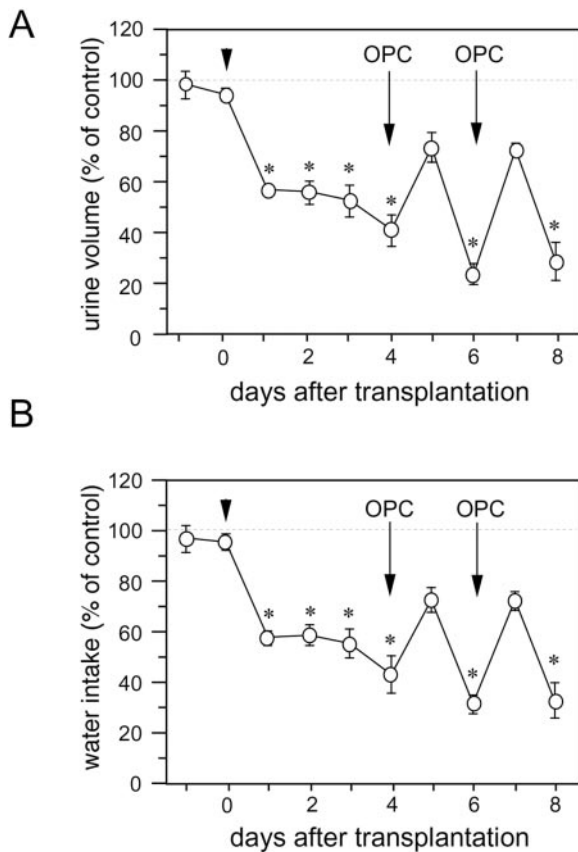


FIG. 7. The effect of OPC31260 on the antidiuresis induced by transplanted L6VP cells. On d 4 or 6 after L6VP transplantation, Brattleboro rats received OPC31260 administration. Daily urine volume (A) and water intake (B) were measured in both groups ($n = 3$ in each group). Data are shown as percentage of control L6-transplanted Brattleboro rats. Data are mean \pm SEM. *, $P < 0.05$ vs. control. Arrowheads represent the day of transplantation.

d 28. Food intake during the first 14 d after electroporation was similar in the pCAGGS-AVP/Fur and control (pCAGGS) rats (27.9 ± 0.5 vs. 25.9 ± 1.3 g/rat·d, respectively). Simple muscular injection of naked plasmid (pCAGGS-AVP/Fur) without electroporation failed to decrease urine volume (data not shown). Vasopressin expression in the muscle tissue receiving electroporation was confirmed by RT-PCR and protein analyses (Fig. 9, A and B). In the latter analysis, we observed substantial amounts of immunoreactive vasopressin in the muscle tissue 7 d after electroporation (384 ± 39 pg/g wet tissue), but not in the control (pCAGGS) rats (Fig. 9B). In addition, we observed a physiological concentration of plasma vasopressin in pCAGGS-AVP/Fur-introduced rats 7 d after electroporation (3.03 ± 0.66 pg/ml), compared with an almost undetectable level (0.06 ± 0.04 pg/ml) in the control rats (Fig. 9C). Collectively, we clearly demonstrated that nonendocrine cells such as myocytes can produce bioactive small peptide hormones like vasopressin *in vivo*.

Discussion

Gene therapies for supplying proteins to deficient patients are currently undergoing steady progress (33–35). In this

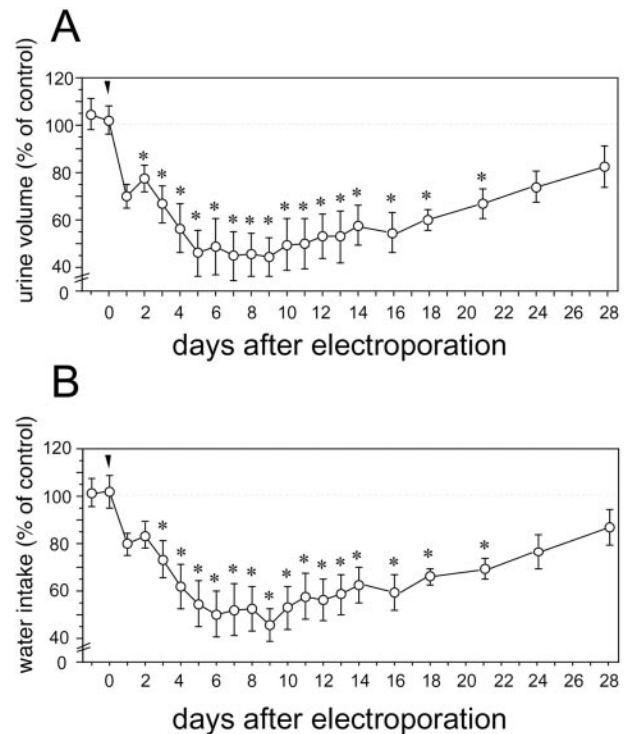


FIG. 8. Antidiuretic effect of vasopressin expressed in the skeletal muscle of Brattleboro rats. A and B, Direct introduction of pCAGGS/AVP/Fur or pCAGGS vector into the tibial and soleal muscles of Brattleboro rats by electroporation *in vivo* ($n = 4$ or 3 , respectively). Daily urine volume (A) and water intake (B) were measured in both groups (open circles, data are shown as % of control pCAGGS electroporated rats). Data are mean \pm SEM. *, $P < 0.05$ vs. control. Arrowheads represent the day of electroporation.

paper, we tried to apply a nonviral gene transfer technique for the replacement therapy of small peptide hormones like arginine vasopressin. Our data clearly show that bioactive vasopressin can be produced efficiently even in nonendocrine cells both *in vitro* and *in vivo* so that fibroblast- or myocyte-derived vasopressin is enough to substitute for the degenerative vasopressinergic neurons of CDI patients. When the modified furin-processible gene was introduced into skeletal muscle of the hereditarily vasopressin-deficient Brattleboro rat, polyuria was markedly improved, promising the feasibility of these techniques to gene therapy for human CDI. Furthermore, the successful production of processed bioactive peptide hormones in nonendocrine cells/tissues is applicable to the replacement therapy of other peptide hormones.

The vasopressin gene encodes preprovasopressin, which consists of a signal peptide, neurophysin II, and glycoprotein, as well as vasopressin. After the removal of the signal peptide, provasopressin is further processed into the three end products by neuroendocrine cell-specific endoprotease PC1/3 or PC2. Both enzymes associate with the processing of proopiomelanocortin (36), proinsulin (37), and proglucagon (38). In nonendocrine cells without these enzymes, appropriately processed mature vasopressin is not produced, even though the vasopressin gene is efficiently expressed (16). We showed that coexpression of PC1/3, but not PC2, facilitated the processing between vasopressin and neuro-

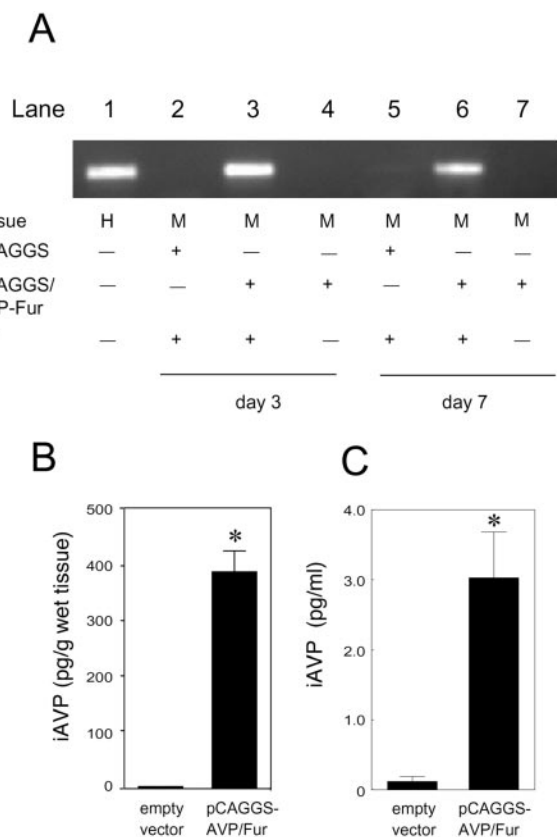


FIG. 9. A, Vasopressin mRNA expression in the electroporated muscle detected by RT-PCR. Amplified products from muscle tissues of DI rat (M), or from the hypothalamus of a normal Wistar rat (H) as a control, are shown. B, Local immunoreactive vasopressin (iAVP) content of muscular tissue 7 d after electroporation of pCAGGS/AVP/Fur or control plasmid (pCAGGS). C, Plasma vasopressin concentration in pCAGGS/AVP-Fur or control plasmid (pCAGGS)-electroporated rats on d 7 ($n = 4$ and 3 , respectively). Data are mean \pm SEM. *, $P < 0.05$ vs. empty plasmid-introduced group.

physin II, resulting in improved secretion of immunoreactive vasopressin of an appropriate size even in nonendocrine cells. Alternatively, we constructed a modified vasopressin gene, the protein product of which is made processible by the ubiquitous endoprotease furin. This strategy is also effective, producing vasopressin much more efficiently than the WT gene. In this approach, the immunoreactive vasopressin is bioactive as well, as confirmed by both *in vivo* and *in vitro* assays. Thus, small peptide hormones like vasopressin can be produced in nonsecretory cells by either technique, *i.e.* coexpression of the target protein with its processing enzyme, or modification of hormone precursor genes into a processible form. The latter strategy has already been successfully applied for insulin gene expression (39–41). In addition, our data suggest that PC1/3 is the enzyme mainly responsible for the processing between vasopressin and neurophysin II. The mRNA of PC1/3 is known to colocalize with vasopressin mRNA in the magnocellular neurons of the hypothalamus (13).

Successful clinical applications of gene therapy rely on efficiencies in gene delivery, simplicity, safety, and duration of expression. The advantages of nonviral vectors over viral vectors are lower toxicity, lower immunogenicity, simplicity of use, and ease of large-scale production (34). Electropora-

tion *in vivo* into skeletal muscle is more than 100-fold efficient compared with simple naked DNA injection (21), and successful gene delivery has been reported in a variety of cells and/or tissues (42–44). Moreover, skeletal muscle has the advantage of accessibility for gene delivery. The electroporation strategy in this study worked well and improved the polyuria of CDI rats for 3 wk. We performed electroporation with low-voltage and long-pulse currents, which is a highly efficient condition for gene transfer according to previous reports (21, 22). The duration of the effect of *in vivo* vasopressin expression was unexpectedly long, maintaining the improvement of polyuria for approximately 3 wk after a single electroporation procedure. Moreover, after the introduction of the expression vector, the plasma vasopressin concentration was within the physiological range, indicating that the myocyte-derived vasopressin can exert a similar bioactivity *in vivo* as does native vasopressin. Our data suggest that the expression of the processible form of vasopressin in skeletal muscle is a potential approach for long-term remission of CDI.

Implantation of L6VP cells exerted potent antidiuresis, but these cells were finally rejected with no immunosuppressive agents, suggesting that additional method(s) to prevent immunorejection would be necessary. Previous works have shown that the transplantation of bioengineered cells for supplying the desired gene products is a successful approach for gene therapy (2, 3, 45). For clinical application, the microencapsulation technique may be used for this purpose and also for preventing spreading of the transplanted cells (46). Alternatively, immunorejection may be avoided by use of host-derived myoblasts, fibroblasts, or even differentiated stem cells transfected *ex vivo* with therapeutic gene constructs and subsequent reimplantation (47–50).

Finally, we have recognized that diabetes insipidus is a convenient model system for developing gene/cell therapy. Vasopressin is known to be effective for causing antidiuresis with very low plasma concentration (0.5–5 μ M). The efficacy can be assessed easily, by the decrease in urine volume or the increase in urine osmolality, using the Brattleboro rat, or also probably the normal rat, if water loading is carried out. Furthermore, for clinical application, a relatively small amount of vasopressin is enough to decrease the daily urine volume to a convenient range. One remaining problem is that we cannot regulate the degree of plasma vasopressin when the vasopressin gene is constitutively expressed either in the transfected cells or in muscle. In the present study, we showed that the antidiuretic effect by expressed vasopressin was effectively inhibited by the selective vasopressin V2 receptor antagonist OPC31260, which is a nonpeptidic and orally effective agent (28, 29). Thus, the administration of V2 antagonists may be a useful approach to avoid water intoxication or regulate the urine volume under continuous vasopressin replacement. Overall, the strategies tested in this study using the DI rat will be helpful for future gene therapies for a variety of hormone deficiencies.

Acknowledgments

We wish to thank Prof. Sadao Yamaoka for providing Brattleboro rats, and Prof. Jun-ichi Miyazaki for providing a pCAGGS expression vector. We also thank NEPA GENE Co., Ltd. for the Square Electroporator.

Received March 25, 2003. Accepted September 25, 2003.

Address all correspondence and requests for reprints to: Yasumasa Iwasaki, M.D., Ph.D., Department of Clinical Pathophysiology, Nagoya University Graduate School of Medicine and Hospital, 65 Tsurumai-cho, Showa-ku, Nagoya 466-8550, Japan. E-mail: iwasakiy@med.nagoya-u.ac.jp.

This work was supported in part by a grant from Japanese Ministry of Health, Labor and Welfare (to Y.I.).

References

- Robertson GL 1976 The regulation of vasopressin function in health and disease. *Recent Prog Horm Res* 33:333–385
- Barr E, Leiden JM 1991 Systemic delivery of recombinant proteins by genetically modified myoblasts. *Science* 254:1507–1509
- Dhawani J, Pan LC, Pavlath GK, Travis MA, Lanctot AM, Blau HM 1991 Systemic delivery of human growth hormone by injection of genetically engineered myoblasts. *Science* 254:1509–1512
- Al-Hendy A, Hortelano G, Tannenbaum GS, Chang PL 1995 Correction of the growth defect in dwarf mice with non-autologous microencapsulated myoblasts—an alternate approach to somatic gene therapy. *Hum Gene Ther* 6:165–175
- Rivera VM, Ye X, Courage NL, Sachar J, Cerasoli Jr F, Wilson JM, Gilman M 1999 Long-term regulated expression of growth hormone in mice after intramuscular gene transfer. *Proc Natl Acad Sci USA* 96:8657–8662
- Schmale H, Richter D 1984 Single base deletion in the vasopressin gene is the cause of diabetes insipidus in Brattleboro rats. *Nature* 308:705–709
- Geddes BJ, Harding TC, Lightman SL, Uney JB 1997 Long-term gene therapy in the CNS: reversal of hypothalamic diabetes insipidus in the Brattleboro rat by using an adenovirus expressing arginine vasopressin. *Nat Med* 12:1402–1404
- Valtin H 1967 Hereditary hypothalamic diabetes insipidus in rats (Brattleboro strain). A useful experimental model. *Am J Med* 42:814–827
- Majzoub JA, Pappay A, Burg R, Habener JF 1984 Vasopressin gene is expressed at low levels in the hypothalamus of the Brattleboro rat. *Proc Natl Acad Sci USA* 17:5296–5299
- Blotner H 1958 Primary or idiopathic diabetes insipidus: a system disease. *Metabolism* 7:191–200
- Bergeron C, Kovacs K, Ezrin C, Mizzen C 1991 Hereditary diabetes insipidus: an immunohistochemical study of the hypothalamus and pituitary gland. *Acta Neuropathol (Berl)* 3:345–348
- Ivell R, Richter D 1984 Structure and comparison of the oxytocin and vasopressin genes from rat. *Proc Natl Acad Sci USA* 81:2006–2010
- Dong W, Seidel B, Marcinkiewicz M, Chretien M, Seidah NG, Day R 1997 Cellular localization of the prohormone convertases in the hypothalamic paraventricular and supraoptic nuclei: selective regulation of PC1 in corticotrophin-releasing hormone parvocellular neurons mediated by glucocorticoids. *J Neurosci* 17:563–575
- Coates LC, Birch NP 1998 Differential cleavage of provasopressin by the major molecular forms of SPC3. *J Neurochem* 70:1670–1678
- Zhou A, Webb G, Zhu X, Steiner DF 1999 Proteolytic processing in the secretory pathway. *J Biol Chem* 274:20745–20748
- Cwikel BJ, Habener JF 1987 Provasopressin-neurophysin II processing is cell-specific in heterologous cell lines expressing a metallothionein-vasopressin fusion gene. *J Biol Chem* 262:14235–14240
- Nakayama K 1997 Furin: a mammalian subtilisin/Kex2p-like endoprotease involved in processing of a wide variety of precursor proteins. *Biochem J* 327:625–635
- Aihara H, Miyazaki J 1998 Gene transfer into muscle by electroporation in vivo. *Nat Biotechnol* 16:867–870
- Mir LM, Bureau MF, Gehl J, Rangara R, Rouy D, Caillaud JM, Delaere P, Branellec D, Schwartz B, Scherman D 1999 High-efficiency gene transfer into skeletal muscle mediated by electric pulses. *Proc Natl Acad Sci USA* 96:4262–4267
- Rizzuto G, Cappelletti M, Maione D, Savino R, Lazzaro D, Costa P, Mathiesen I, Cortese R, Ciliberto G, Laufer R, La Monica N, Fattori E 1999 Efficient and regulated erythropoietin production by naked DNA injection and muscle electroporation. *Proc Natl Acad Sci USA* 96:6417–6422
- Somiari S, Glasspool-Malone J, Drabick JJ, Gilbert RA, Heller R, Jaroszeski MJ, Malone RW 2000 Theory and in vivo application of electroporative gene delivery. *Mol Ther* 2:178–187
- Wolff JA, Malone RW, Williams P, Chong W, Acsadi G, Jani A, Felgner PL 1990 Direct gene transfer into mouse muscle in vivo. *Science* 247:1465–1468
- Tokui M, Takei I, Tashiro F, Shimada A, Kasuga A, Ishii M, Ishii T, Takatsu K, Saruta T, Miyazaki J 1997 Intramuscular injection of expression plasmid DNA is an effective means of long-term systemic delivery of interleukin-5. *Biochem Biophys Res Commun* 233:527–531
- Tsurumi Y, Takeshita S, Chen D, Kearney M, Rossow ST, Passeri J, Horowitz JR, Symes JF, Isner JM 1996 Direct intramuscular gene transfer of naked DNA encoding vascular endothelial growth factor augments collateral development and tissue perfusion. *Circulation* 94:3281–3290
- Niwa H, Yamamura K, Miyazaki J 1991 Efficient selection for high-expression transfectants with a novel eukaryotic vector. *Gene* 108:193–199
- Zhou A, Bloomquist BT, Mains RE 1993 The prohormone convertases PC1 and PC2 mediate distinct endoproteolytic cleavages in a strict temporal order during proopiomelanocortin biosynthetic processing. *J Biol Chem* 268:1763–1769
- Iwasaki Y, Oiso Y, Saito H, Majzoub JA 1997 Positive and negative regulation of the rat vasopressin gene promoter. *Endocrinology* 138:5266–5274
- Yamamura Y, Ogawa H, Yamashita H, Chihara T, Miyamoto H, Nakamura S, Onogawa T, Yamashita T, Hosokawa T, Mori T 1992 Characterization of a novel aquaretic agent, OPC-31260, as an orally effective, nonpeptide vasopressin V2 receptor antagonist. *Br J Pharmacol* 105:787–791
- Fujisawa G, Ishikawa S, Tsuboi Y, Okada K, Saito T 1993 Therapeutic efficacy of non-peptide ADH antagonist OPC-31260 in SIADH rats. *Kidney Int* 44:19–23
- Nagasaki H, Yokoi H, Arima H, Hirabayashi Y, Ishizaki S, Tachikawa K, Murase T, Miura Y, Oiso Y 2002 Overexpression of vasopressin in the rat transgenic for the metallothionein-vasopressin fusion gene. *J Endocrinol* 173:35–44
- Oiso Y, Iwasaki Y, Kondo K, Takatsuki K, Tomita A 1988 Effect of the opioid kappa-receptor agonist U50488H on the secretion of arginine vasopressin. Study on the mechanism of U50488H-induced diuresis. *Neuroendocrinology* 48:658–662
- Ausiello DA, Hall DH, Dayer JM 1980 Modulation of cyclic AMP-dependent protein kinase by vasopressin and calcitonin in cultured porcine renal LLC-PK1 cells. *Biochem J* 186:773–780
- Anderson WF 1998 Human gene therapy. *Nature* 392:25–30
- Nishikawa M, Huang L 2001 Nonviral vectors in the new millennium: delivery barriers in gene transfer. *Hum Gene Ther* 12:861–870
- Barzon L, Bonaguro R, Palu G, Boscaro M 2000 New perspectives for gene therapy in endocrinology. *Eur J Endocrinol* 143:447–466
- Bloomquist BT, Eipper BA, Mains RE 1991 Prohormone-converting enzymes: regulation and evaluation of function using antisense RNA. *Mol Endocrinol* 5:2014–2024
- Davidson HW, Rhodes CJ, Hutton JC 1988 Intraorganellar calcium and pH control proinsulin cleavage in the pancreatic β cell via two distinct site-specific endopeptidases. *Nature* 333:93–96
- Rothenberg ME, Eilertson CD, Klein K, Zhou Y, Lindberg I, McDonald JK, Mackinnon RB, Noe BD 1995 Processing of mouse proglucagon by recombinant prohormone convertase 1 and immunopurified prohormone convertase 2 in vitro. *J Biol Chem* 270:10136–10146
- Yanagita M, Nakayama K, Takeuchi T 1992 Processing of mutated proinsulin with tetrabasic cleavage sites to bioactive insulin in the non-endocrine cell line, COS-7. *FEBS Lett* 311:55–59
- Gros L, Riu E, Montoliu L, Ontiveros M, Lebrigand L, Bosch F 1999 Insulin production by engineered muscle cells. *Hum Gene Ther* 10:1207–1217
- Lee HC, Kim SJ, Kim KS, Shin HC, Yoon JW 2000 Remission in models of type 1 diabetes by gene therapy using a single-chain insulin analogue. *Nature* 408:483–488
- Neumann E, Schaefer-Ridder M, Wang Y, Hofschneider PH 1982 Gene transfer into mouse lymphoma cells by electroporation in high electric fields. *EMBO J* 1:841–845
- Titomirov AV, Sukharev S, Kistanova E 1991 In vivo electroporation and stable transformation of skin cells of newborn mice by plasmid DNA. *Biochim Biophys Acta* 1088:131–134
- Heller R, Jaroszeski M, Atkin A, Moradpour D, Gilbert R, Wands J, Nicolau C 1996 In vivo gene electroinjection and expression in rat liver. *FEBS Lett* 89:225–228
- Gage FH 1998 Cell therapy. *Nature* 392:18–24
- Chang PL 1997 Microcapsules as bio-organs for somatic gene therapy. *Ann NY Acad Sci* 831:461–473
- Campbell AI, Zhao Y, Sandhu R, Stewart DJ 2001 Cell-based gene transfer of vascular endothelial growth factor attenuates monocrotaline-induced pulmonary hypertension. *Circulation* 104:2242–2248
- Suzuki K, Murtuza B, Smolenski RT, Sammut IA, Suzuki N, Kaneda Y, Yacoub MH 2001 Cell transplantation for the treatment of acute myocardial infarction using vascular endothelial growth factor-expressing skeletal myoblasts. *Circulation* 104:1207–1212
- Raymond HK, Thode S, Gage FH 1997 Application of ex vivo gene therapy in the treatment of Parkinson's disease. *Exp Neurol* 144:82–91
- Chen BF, Chang WC, Chen ST, Chen DS, Hwang LH 1995 Long-term expression of the biologically active growth hormone in genetically modified fibroblasts after implantation into a hypophysectomized rat. *Hum Gene Ther* 6:917–926

Endocrinology is published monthly by The Endocrine Society (<http://www.endo-society.org>), the foremost professional society serving the endocrine community.

Protection Against Autoimmune Myocarditis by Gene Transfer of Interleukin-10 by Electroporation

Kenichi Watanabe, MD, PhD; Mikio Nakazawa, PhD; Koichi Fuse, MD, PhD; Haruo Hanawa, MD, PhD; Makoto Kodama, MD, PhD; Yoshifusa Aizawa, MD, PhD; Toshio Ohnuki, PhD; Fumitake Gejyo, MD, PhD; Hiroki Maruyama, MD, PhD; Jun-ichi Miyazaki, MD, PhD

Background—Although immunosuppressive therapy for myocarditis has attracted a great deal of attention, its effectiveness is controversial. Interleukin (IL)-10 has a variety of immunomodulatory properties. Among the nonviral techniques for gene transfer *in vivo*, the direct injection of plasmid DNA into muscle is simple, inexpensive, and safe.

Methods and Results—We examined the applicability of murine IL-10 (mIL-10) gene transfer to the treatment of rats with experimental autoimmune myocarditis. Nine-week-old Lewis rats were inoculated with pig myosin (day 0). A plasmid vector expressing mIL-10 cDNA (800 μ g per rat) was transferred into the tibialis anterior muscles by electroporation 3 times (5 days before immunization and at days 4 and 13); control rats received empty plasmid. Electroporation increased the serum mIL-10 levels to >250 pg/mL. The 21-day survival rate in rats treated with mIL-10 cDNA was higher (15 of 15; 100%) than that of the control group (9 of 15; 60%). Furthermore, mIL-10 treatment significantly attenuated myocardial lesions and improved hemodynamic parameters.

Conclusions—These findings showed that gene transfer into muscle by electroporation *in vivo* is an effective means of delivery of IL-10 for the treatment of autoimmune myocarditis. (*Circulation*. 2001;104:1098-1100.)

Key Words: interleukins ■ myocarditis ■ gene therapy ■ immune system ■ cardiomyopathy

Human myocarditis can be classified into lymphocytic myocarditis and giant cell myocarditis according to histopathological findings. Giant cell myocarditis is a fatal disease, and survivors are more likely to develop dilated cardiomyopathy than patients with lymphocytic myocarditis.^{1,2} The efficiency of immunosuppressive therapy for this disease is controversial.^{1,2}

In a rat model in which myocarditis was induced by purified cardiac myosin, T cells were reported to play an important role in inducing myocarditis.³⁻⁵ Immune dysfunction associated with autoimmune disease may be related to an imbalance between T helper type 1 and 2 cells.⁶ The T helper type 2-associated cytokine interleukin (IL)-10 has a variety of immunomodulatory properties, including the inhibition of T helper type 1 cells and the production of proinflammatory cytokines.^{7,8} Recent reports have suggested that the immunosuppressive effects associated with IL-10 are effective in suppressing the rejection of transplanted organs and immune complex diseases, and clinical trials of IL-10 have been performed in patients with these disorders.^{9,10}

Electroporation has been widely used to introduce DNA into various types of cells *in vitro*. Gene transfer by electroporation *in vivo* has been effective for introducing DNA into mouse skin, chick embryos, rat liver, and murine melanoma and muscle.¹¹⁻¹³

We previously showed that gene transfer into muscles by electroporation *in vivo* can be used to deliver cytokines systemically.^{13,14} In the present study, we applied this method for the delivery of IL-10 in a rat model of autoimmune myocarditis.

Methods

Animals

Nine-week-old male Lewis rats were injected with the antigen-adjuvant emulsion in their foot pads according to the procedure described previously.³⁻⁵ The morbidity of experimental autoimmune myocarditis was 100% in rats immunized by this method.³⁻⁵ Throughout the studies, all animals were treated in accordance with the guidelines for animal experiments of our institute.⁵

Construction of Mouse IL-10 Expression Vector

Mouse IL-10 (mIL-10) cDNA cloned by polymerase chain reaction was inserted into the unique *Xho* I site between the cytomegalovirus immediate early enhancer-chicken β -actin hybrid promoter and rabbit β -globin poly A site of the pCAGGS expression plasmid.^{13,14} The resulting plasmid, pCAGGS-IL-10, was grown in *Escherichia coli* DH 5 α and prepared using plasmid purification columns (EndFree plasmid giga kit; Qiagen). The plasmid DNA was dissolved in a buffer

Received April 30, 2001; revision received July 17, 2001; accepted July 18, 2001.

From the Department of Clinical Pharmacology (K.W.) and the Department of Pharmacology (T.O.), Niigata College of Pharmacy; the Department of Medical Technology, School of Health Sciences, Niigata University School of Medicine (M.N.); the Division of Cardiology (K.F., H.H., M.K., Y.A.) and the Division of Clinical Nephrology and Rheumatology (F.G., H.M.), Niigata Graduate School of Medicine and Dental Science, Niigata, Japan; and the Department of Nutrition and Physiological Chemistry, Osaka University Graduate School of Medicine, Osaka, Japan (J.M.).

Correspondence to Kenichi Watanabe, MD, Department of Clinical Pharmacology, Niigata College of Pharmacy, Kamisin-ei-cho, Niigata, 950-2081, Japan. E-mail watanabe@niigata-pharm.ac.jp

© 2001 American Heart Association, Inc.

Circulation is available at <http://www.circulationaha.org>

(10 mmol/L Tris-HCl and 1 mmol/L EDTA; pH 8.0). The purified plasmid DNA was stored at -20°C and diluted to $4\ \mu\text{g}/\mu\text{L}$ with phosphate-buffered saline (pH 7.4) immediately before use.

Intramuscular DNA Injection and Electroporation

Rats were anesthetized with diethyl ether. Aliquots of $50\ \mu\text{L}$ of plasmid DNA (pCAGGS-IL-10 or control pCAGGS) at $4\ \mu\text{g}/\mu\text{L}$ in phosphate-buffered saline were injected 4 times (total amount of DNA was $800\ \mu\text{g}$ per rat) into the bilateral tibialis anterior muscles using a disposable insulin syringe with a 27-gauge needle.¹³ A pair of electrode needles with a gap of 5 mm were inserted into the muscle to a depth of 5 mm to encompass the DNA injection sites, and electrical pulses were delivered 4 times at 100 V using an electrical pulse generator (Electro Porator CUY21; TR Tech).¹³

Treatment Protocols

Protocol 1: Time Course of Changes in Serum mIL-10 Levels After Administration of mIL-10 Plasmid to Normal Rats

Single Administration of mIL-10 Plasmid

The mIL-10 expression plasmid pCAGGS-IL-10 was transferred once at a dose of $800\ \mu\text{g}$ per rat into the tibialis anterior muscles of normal Lewis rats ($n=5$) by electroporation *in vivo*, and the serum mIL-10 levels were monitored. The time course of changes in serum mIL-10 levels was examined on days 0, 2, 4, 6, 8, 10, and 14 after transfer of pCAGGS-IL-10 using an ELISA kit (Endogen).

Administration of mIL-10 Plasmid 3 Times

The mIL-10 plasmid was administered 3 times to normal rats ($n=5$). After the first injection of mIL-10 plasmid, second and third injections were added on days 10 and 20. Serum mIL-10 levels were examined on days 6, 16, and 26.

Protocol 2: Preventive Effects of mIL-10 Plasmid Administration in Myocarditis

Lewis rats were inoculated with pig myosin (day 0). The results of protocol 1 indicated that the serum levels of mIL-10 were enhanced to $>50\ \text{pg}/\text{mL}$ until day 10 after mIL-10 plasmid administration. pCAGGS-IL-10 (at a dose of $800\ \mu\text{g}$ per rat) was administered 3 times (5 days before immunization and on days 7 and 14) to rats (group IL-10; $n=15$), and controls received empty pCAGGS (group V; $n=15$). Lewis rats without any treatment were used as age-matched normal controls (group N; $n=10$).

Myocardial histopathology and hemodynamic parameters were examined on day 21 as described previously.⁵ Briefly, rats were anesthetized with 2% halothane in O_2 during surgical procedures, and then the halothane concentration was reduced to 0.5% to minimize hemodynamic effects. Mean blood pressure, central venous pressure, peak left ventricular pressure, left ventricular end-diastolic pressure, and dP/dt were recorded as described previously.⁵ The heart weight was measured, and the ratio of heart weight to body weight (g/kg) was calculated. After embedding in paraffin, several transverse sections were cut from the mid-ventricle slice and stained with hematoxylin-eosin and Azan-Mallory.

Statistical Analysis

Data are presented as mean \pm SEM. Statistical analysis between the groups was performed by one-way ANOVA followed by Tukey's method. Differences were considered significant at $P<0.05$.

Results

Protocol 1: Time Course of Changes in Serum mIL-10 Levels After Administration of mIL-10 Plasmid to Normal Rats

Single Administration of mIL-10 Plasmid

The levels of serum mIL-10 on days 2 ($126\pm 14\ \text{pg}/\text{mL}$), 4 ($308\pm 16\ \text{pg}/\text{mL}$), 6 ($320\pm 23\ \text{pg}/\text{mL}$), 8 ($192\pm 34\ \text{pg}/\text{mL}$), 10 ($82\pm 9\ \text{pg}/\text{mL}$), and 14 ($35\pm 8\ \text{pg}/\text{mL}$) were significantly higher (all $P<0.01$) than on day 0 (not detected). The level of

mIL-10 peaked on day 6. These mIL-10 levels were $>50\ \text{pg}/\text{mL}$ until day 10 and were greater than the peak value of serum rat IL-10 during the natural course of progression of myocarditis in this model ($42\pm 4\ \text{pg}/\text{mL}$ on day 27).

Administration of mIL-10 Plasmid 3 Times

The levels of serum mIL-10 on days 6, 16, and 26 were 332 ± 46 , 286 ± 48 , and $218\pm 42\ \text{pg}/\text{mL}$, respectively.

Protocol 2: Preventive Effects of mIL-10 Plasmid Administration in Myocarditis

Clinical Course in Rats with Myocarditis

Rats in the myosin-immunized group became ill and immobile on day 14. The 21-day survival rates in groups IL-10 and N were higher (15 of 15 and 10 of 10; 100%) than that in group V (9 of 15; 60%). Six rats in group V died between days 19 and 21, and all hearts from these rats showed extensive myocarditis and massive pericardial effusion.

Body Weight, Heart Weight, and Serum Levels of mIL-10

Body weights did not differ between rats in groups IL-10 and V. Heart weight and the heart weight to body weight ratio were significantly greater in group V ($1.62\pm 0.05\ \text{g}$ and $6.50\pm 0.23\ \text{g}/\text{kg}$, respectively) than those in groups IL-10 ($1.17\pm 0.02\ \text{g}$ and $4.80\pm 0.10\ \text{g}/\text{kg}$; both $P<0.01$) and N ($1.02\pm 0.02\ \text{g}$ and $2.45\pm 0.06\ \text{g}/\text{kg}$; both $P<0.01$).

Although serum levels of mIL-10 in both groups V and N were below the level of detection, that in group IL-10 was $125\pm 16\ \text{pg}/\text{mL}$ on day 21.

Hemodynamic Parameters

Central venous pressure and left ventricular end-diastolic pressure were significantly higher and mean blood pressure,

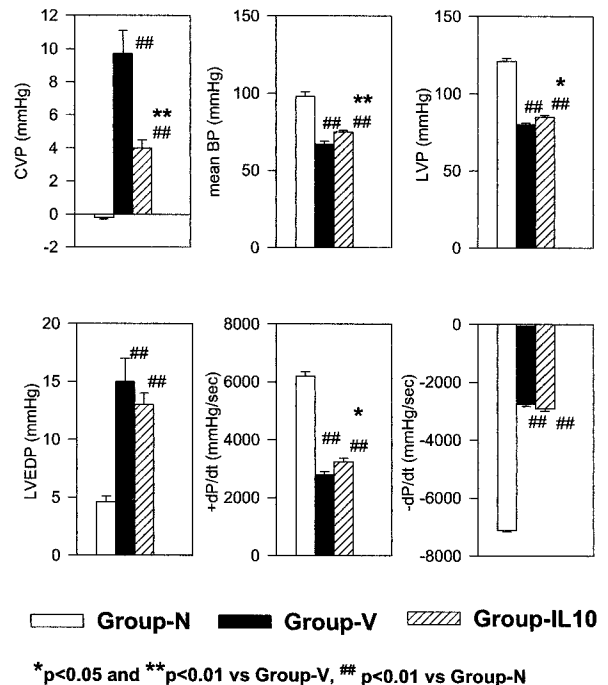


Figure 1. Effects of mIL-10 on hemodynamic parameters. Administration of mIL-10 improved central venous pressure (CVP), mean blood pressure (mean BP), peak left ventricular pressure (LVP) and $+dP/dt$. LVEDP indicates left ventricular end-diastolic pressure. There were 9 rats in groups V and N and 8 rats in group IL-10.

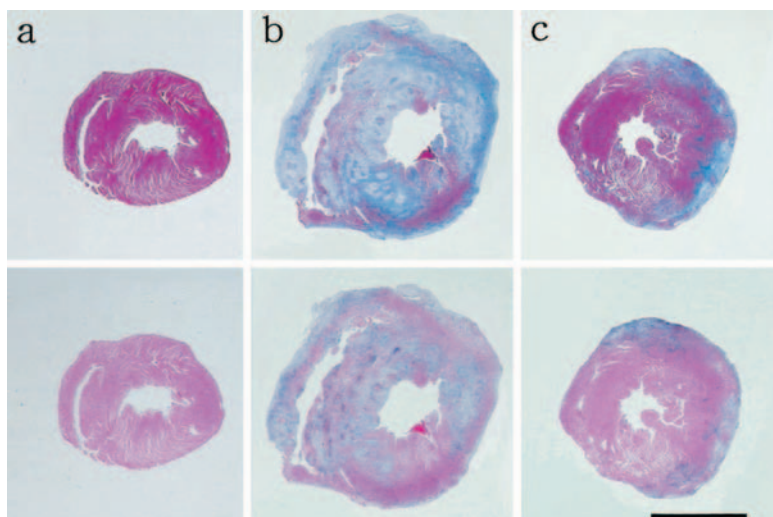


Figure 2. Effects of mIL-10 on myocardial infiltration and heart size. Figures show representative data for each group. Top, Azan-Mallory staining; bottom, hematoxylin-eosin staining. a, Group N; b, group V; and c, group IL-10. Scale bar is 5 mm.

left ventricular pressure, and dP/dt were lower in group V than in group N (all $P < 0.01$; Figure 1).

Central venous pressure was significantly lower and the mean blood pressure, left ventricular pressure, and +dP/dt were significantly higher in group IL-10 than group V. The left ventricular end-diastolic pressure and -dP/dt did not differ between groups IL-10 and V.

Quantitative Analysis of Myocardial Inflammation

Although massive pericardial effusion was observed in most of the surviving rats in group V on day 21, there was little effusion in group IL-10.

Figure 2 shows representative photographs of thin sections stained with hematoxylin-eosin and Azan-Mallory. The normal heart did not show inflammation, but hearts in group V rats showed massive inflammation (stained light blue, which indicates inflammation). The area of myocarditis in group IL-10 was smaller than that in group V (Figure 2).

Discussion

In the present study using a rat model of autoimmune myocarditis, we examined the effects of IL-10 on the prevention of myocarditis. We found that IL-10 reduced heart weight and myocardial inflammation and increased positive dP/dt.

Human dilated cardiomyopathy is thought to have a variety of causes. Cardiac myosin-induced autoimmune myocarditis, which is not exclusively related to viral infection, develops clinicopathologically to resemble dilated cardiomyopathy in the chronic phase. Thus, the present results provided some insight into the effectiveness of IL-10 treatment against not only myocarditis but also dilated cardiomyopathy after myocarditis.

Gene transfer by electroporation, which uses plasmid DNA as a vector, has several advantages over transfer using viral vectors. A large quantity of highly purified plasmid DNA can be obtained easily and inexpensively. Gene transfer can be repeated without apparent immunological responses to the DNA vector. There is less likelihood of recombination events with the cellular genome, eliminating the risk of insertional mutagenesis that is associated with the use of viral vectors.

The present study indicated that delivery of IL-10 expression plasmid DNA by electroporation provided marked cardioprotection in a rat model of autoimmune myocarditis and may help clarify the mechanisms of the protective effect of IL-10 when used for the treatment of myocarditis in humans.

Acknowledgments

This research was supported by grants from the Ministry of Education, Science, Sports and Culture of Japan and the Promotion and Mutual Aid Corporation for Private Schools of Japan.

References

- Dec GW, Palacios IF, Fallon JT, et al. Acute myocarditis in the spectrum of acute dilated cardiomyopathies: clinical features, histologic correlates, and clinical outcome. *N Engl J Med*. 1985;312:885–890.
- Davidoff R, Palacios I, Southern J, et al. Giant cell versus lymphocytic myocarditis: a comparison of their clinical features and long-term outcomes. *Circulation*. 1991;83:953–961.
- Kodama M, Matsumoto Y, Fujiwara M, et al. A novel experimental model of giant cell myocarditis induced in rats by immunization with cardiac myosin fraction. *Clin Immunol Immunopathol*. 1991;57:250–262.
- Kodama M, Hanawa H, Saeki M, et al. Rat dilated cardiomyopathy after autoimmune giant cell myocarditis. *Circ Res*. 1994;75:278–284.
- Watanabe K, Ohta Y, Nakazawa M, et al. Low dose carvedilol inhibits progression of heart failure in rats with dilated cardiomyopathy. *Br J Pharmacol*. 2000;130:1489–1495.
- Liblau RS, Singer SM, McDevitt HO. Th1 and Th2 CD4+ T cell in the pathogenesis of organ-specific autoimmune diseases. *Immunol Today*. 1995;16:34–38.
- Fiorentino DF, Bond MW, Mosmann TR. Two types of mouse T helper cell, IV: Th2 clones secrete a factor that inhibits cytokine production by Th1 clones. *J Exp Med*. 1989;170:2081–2095.
- Lentsch AB, Shanley TP, Sarma V, et al. In vivo suppression of NF-kappa B and preservation of I kappa B alpha by interleukin-10 and interleukin-13. *J Clin Invest*. 1997;100:2443–2448.
- Shanley TP, Schmal H, Friedl HP, et al. Regulatory effects of intrinsic IL-10 in IgG immune complex-induced lung injury. *J Immunol*. 1995;154:3454–3460.
- Nishio R, Matsumori A, Shioi T, et al. Treatment of experimental viral myocarditis with interleukin-10. *Circulation*. 1999;100:1102–1108.
- Heller R, Jaroszeski M, Atkin A, et al. In vivo electroinjection and expression in rat liver. *FEBS Lett*. 1996;389:225–228.
- Rols MP, Delteil C, Golzio M, et al. In vivo electrically mediated protein and gene transfer in murine melanoma. *Nat Biotechnol*. 1998;16:168–171.
- Aihara H, Miyazaki J. Gene transfer into muscle by electroporation in vivo. *Nat Biotechnol*. 1998;16:867–870.
- Maruyama H, Sugawa M, Moriguchi Y, et al. Continuous erythropoietin delivery by muscle-targeted gene transfer using in vivo electroporation. *Hum Gene Ther*. 2000;11:429–437.

Skeletal muscle targeting *in vivo* electroporation-mediated HGF gene therapy of bleomycin-induced pulmonary fibrosis in mice

Yukio Umeda^{1,*}, Tsutomu Marui^{1,*}, Yukihiro Matsuno¹, Koyo Shirahashi¹, Hisashi Iwata¹, Hisato Takagi¹, Kunio Matsumoto², Toshikazu Nakamura², Atsushi Kosugi³, Yoshio Mori¹ and Hirofumi Takemura¹

¹Advanced Surgery, Department of Organ Pathobiology, Gifu University School of Medicine, Gifu, Japan;

²Molecular Regenerative Medicine, Course of Advanced Medicine, Osaka University Graduate School of Medicine, Suita, Osaka, Japan and ³School of Allied Health Sciences, Faculty of Medicine, Osaka University, Suita, Osaka, Japan

Lung fibrosis is a common feature of interstitial lung diseases, and apoptosis and fibrinogenesis play critical roles in its formation and progression. Hepatocyte growth factor (HGF) is one of the ideal therapeutic agents for prevention of lung fibrosis because of its antiapoptotic and fibrinolytic effects. The aim of this study is to establish nonviral HGF gene therapy of bleomycin-induced lung fibrosis avoiding the viral vector-related side effects. C57BL/6 mice were injected with 3.0 mg/kg body weight of bleomycin intratracheally. Following bleomycin injection, 50 μ l of pUC-HGF (1 mg/ml) was injected into each of the quadriceps muscle. Immediately after plasmid injection, *in vivo* electroporation was performed with pulse generator. Skeletal muscle-targeting electroporation induced transgene expression on day 1 and persisted for 4 weeks, and human HGF was also detected in the lung. In mice transferred with HGF, pathological score (1.0 ± 0.3 vs 3.2 ± 0.6), TUNEL-positive cell index (4.5 ± 1.1 vs 14.2 ± 3.1), and hydroxyproline content (9.0 ± 1.3 vs 14.4 ± 5.1 μ mol/g) were significantly reduced compared with the control. Furthermore, survival rate of HGF mice was significantly improved compared with the control. Our data indicate that HGF gene therapy with a single skeletal muscle-targeting electroporation has a therapeutic potential for bleomycin-induced lung fibrosis and this strategy can be applied as a practical gene therapy protocol for various organs.

Laboratory Investigation (2004) 84, 836–844, advance online publication, 3 May 2004; doi:10.1038/labinvest.3700098

Keywords: lung fibrosis; hepatocyte growth factor (HGF); gene therapy; *in vivo* electroporation

Pulmonary fibrosis is a common feature of interstitial pulmonary diseases. These disorders are progressive and refractory to current therapy and the limited fundamental therapeutic options are available to date.¹ A number of animal models and therapeutic agents were developed to explore the possibility of a new fundamental strategy against pulmonary fibrosis. Bleomycin-induced pneumopathy is a well-established model of pulmonary fibrosis, and the acute toxicity of bleomycin is characterized as the DNA damage of pulmonary

tissue, which results in apoptosis.² Following the induction of apoptosis, immunological mechanisms including the further induction of apoptosis are also involved in the progression of the bleomycin-induced pulmonary fibrosis.³

On the other hand, hepatocyte growth factor (HGF) is mitogenic and antiapoptotic factor for alveolar and bronchial epithelial cells. It also stimulates the migration and morphogenesis of those cells as reported in the previous *in vitro* studies.^{4,5} Yaekashiwa *et al*⁶ demonstrated that continuous systemic injection of recombinant HGF suppressed pulmonary fibrosis induced by bleomycin in the mice model. HGF had significant effect when it was administered simultaneously or subsequently to bleomycin treatment.⁶ Although these studies suggested the therapeutic potential of recombinant HGF for bleomycin-induced pulmonary fibrosis, the feasibility of HGF gene transfer has not

Correspondence: Dr Y Umeda, MD, PhD, Advanced Surgery, Department of Organ Pathobiology, Gifu University, 40 Tsukasamachi, Gifu 5008705, Japan.
E-mail: umeda@cc.gifu-u.ac.jp

*YU and TM equally contributed to this paper.

Received 21 October 2003; revised 15 February 2004; accepted 17 February 2004; published online 3 May 2004

been fully explored. When delivered to the lung *in vivo*, in addition to the innate immune response or nonspecific inflammation, cellular and humoral immune responses are especially critical issues in the use of viral vectors. Furthermore, pathologically abnormal lungs present disease-specific barriers that can limit gene transfer.⁷

In current clinical gene therapy, viral vector-mediated gene transfer is the most popular gene delivery system. On the other hand, serious concerns regarding the possibility of insertional mutagenesis and induction of the host immune response limit their clinical desirability. When a retroviral vector-mediated gene transfer was used, an anti-hypertensive gene was transmitted to the offspring and integrated into its genome.⁸ In liver-directed clinical gene therapy, adenoviral vector-mediated gene transfer induced fulminant hepatic failure that lead to mortality.⁹ Adenoassociate virus (AAV) vector have been found to be efficient for transducing nonproliferating cells and is considered to be nonpathogenic. Gene delivery by AAV vector also appears to be the least immunogenic of the viral vector systems. However, a major problem associated with the use of AAV vector has been the difficulty in producing large quantities of high-titer stock.

Previously, to avoid these viral-vector related side effects and complexity of viral gene transfer, we developed nonviral gene gun-mediated gene transfer^{10–12} and *in vivo* electroporation.¹³ However, these nonviral gene transfer methods also induced infiltration of inflammatory cells and mechanical damage in targeted organs. Clinically, these nonviral gene transfer-related side effects in diseased organs are also critical.

We hypothesized that these nonviral gene transfer-related side effects would be avoided with the use of nondiseased-organ-targeting gene transfer. Especially in lung disease, as a result of skeletal muscle targeting gene transfer, secreted transgene product would reach the lung through the bloodstream with a certain concentration. Therefore, we investigated the possibility of the *in vivo* electroporation-mediated HGF gene transfer targeting skeletal muscle for bleomycin-induced pulmonary fibrosis in current study.

Materials and methods

Construction of Plasmid DNA

Human HGF cDNA (2.2 kb) was inserted between the *EcoRI* and *NotI* sites of the pUC-SR alpha expression vector plasmid.¹⁴ In this plasmid, transcription of HGF cDNA was under the control of the SR alpha promoter. pCAGGS-EGFP was generated as a control vector using the modified pCAGGS expression vector.¹⁵

Animal Model of Pulmonary Fibrosis

Male pathogen-free C57BL/6 mice, 8 weeks old, were obtained from Japan SLC (Shizuoka, Japan). After measurement of their body weight, the animals were anesthetized with intraperitoneal injection of pentobarbital sodium (Dainippon Pharmaceutical, Osaka, Japan), and the trachea was exposed following a cervical incision. Bleomycin (3.0 mg/kg of body weight, Nippon Kayaku, Tokyo, Japan) was dissolved in 50 μ l of sterile saline and then injected intratracheally with a 30-gauge needle.

In Vivo Electroporation-mediated Gene Transfer

Following bleomycin treatment, the bilateral quadriceps muscles were exposed by bilateral longitudinal incisions of the thigh. A volume of 50 μ l of pUC-HGF (1 mg/ml) was injected into each of the quadriceps muscle with 30-gauge needle. Immediately after intramuscular injection of pUC-HGF, the muscle was held by an electrode (Figure 1a) and *in vivo* electroporation was performed with pulse generator (Square Electroporator CUY 21; NEPA GENE, Chiba, Japan). The voltage, pulse length, and number of pulses of electroporation were 40 V, 50 ms, and 18 times, respectively. A total of 49 mice were transferred with pUC-HGF, and another 49 mice were transferred with pCAGGS-EGFP as the control. In all, 25 mice of each treatment group were served for survival analysis until 28 days after bleomycin injection and *in vivo* electroporation. Six of residual 24 mice of each group were killed on 1, 3, 5, and 7 days after bleomycin injection and *in vivo* electroporation. Then, gene expression of HGF or green fluorescent protein (GFP), collagen content of the lung, and histological findings including the apoptosis were evaluated.

Detection of GFP and Human HGF Expression

The right quadriceps muscle and the left lobe of the lung were excised then GFP expression was detected with fluorescent stereomicroscopy. The left quadriceps muscle and the right upper lobe of the lung were excised and homogenized on ice after dilution with an adequate volume of human HGF extraction buffer (Institute of Immunology, Tokyo, Japan). After centrifugation, the supernatant was collected and stored at -80°C until assay. The concentration of human HGF was determined by means of enzyme-linked immunosorbent assay (ELISA) using anti-human HGF monoclonal antibody (Institute of Immunology, Tokyo, Japan). The antibody used in this study reacts specifically with human HGF and has little crossreactivity with mouse endogenous HGF.

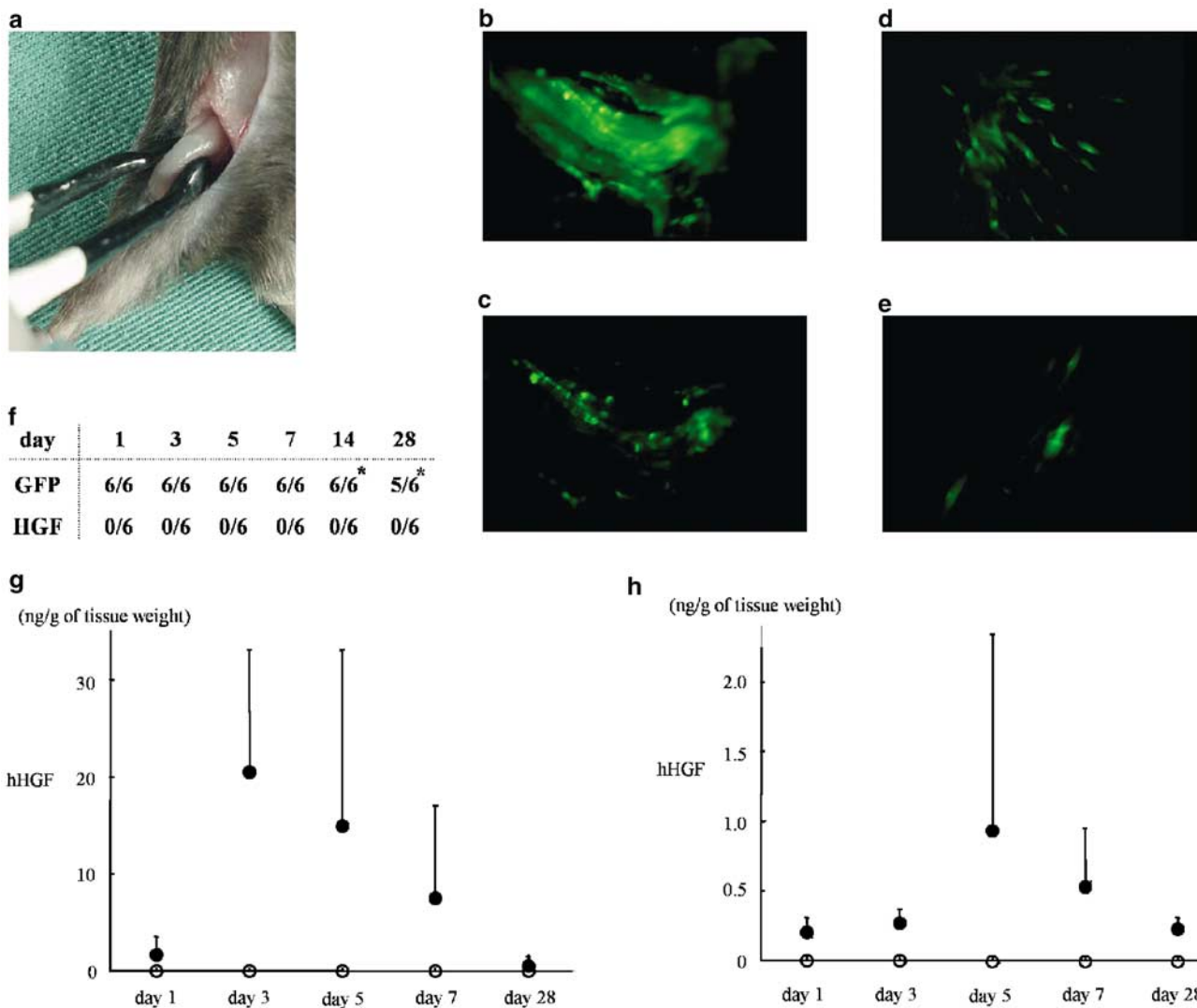


Figure 1 (a) Procedure of the skeletal muscle-targeting *in vivo* electroporation following intramuscular injection of plasmid DNA. (b–e) Expression of GFP in the quadriceps muscle at day 1 (b), 5 (c), 7 (d), and 28 (e). Panel f represents the number of GFP positive mice. Asterisk (*) indicates the data from bleomycin-untreated mice. (g and h) Concentration of human HGF in the unilateral quadriceps muscle (g) or lung (h) at days 1, 3, 5, 7, 14, and 28; (●) human HGF level of mice transferred with pUC-HGF; (○) human HGF level of mice transferred with pCAGGS-EGFP. Each plot represents the mean value from six mice.

Histological Analysis of *In Vivo* Electroporation-Induced Tissue Damage

To evaluate the tissue damage related to the *in vivo* electroporation, the right quadriceps muscle was fixed with 10% formaldehyde after the fluorescent stereomicroscopy for GFP expression analysis. The tissue was embedded in paraffin, and 4 μ m section of the quadriceps muscle was stained with hematoxylin–eosin.

Histological Analysis for Bleomycin-Induced Pulmonary Fibrosis

The left lobe of the lung was obtained after the fluorescent stereomicroscopy for GFP expression

analysis. After perfusion of the lung sample with phosphate-buffered saline solution (PBS), lung tissue was fixed by instilling 10% formaldehyde and embedded in paraffin. A 4 μ m section of the lung was used for Masson's trichrome staining. The section was reviewed under CCD microscopy (CCD; DP-70 (Olympus, Tokyo, Japan), microscope; Optiphot-2 (Nikon, Tokyo, Japan), objective lens; $\times 20$, adapter lens; $\times 0.45$, display size; 21"). The extent of pulmonary fibrosis was evaluated according to the scoring system of Ashcroft *et al.*¹⁶ A score ranging from 0 (normal lung) to 8 (total fibrosis) was assigned for each of the five microscopic fields. The mean score of all fields was taken as the fibrosis score of lung section.

Evaluation of Lung Collagen Content by Hydroxyproline Assay

The right lower lobe of the lung was excised and its hydroxyproline was measured. Briefly, after acid hydrolysis of the lung with 6 N HCl at 110°C for 14 h in a sealed glass tube, hydroxyproline content was determined using high-performance liquid chromatography.

Quantification of Apoptosis in Lung Tissue by Terminal Deoxynucleotidyltransferase dUTP Nick End Labeling

Terminal deoxynucleotidyltransferase dUTP nick end labeling (TUNEL) in the left lobe of the lung was performed with an *in situ* apoptosis detection kit (Takara, Shiga, Japan) according to the manufacturer's protocol. The number of TUNEL-positive signals was counted in five fields under CCD microscopy. Apoptotic cell index was presented as the number of TUNEL-positive cells per 100 total cells.

Statistical Analysis

Data are expressed as mean \pm s.d. The statistically significant difference between treatments was assessed using a one-way analysis of variance followed by a parametric Student's *t*-test. Survival rates were estimated from survival curves based on the Kaplan–Meier method and compared with the Mantel–Cox log rank test. A *P*-value of less than 0.05 was considered significant.

Results

In Vivo Electroporation-mediated GFP Gene Expression

To confirm the efficacy of gene transfer by skeletal muscle-targeting *in vivo* electroporation, we detected GFP expression under fluorescent stereomicroscopy. The expression of GFP was exclusively detected along the muscle fiber of enhanced GFP (EGFP)-transferred quadriceps muscle on the day after electroporation and persisted for 4 weeks (Figure 1b–f). Although GFP expression at day 28 was observed in five of six mice transferred with EGFP, the intensity of GFP in the quadriceps muscle at day 28 was slightly reduced compared with that measured in the early days. GFP expression was not detected in the HGF-transferred mice nor the other organs including the lungs of EGFP-transferred mice.

In Vivo Electroporation-mediated HGF Gene Expression

The expression of human HGF was detected in the quadriceps muscle of HGF-transferred mice from the day after *in vivo* electroporation to day 28 using human HGF-specific ELISA (Figure 1g). Concentration of human HGF in the unilateral quadriceps muscle was peaked at day 3 (20.37 ± 12.69 ng/g of tissue weight) and gradually decreased until day 28 (0.49 ± 1.01 ng/g of tissue weight). Although human HGF in the lung was also detected in the HGF-transferred mice and peaked at day 5 (0.93 ± 1.41 ng/g of tissue weight), its concentration

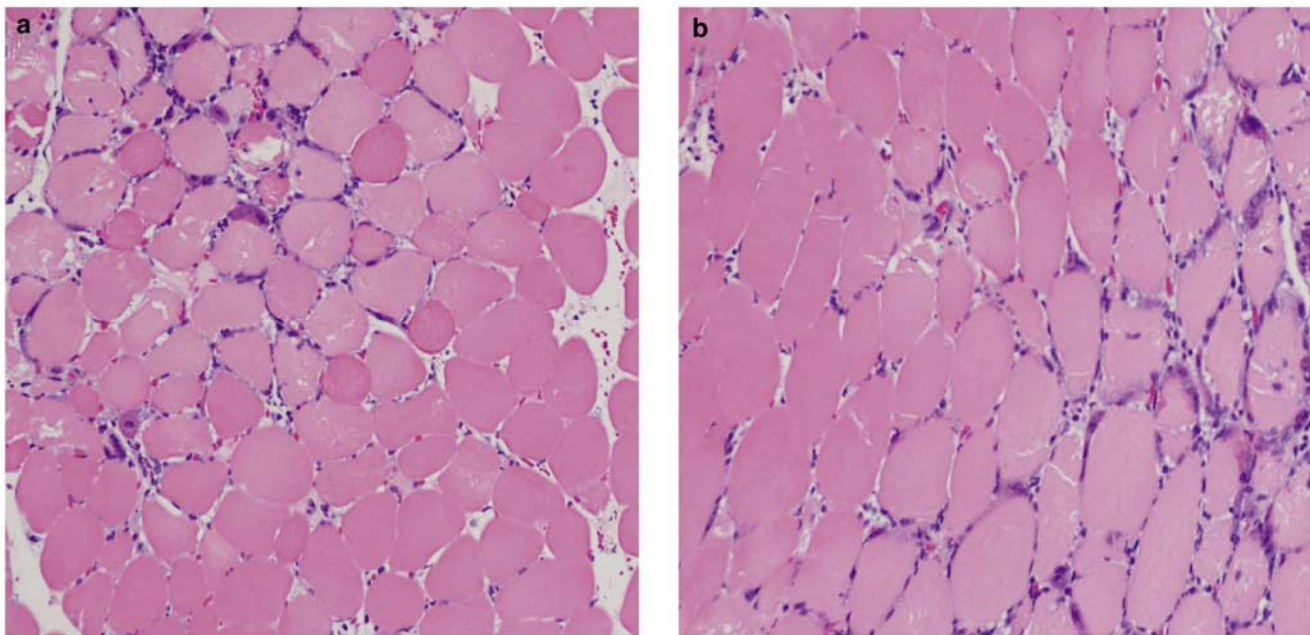


Figure 2 Histological damage of the quadriceps muscle induced by *in vivo* electroporation in GFP (a) or HGF (b)-transferred mice (hematoxylin–eosin staining).

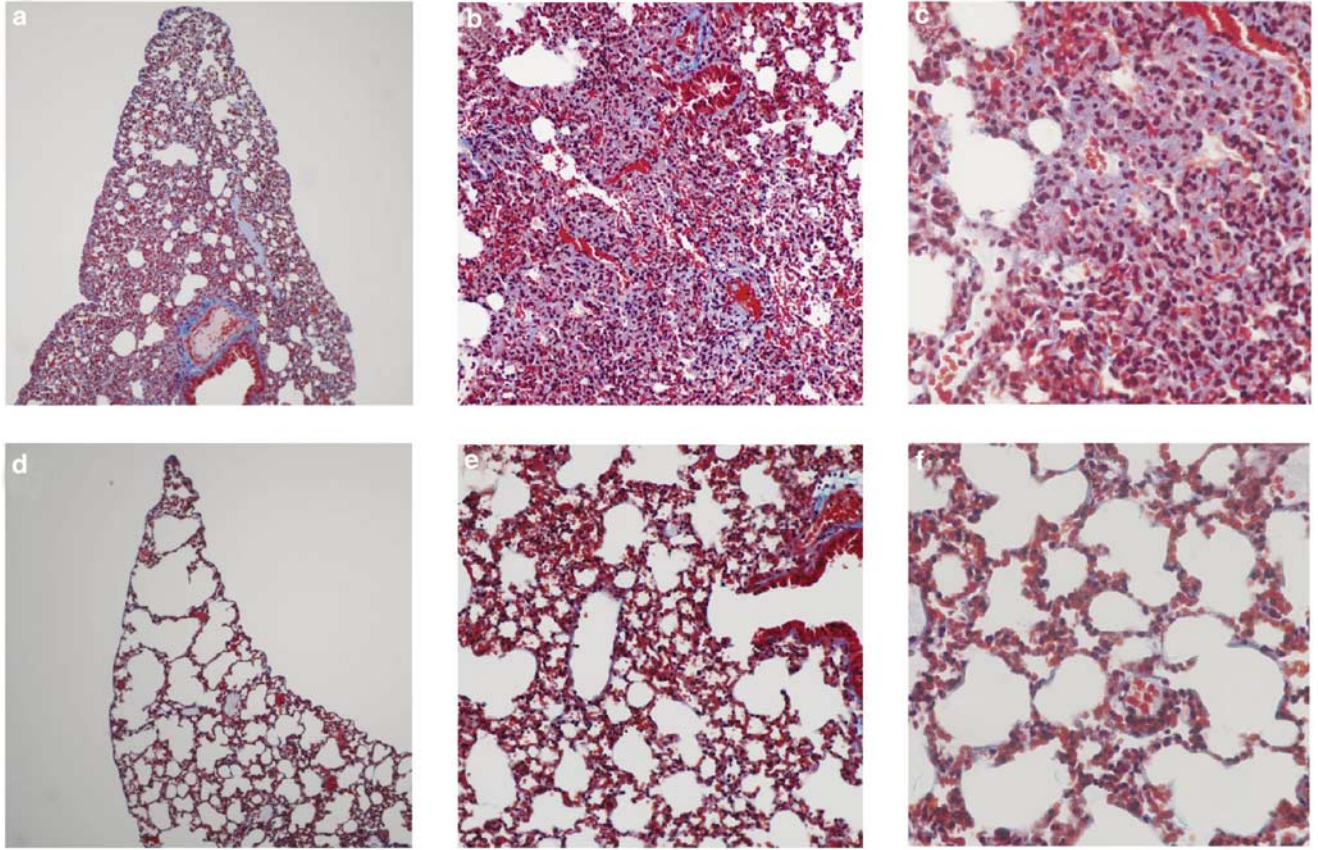


Figure 3 (a–f) Lung sections of mice treated with bleomycin (Masson trichrome staining). (a–c) Lung sections of mice transferred with pCAGGS-EGFP at day 7. (d–f) Lung sections of mice transferred with pUC-HGF at day 7.

was significantly lower than that in the quadriceps muscle (Figure 1h). Throughout this experiment, human HGF was not detected in the EGFP-transferred mice (Figure 1g, h).

Effect of *In Vivo* Electroporation on the Skeletal Muscle

Histologically, skeletal muscle-targeting *in vivo* electroporation induced minimal damage of the skeletal muscle fiber and mild degree of influx of inflammatory cells (Figure 2a, b). However, no dysfunction of the lower limb was observed in either group.

Effect of HGF Gene Transfer on Bleomycin-induced Pulmonary Fibrosis

Histologic finding in control mice showed increased cellularity and severe fibrotic changes. However, those changes were minimum in the mice injected with HGF. The fibrotic change of the lungs was assessed by the Ashcroft's numerical score at day 7. The scores in the bleomycin-injected mice transferred with GFP (Figure 3a–c) and HGF (Figure 3d–f) were 3.2 ± 0.6 and 1.0 ± 0.3 , respectively (Figure 4a, $P < 0.01$).

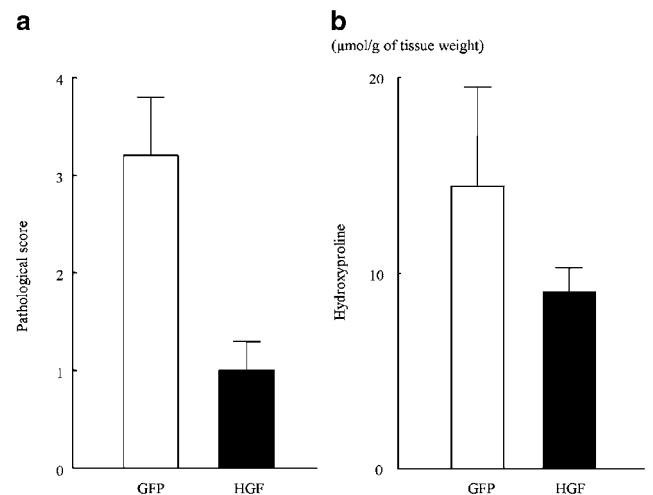


Figure 4 (a) Assessment of lung fibrosis using the Ashcroft's criteria for grading lung fibrosis at day 7. (b) Assessment of lung collagen content using hydroxyproline assay at day 7.

Effect of HGF Gene Transfer on Hydroxyproline Content of Bleomycin-injected Lung

Collagen content of the bleomycin-injected lung was assessed by the hydroxyproline assay. There was a

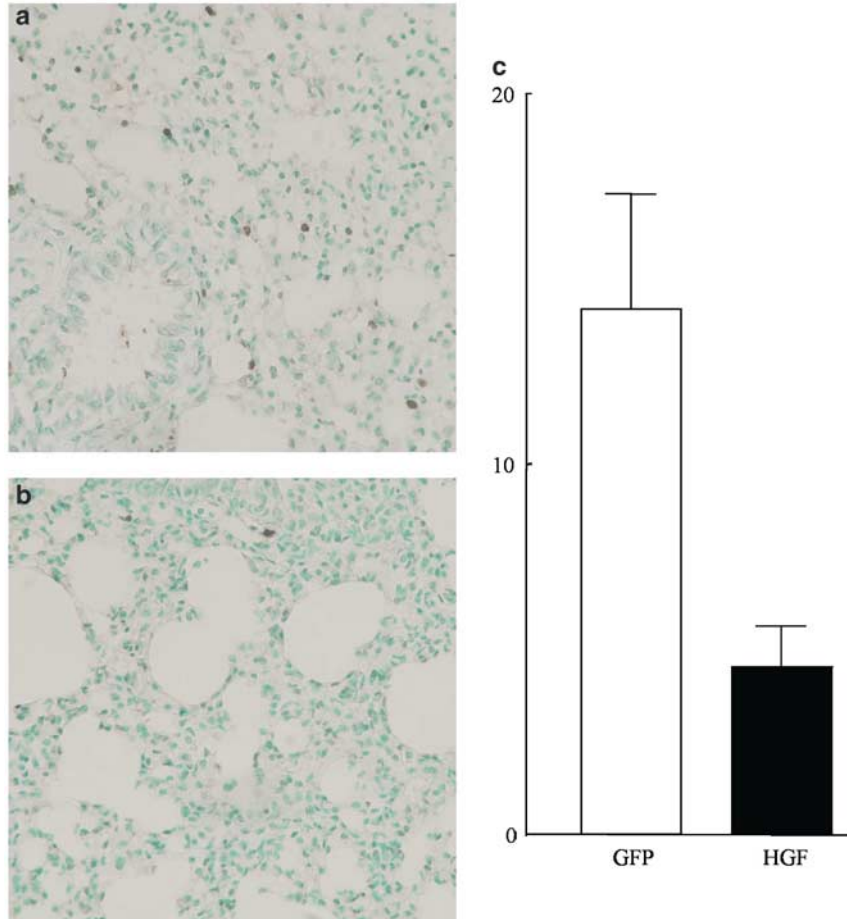


Figure 5 (a and b) Lung sections of mice treated with bleomycin (TUNEL staining). (a) Lung sections of mice transferred with pCAGGS-EGFP at day 5. (b) Lung sections of mice transferred with pUC-HGF at day 5. (c) Apoptotic cell index at day 5 was presented as the number of TUNEL-positive cells per 100 total cells.

significant decrease in lung hydroxyproline content in mice transferred with HGF ($9.0 \pm 1.3 \mu\text{mol/g}$ of tissue weight) compared with that in control mice ($14.4 \pm 5.1 \mu\text{mol/g}$ of tissue weight) at day 7 (Figure 4b, $P < 0.05$).

Effect of HGF Gene Transfer on Apoptosis in Bleomycin-injected Lung

Apoptotic cell index in bleomycin-injected lungs was significantly reduced in mice transferred with HGF (4.5 ± 1.1) compared with GFP (14.2 ± 3.1) at day 5 (Figure 5a–c, $P < 0.0001$).

Effect of HGF Gene Transfer on Survival after Bleomycin Injection

In total, 25 mice transferred with HGF after bleomycin treatment and 25 mice with GFP were served for survival analysis. Within 28 days, three of the mice with HGF and 20 with GFP had died. The Mantel–Cox log rank test showed that the survival

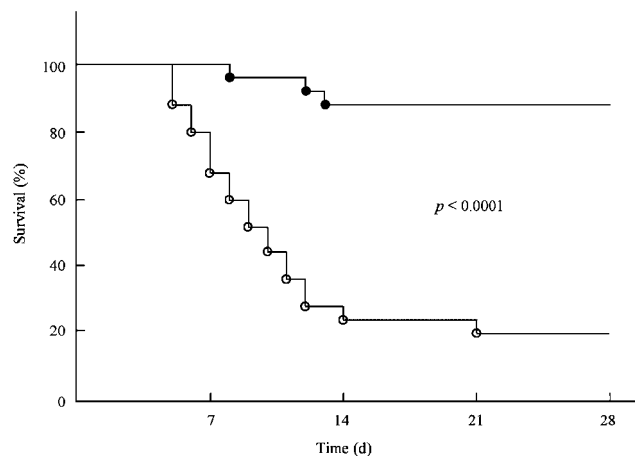


Figure 6 Survival of the bleomycin-treated mice: (●) mice transferred with pUC-HGF and (○) mice transferred with pCAGGS-EGFP. Survival curves were presented as a Kaplan–Meier plot. Mantel–Cox log rank test was used for comparison of survival curves.

rate of mice with HGF was significantly improved compared with that of control mice (Figure 6, $P < 0.0001$).

Discussion

HGF¹⁷ is a multipotent growth factor that acts as mitogen,¹⁴ motogen,¹⁸ and morphogen¹⁹ on various epithelial cells. Furthermore, HGF also has an anti-apoptotic effect on these cells²⁰ and fibrinolytic activity via upregulating urokinase-type plasminogen activator expression.^{21,22} Therefore, HGF has been obtained as a protective agent for a variety of organ disorders, such as liver cirrhosis,²³ intestinal ischemia,²⁴ myocardial ischemia,²⁵ and acute renal failure.²⁶

On the other hand, pulmonary fibrosis is the most common feature of interstitial pulmonary diseases and this disorder is progressive and refractory to current therapy. Limited fundamental therapeutic options are available to date.¹ A number of animal models and therapeutic agents were developed to explore the possibility of a new fundamental strategy against pulmonary fibrosis. Bleomycin-induced pneumopathy is a well-established model of pulmonary fibrosis. Acute toxicity of bleomycin is characterized as the DNA damage of pulmonary tissue, which results in apoptosis.² As found in bleomycin-treated mice,²⁷ Fas expression in bronchiolar and alveolar epithelial cells and upregulation of Fas ligand (FasL) expression are also found in clinical idiopathic pulmonary fibrosis patients.²⁸ Furthermore, an activation of apoptotic pathway was found in acute respiratory distress syndrome (ARDS),²⁹ or other experimental models, such as lipopolysaccharide,^{30,31} hyperoxia,^{32,33} asbestos,³⁴ and ischemia/reperfusion-induced lung injury.³⁵ Thus, apoptosis is a common feature found in both clinical and experimental models of lung injury. Following the acute toxicity of bleomycin, immunological mechanisms by T cells, its cytokines and natural killer cells also concern the progression of lung fibrosis.^{3,36,37} In concurrence with these processes, extravasation of plasma through hyperpermeable vasculatures and injured alveolar walls occurs and tissue factor triggers the coagulation cascade, leading to fibrin deposition.³⁸ Fibrin matrix serves as a scaffold in which fibroblasts migrate and induce collagen deposition.

From the therapeutic point of view, suppressions of apoptosis and fibrinogenesis are critical in prevention of the onset and progression of lung fibrosis. As HGF has both antiapoptotic and fibrinolytic potential as described above, HGF is one of the ideal therapeutic agents for lung fibrosis. Yaekashiwa *et al*⁶ reported that systemic injection of recombinant HGF suppressed pulmonary fibrosis induced by bleomycin in a mice model. Although their study suggested the therapeutic potential of HGF for bleomycin-induced pulmonary fibrosis, relatively high dose and continuous administration of recombinant HGF were required to induce those therapeutic effects. Since HGF has a short half-life ($T_{1/2}$ 3–5 min), HGF gene therapy would be desirable from a clinical point of view.

In current clinical gene therapy, viral vector-mediated gene transfer is the most popular gene delivery system. However, in the use of adenoviral vector or retroviral vector, serious concerns regarding the possibility of insertional mutagenesis and induction of the host immune response limit their clinical desirability. With regard to newly developed AAV vector, it has been found to be efficient for transducing nonproliferating cells and is considered to be nonpathogenic. Gene delivery by AAV vector also appears to be less immunogenic. However, a major problem associated with the use of AAV vector has been the difficulty in producing large quantities of high-titer stock. Therefore, we previously explored the *in vivo* nonviral gene transfer systems, such as particle delivery using gene gun^{10–12} and electroporation using pulse generator,¹³ to avoid these viral vector related problems.^{8,9} In the gene gun-mediated gene transfer to the mice liver, gene expression was observed even on day 1 and persisted for 2–5 weeks, and exclusive in the gene gun bombarded area.¹⁰ With a regard to *in vivo* electroporation, we investigated the feasibility of HGF gene transfer via the portal vein in dimethylnitrosamine (DMN)-induced rat liver fibrosis. HGF gene transfer attenuated the fibrotic change and prolonged the survival of DMN rats, and also reduced the apoptotic cell death.¹³ However, these nonviral gene transfer methods also induced infiltration of inflammatory cells and mechanical damage in the site of gene transfer. On the other hand, *in vivo* lung-targeting gene therapy has been challenging due to the physical extracellular barriers, such as mucus, mucociliary clearance and glycocalyx proteins, and the innate or adaptive immunological systems.⁷ Preclinical and clinical studies of gene therapy for cystic fibrosis suggested that current levels of gene expression were too low to achieve clinical benefit. Repetitive administrations of viral vectors were also limited by the formation of neutralizing antibodies. In addition, almost all previous studies including the lung-directed one used the diseased organ as a target site to induce efficient transgene expression locally. However, we should avoid putting the diseased organ at risk as the targets of gene transfer. Therefore, in this study, we selected the skeletal muscle as a gene transfer site using nonviral *in vivo* electroporation system to avoid these problems in lung gene therapy.

In vivo electroporation-mediated gene transfer achieved rapid and persistent gene expression in the skeletal muscle in this study. GFP expression was detected on the day after gene transfer and persisted for 28 days. GFP expression was exclusively restricted to the quadriceps muscle. These data were identical to the previous reports of *in vivo* electroporation.^{39,40} On the other hand, in addition to the electroporation-related tissue damage described above, another problem of nonviral gene transfer is lower transfection efficiency compared with viral vector. Although human HGF in the

quadriceps muscle and the lung were also detected at day 1 and peaked at days 3 and 5, respectively, human HGF concentration in the lung was significantly lower compared with that in the skeletal muscle. However, its level would be efficient to demonstrate the physiological effects according to the previous reports on HGF gene therapy.^{13,41} As a result of our observations, skeletal muscle-targeting *in vivo*-electroporation could be performed with the advantages of simplicity, safety, and without toxicity to the diseased organ.

Suppressions of fibrinogenesis and apoptosis are principal points in the therapy of lung fibrosis as described above. Our results of hydroxyproline assay and histological evaluation indicated the certain effects of HGF gene transfer on suppression of fibrinogenesis in the bleomycin-injected lung. Furthermore, HGF gene transfer also reduced the apoptosis of the bleomycin-injected lung significantly. Concerning the survival analysis of bleomycin-injected mice, Hattori *et al*⁴² reported the significant improvement of the survival rate of the mice deleted for the plasminogen activator inhibitor-1 (PAI-1) gene compared with that of wild-type mice. They suggested that the protective effect of PAI deletion could be attributed to the accelerated clearance of fibrin matrices. Their result emphasized the importance of fibrinogenesis suppression. In our study, the survival ratio of the bleomycin-injected mice was significantly improved in HGF-transferred mice compared with GFP mice.

With regard to the limitations of this study, concentration of human HGF in the muscle and the lung decreased to around undetectable level of ELISA system at 28 days after gene transfer. However, clinical efficiency of our gene therapy protocol could be suggested by the following point. First, the expression of GFP in skeletal muscle was confirmed in five of six mice at day 28 in our study. And in previous reports regarding the skeletal muscle-targeting electroporation, gene expression was confirmed even in 15 weeks after gene transfer.⁴³ Second, the physiological effect of HGF would be expectable even when its concentration decreased to undetectable level as reported previously.⁴¹ Third, skeletal muscle-targeting electroporation-mediated gene transfer could be repeated without apparent immune responses.⁴⁴

Another problem of this study is electroporation-related skeletal muscle damage. However, electroporation induced minimal damage of the skeletal muscle and mild degree of influx of inflammatory cells. And no dysfunction of the lower limb was observed in either group. These changes induced by electroporation were recovered within about 2 weeks in our preliminary study.

In conclusion, we developed a nonviral HGF gene therapy of bleomycin-induced lung fibrosis with a single skeletal muscle-targeting *in vivo* electroporation for the first time. This procedure could be

applied as a practical gene therapy protocol of various diseased organs.

Acknowledgements

We thank Dr Emi Yokoyama for editing the manuscript. This work was supported in part by Grant-in-Aid for Scientific Research (No. 14770677 to YU) from Ministry of Education, Culture, Sports, Science and Technology of Japan.

References

- 1 Green FH. Overview of pulmonary fibrosis. *Chest* 2002;122:334S–339S.
- 2 Harrison Jr JH, Hoyt DG, Lazo JS. Acute pulmonary toxicity of bleomycin: DNA scission and matrix protein mRNA levels in bleomycin-sensitive and -resistant strains of mice. *Mol Pharmacol* 1989;36: 231–238.
- 3 Schrier DJ, Phan SH, McGarry BM. The effects of the nude (nu/nu) mutation on bleomycin-induced pulmonary fibrosis. *Am Rev Respir Dis* 1983;127:614–617.
- 4 Mason RJ, Leslie CC, McCormick-Shannon K, *et al*. Hepatocyte growth factor is a growth factor for rat alveolar type II cells. *Am J Respir Cell Mol Biol* 1994;11:561–567.
- 5 Shiratori M, Michalopoulos G, Shinozuka H, *et al*. Hepatocyte growth factor stimulates DNA synthesis in alveolar epithelial type II cells *in vitro*. *Am J Respir Cell Mol Biol* 1995;12:171–180.
- 6 Yaekashiwa M, Nakayama S, Ohnuma K, *et al*. Simultaneous or delayed administration of hepatocyte growth factor equally represses the fibrotic changes in murine lung injury induced by bleomycin. *Am J Respir Crit Care Med* 1997;156:1937–1944.
- 7 Ferrari S, Griesenbach U, Geddes DM, *et al*. Immunological hurdles to lung gene therapy. *Clin Exp Immunol* 2003;132:1–8.
- 8 Wang H, Reaves PY, Gardon ML, *et al*. Angiotensin I-converting enzyme antisense gene therapy causes permanent antihypertensive effects in the SHR. *Hypertension* 2000;35:202–208.
- 9 Marshall E. Gene therapy death prompts review of adenovirus vector. *Science* 1999;286:2244–2245.
- 10 Umeda Y, Hirose H, Yoshikawa S, *et al*. Nonviral gene gun-mediated CTLA4-Ig gene transfer for modification of donor organs. *Transplant Proc* 2001;33:243–245.
- 11 Umeda Y, Iwata H, Yoshikawa S, *et al*. Gene gun-mediated CTLA4I-gene transfer for modification of allogeneic cardiac grafts. *Transplant Proc* 2002;34:2622–2623.
- 12 Matsuno Y, Iwata H, Yoshikawa S, *et al*. Suppression of graft coronary arteriosclerosis by gene gun-mediated CTLA4-Ig gene transfer. *Transplant Proc* 2002;34: 2619–2621.
- 13 Matsuno Y, Iwata H, Umeda Y, *et al*. Hepatocyte growth factor gene transfer into the liver via the portal vein using electroporation attenuates the rat liver cirrhosis. *Gene Therapy* 2003;10:1559–1566.
- 14 Nakamura T, Nishizawa T, Hagiya M, *et al*. Molecular cloning and expression of human hepatocyte growth factor. *Nature* 1989;342:440–443.

- 15 Niwa H, Yamamura K, Miyazaki J. Efficient selection for high-expression transfectants with a novel eukaryotic vector. *Gene* 1991;108:193–199.
- 16 Ashcroft T, Simpson JM, Timbrell V. Simple method of estimating severity of pulmonary fibrosis on a numerical scale. *J Clin Pathol* 1988;41:467–470.
- 17 Nakamura T, Nawa K, Ichihara A. Partial purification and characterization of hepatocyte growth factor from serum of hepatectomized rats. *Biochem Biophys Res Commun* 1984;122:1450–1459.
- 18 Weidner KM, Arakaki N, Hartmann G, *et al*. Evidence for the identity of human scatter factor and human hepatocyte growth factor. *Proc Natl Acad Sci USA* 1991;88:7001–7005.
- 19 Montesano R, Matsumoto K, Nakamura T, *et al*. Identification of a fibroblast-derived epithelial morphogen as hepatocyte growth factor. *Cell* 1991;67:901–908.
- 20 Schmidt C, Bladt F, Goedecke S, *et al*. Scatter factor/hepatocyte growth factor is essential for liver development. *Nature* 1995;373:699–702.
- 21 Dohi M, Takashi H, Yamamoto K, *et al*. Hepatocyte growth factor attenuates collagen accumulation in a murine model of pulmonary fibrosis. *Am J Respir Crit Care Med* 2000;162:2302–2307.
- 22 Pepper MS, Matsumoto K, Nakamura T, *et al*. Hepatocyte growth factor increases urokinase-type plasminogen activator (u-PA) and u-PA receptor expression in Madin–Darby canine kidney epithelial cells. *J Biol Chem* 1992;267:20493–20496.
- 23 Matsuda Y, Matsumoto K, Ichida T, *et al*. Hepatocyte growth factor suppresses the onset of liver cirrhosis and abrogates lethal hepatic dysfunction in rats. *J Biochem* 1995;118:643–649.
- 24 Kuenzler KA, Pearson PY, Schwartz MZ. Hepatocyte growth factor pretreatment reduces apoptosis and mucosal damage after intestinal ischemia–reperfusion. *J Pediatr Surg* 2002;37:1093–1097.
- 25 Nakamura T, Mizuno S, Matsumoto K, *et al*. Myocardial protection from ischemia/reperfusion injury by endogenous and exogenous HGF. *J Clin Invest* 2000;106:1511–1519.
- 26 Nagano T, Mori-Kudo I, Tsuchida A, *et al*. Ameliorative effect of hepatocyte growth factor on glycerol-induced acute renal failure with acute tubular necrosis. *Nephron* 2002;91:730–738.
- 27 Kuwano K, Hagimoto N, Kawasaki M, *et al*. Essential roles of the Fas–Fas ligand pathway in the development of pulmonary fibrosis. *J Clin Invest* 1999;104:13–19.
- 28 Kuwano K, Miyazaki H, Hagimoto N, *et al*. The involvement of Fas–Fas ligand pathway in fibrosing lung diseases. *Am J Respir Cell Mol Biol* 1999;20:53–60.
- 29 Matute-Bello G, Liles WC, Steinberg KP, *et al*. Soluble Fas ligand induces epithelial cell apoptosis in humans with acute lung injury (ARDS). *J Immunol* 1999;163:2217–2225.
- 30 Kitamura Y, Hashimoto S, Mizuta N, *et al*. Fas/FasL-dependent apoptosis of alveolar cells after lipopolysaccharide-induced lung injury in mice. *Am J Respir Crit Care Med* 2001;163:762–769.
- 31 Vernooij JH, Dentener MA, van Suylen RJ, *et al*. Intratracheal instillation of lipopolysaccharide in mice induces apoptosis in bronchial epithelial cells: no role for tumor necrosis factor- α and infiltrating neutrophils. *Am J Respir Cell Mol Biol* 2001;24:569–576.
- 32 Otterbein LE, Chin BY, Mantell LL, *et al*. Pulmonary apoptosis in aged and oxygen-tolerant rats exposed to hyperoxia. *Am J Physiol Lung Cell Mol Physiol* 1998;275:L14–L20.
- 33 Howlett CE, Hutchison JS, Veinot JP, *et al*. Inhaled nitric oxide protects against hyperoxia-induced apoptosis in rat lungs. *Am J Physiol Lung Cell Mol Physiol* 1999;277:L596–L605.
- 34 Aljandali A, Pollack H, Yeldandi A, *et al*. Asbestos causes apoptosis in alveolar epithelial cells: role of iron-induced free radicals. *J Lab Clin Med* 2002;137:330–339.
- 35 Stammberger U, Gaspert A, Hillinger S, *et al*. Apoptosis induced by ischemia and reperfusion in experimental lung transplantation. *Ann Thorac Surg* 2000;69:1532–1536.
- 36 Maeyama T, Kuwano K, Kawasaki M, *et al*. Attenuation of bleomycin-induced pneumopathy in mice by monoclonal antibody to interleukin-12. *Am J Physiol Lung Cell Mol Physiol* 2001;280:L1128–L1137.
- 37 Sharma SK, MacLean JA, Pinto C, *et al*. The effect of an anti-CD3 monoclonal antibody on bleomycin-induced lymphokine production and lung injury. *Am J Respir Crit Care Med* 1996;154:193–200.
- 38 Idell S, Gonzalez KK, MacArthur CK, *et al*. Bronchoalveolar lavage procoagulant activity in bleomycin-induced lung injury in marmosets. Characterization and relationship to fibrin deposition and fibrosis. *Am Rev Respir Dis* 1987;136:124–133.
- 39 Aihara H, Miyazaki J. Gene transfer into muscle by electroporation *in vivo*. *Nat Biotechnol* 1998;16:867–870.
- 40 Xue F, Takahara T, Yata Y, *et al*. Attenuated acute liver injury in mice by naked hepatocyte growth factor gene transfer into skeletal muscle with electroporation. *Gut* 2002;50:558–562.
- 41 Ueki T, Kaneda Y, Tsutsui H, *et al*. Hepatocyte growth factor gene therapy of liver cirrhosis in rats. *Nat Med* 1999;5:226–230.
- 42 Hattori N, Degen JL, Sisson TH, *et al*. Bleomycin-induced pulmonary fibrosis in fibrinogen-null mice. *J Clin Invest* 2000;106:1341–1350.
- 43 Maruyama H, Ataka K, Gejyo F, *et al*. Long-term production of erythropoietin after electroporation-mediated transfer of plasmid DNA into the muscles of normal and uremic rats. *Gene Therapy* 2001;8:461–468.
- 44 Tanaka T, Ichimaru N, Takahara S, *et al*. *In vivo* gene transfer of hepatocyte growth factor to skeletal muscle prevents changes in rat kidneys after 5/6 nephrectomy. *Am J Transplant* 2002;2:828–836.

Gene transfer into muscle by electroporation in vivo

Hiroyuki Aihara^{1,2} and Jun-ichi Miyazaki^{1*}

¹Department of Nutrition and Physiological Chemistry, Osaka University Medical School, Suita, Osaka 565-0871, Japan. ²The Third Department of Internal Medicine, Tohoku University School of Medicine, Sendai, Miyagi 980-0872, Japan. *Corresponding author (e-mail: jimiyaza@nutri.med.osaka-u.ac.jp).

Received 18 May 1998, accepted 21 July 1998

Among the nonviral techniques for gene transfer in vivo, the direct injection of plasmid DNA into muscle is simple, inexpensive, and safe. Applications of this method have been limited by the relatively low expression levels of the transferred gene. We investigated the applicability of in vivo electroporation for gene transfer into muscle, using plasmid DNA expressing interleukin-5 (IL-5) as the vector. The tibialis anterior muscles of mice were injected with the plasmid DNA, and then a pair of electrode needles were inserted into the DNA injection site to deliver electric pulses. Five days later, the serum IL-5 levels were assayed. Mice that did not receive electroporation had serum levels of 0.2 ng/ml. Electroporation enhanced the levels to over 20 ng/ml. Histochemical analysis of muscles injected with a *lacZ* expression plasmid showed that in vivo electroporation increased both the number of muscle fibers taking up plasmid DNA and the copy number of plasmids introduced into the cells. These results demonstrate that gene transfer into muscle by electroporation in vivo is more efficient than simple intramuscular DNA injection.

Keywords: drug delivery, gene therapy, DNA vaccine, cytokines

Plasmid DNA injected into skeletal muscle is taken up by myofibers, and the genes in the plasmid vector can be expressed for more than 2 months thereafter¹⁻⁵. The postmitotic nature and longevity of myofibers permits the stable expression of transfected genes, although the transfected DNA does not usually undergo chromosomal integration^{1,2}. Among nonviral techniques for gene transfer, this method is simple, inexpensive, and safe^{1,3,6,7}.

The relatively low expression levels attained by this method, however, have limited its applications for uses other than as a DNA vaccine^{5,7}. Conditions that affect the efficiency of gene transfer by intramuscular DNA injection and the fine structures of expression plasmid vectors that may affect expression levels have been analyzed^{4,8,9}. Regenerating muscle produces 80-fold or more protein than that produced by normal muscle following injection of an expression plasmid¹⁰. Muscle regeneration has been induced by treatment with cardiotoxin³ or bupivacaine^{10,11}. By combining a strong promoter and bupivacaine pretreatment, intramuscular injection of an interleukin-5 (IL-5) expression plasmid results in IL-5 production in muscle at a level sufficient to induce marked proliferation of eosinophils in the bone marrow and eosinophil infiltration of various organs¹². A single intramuscular injection of an erythropoietin expression plasmid into adult mice produced physiologic elevations in serum erythropoietin levels and increased hematocrits¹³. Hematocrits in these animals remained elevated at >60% for at least 90 days after a single injection. These results suggested that intramuscular DNA injection is a useful method of systemically delivering cytokines, growth factors, and other serum proteins. These improvements, however, have not been sufficient to extend the application to human gene therapy.

Electroporation has been widely used to introduce DNA into various types of cells in vitro. Gene transfer by electroporation in vivo (DNA injection followed by application of electric fields) has been effective for introducing DNA into mouse skin¹⁴, chick embryos¹⁵, rat liver¹⁶, and murine melanoma¹⁷. Based on these find-

ings, we examined the efficiency of IL-5 gene transfer into muscle by electroporation in vivo.

IL-5 is involved in the growth and differentiation of B cells and eosinophils^{18,19}. IL-5 secreted from muscle into the systemic circulation can be detected by ELISA. We transferred the gene using the pCAGGS-IL-5 plasmid, which drives IL-5 cDNA expression under the CAG (cytomegalovirus immediate-early enhancer-chicken β -actin hybrid) promoter. The CAG promoter has extremely high activity in muscle, as demonstrated in both transgenic mice and intramuscular DNA injection^{12,20}. We show that gene transfer into muscle by electroporation in vivo is more efficient than the traditional method of directly injecting DNA.

Results

In vivo electroporation. The pCAGGS-IL-5 expression plasmid²¹ was used to assess the efficiency of gene transfer into muscle by electroporation in vivo. This vector was prepared by inserting an IL-5 cDNA into the pCAGGS expression vector containing the CAG promoter²². Fifty micrograms each of covalently closed circular DNA of pCAGGS-IL-5 or control pCAGGS were injected into the bilateral tibialis anterior muscles of 8-week-old female mice. Three days before these muscles had been pretreated with bupivacaine to induce muscle regeneration^{10,11}, which increases the efficiency of gene transfer by direct DNA injection. A pair of electrode needles with a 5 mm gap were inserted into the muscle to encompass the DNA injection sites, and electric pulses were delivered using an electric pulse generator. Three pulses of 50 V each were delivered to each injection site at a rate of one pulse per s, each pulse lasting for 50 ms. Then, three pulses of the opposite polarity were applied.

Five days later, blood samples were obtained from the tail vein of the treated mice, and their serum IL-5 levels were measured by ELISA. In the mice injected with control plasmid, the IL-5 levels were below the detection limit of the assay (<10 pg/ml; n = 4), irre-

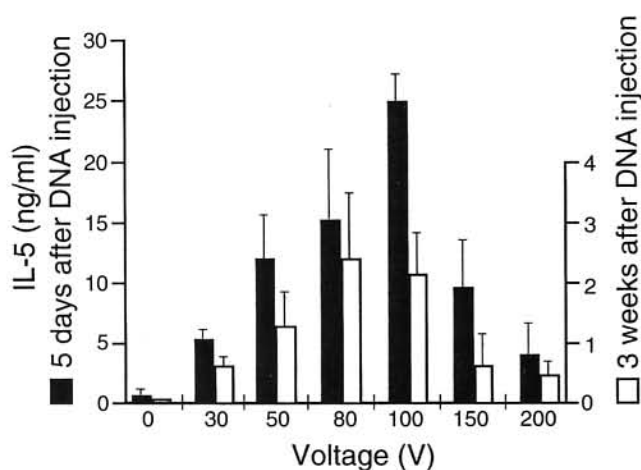


Figure 1. Voltage dependence of the efficiency of gene transfer by electroporation in vivo. The bupivacaine-treated portions of the bilateral tibialis anterior muscles were injected with pCAGGS-IL-5 plasmid DNA. Electric pulses of the indicated voltages were delivered to the DNA injection site. Solid and open bars indicate serum IL-5 levels 5 days and 3 weeks after electroporation, respectively. Each value represents the mean IL-5 concentration + standard deviation (SD) from three mice.

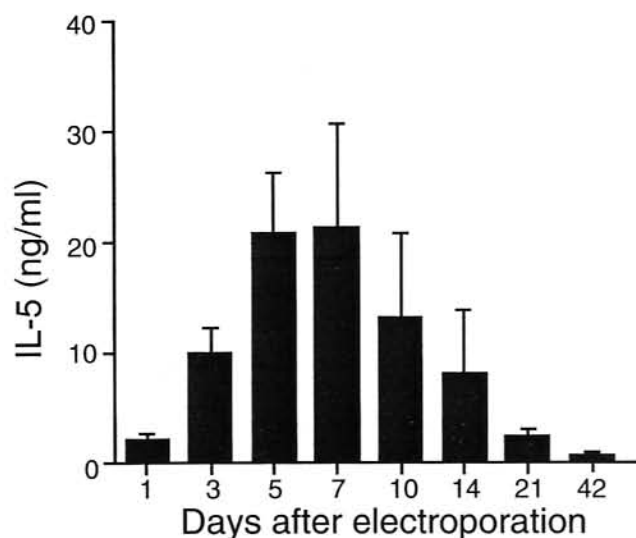


Figure 2. Time course of IL-5 expression after transfer of pCAGGS-IL-5 plasmid by electroporation in vivo. The bilateral tibialis anterior muscles were injected with pCAGGS-IL-5 plasmid DNA. Electric pulses of 100 V were delivered to the DNA injection sites. Serum samples were obtained on the indicated days after electroporation and measured for IL-5 by ELISA. Each value represents the mean IL-5 concentration + SD from three mice.

spective of the administration of electric pulses. The IL-5 levels in the mice injected with pCAGGS-IL-5 were 210 ± 120 pg/ml ($n = 3$) without electropulsation, but $12,000 \pm 3640$ pg/ml ($n = 6$) with electropulsation.

In the following experiments, the conditions affecting the efficiency of gene transfer by electroporation were examined in detail. The amount and concentration of pCAGGS-IL-5 DNA injected were fixed at 50 μ g per site and 1.5 μ g/ μ l in saline, respectively.

Direction of electric field. To determine whether the direction of electric field relative to that of muscle fibers affects the efficiency of gene transfer, electric pulses of 60 V were delivered either in a longitudinal or a transverse direction relative to the muscle fibers. To fit the tibialis anterior muscles between a pair of electrodes, we used electrodes with a 3 mm gap in this experiment. Five days later, serum IL-5 levels were measured by ELISA to evaluate the efficiency of DNA transfer. There were no significant differences between longitudinal (3100 ± 1390 pg/ml; $n = 3$) and transverse (4000 ± 1730 pg/ml; $n = 3$) electric field directions. Because the tibialis anterior muscles of mice are small and it is difficult to insert a pair of electrodes into them in a transverse orientation, electric pulses were delivered in a longitudinal direction in the following experiments.

Effect of bupivacaine pretreatment on gene transfer by electroporation. Bupivacaine or cardiotoxin pretreatment, which induces muscle necrosis and regeneration, enhances the efficiency of gene transfer by intramuscular DNA injection^{3,10,11}. To examine whether bupivacaine pretreatment enhances the efficiency of gene transfer into muscle cells by electroporation in vivo, electric pulses of 50 V were applied to bupivacaine-pretreated and nontreated muscles. Five days later, the serum IL-5 levels were not significantly different between bupivacaine-pretreated mice ($13,800 \pm 3280$ pg/ml; $n = 3$) and nontreated mice ($15,000 \pm 1710$ pg/ml; $n = 3$). Three weeks after electroporation, the serum IL-5 levels of nontreated mice (1930 ± 580 pg/ml) were higher than those of bupivacaine-treated mice (880 ± 420 pg/ml). These results indicate that bupivacaine pretreatment does not improve the effect of electroporation in vivo and that, in fact, the muscle necrosis induced by bupivacaine may reduce the long-term expression of the transferred genes.

Effect of electrode voltage on gene transfer by electroporation. To optimize the voltage of the electric pulses used for electroporation in vivo, we compared the serum IL-5 levels of mice subjected to electroporation at various electrode voltages. In this experiment, the pulse length (50 ms), number of pulses (6), and DNA concentration (1.5 μ g/ μ l in saline), which can all affect the efficiency of gene transfer, were fixed. Immediately after DNA injection, electrode needles with a 5 mm gap were inserted to encompass the DNA injection sites, and electric pulses of different voltages were administered. Five days later, serum IL-5 levels were measured. The serum IL-5 levels increased nearly in proportion to the voltage up to 100 V (Fig. 1); however, administration of voltage >100 V resulted in a marked decrease of the serum IL-5 levels, possibly because of damage to the muscle cells during electroporation at high voltage. Optimal gene expression was achieved at 100 V, resulting in serum IL-5 concentration of $24,900 \pm 2200$ pg/ml ($n = 3$). Serum IL-5 concentration at 0 V was 210 ± 120 pg/ml, which represented the IL-5 expression by intramuscular DNA injection to regenerating muscle. The serum IL-5 concentration 6 weeks after electroporation at 80 V was still >1000 pg/ml.

Time course of IL-5 expression. The time course of gene expression by electroporation in vivo was determined by following the serum IL-5 levels after electroporation at 100 V. The serum IL-5 levels peaked 5–7 days after electroporation and gradually decreased to approximately 10% of the maximum value by 3 weeks after electroporation (Fig. 2).

LacZ expression by electroporation in vivo. To analyze the mechanism by which in vivo electroporation increases gene expression as compared with direct DNA injection, we performed a histochemical analysis of muscles to which a *lacZ* expression plasmid (pCAGGS-*lacZ*) was introduced, with or without electropulsation after bupivacaine pretreatment (Fig. 3). Five days after DNA transfer, the expression of the *lacZ* gene was visualized by X-gal staining for β -galactosidase activity. When the whole muscle was incubated with X-gal, the control muscle (without electropulsation) showed only a small number of stained muscle fibers (Fig. 3B). Electroporation increased both the number of positively stained

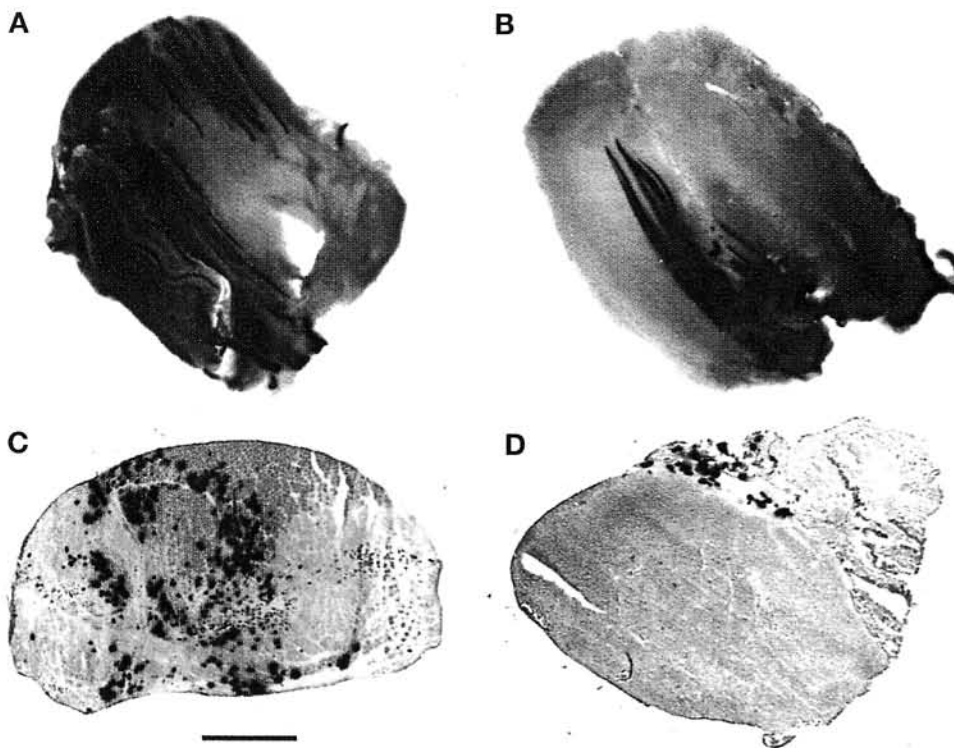


Figure 3. Histochemical staining for β -galactosidase activity in the muscle after gene transfer of pCAGGS-lacZ DNA with or without electropulsion. The bupivacaine-treated portions of the bilateral tibialis anterior muscles were injected with pCAGGS-lacZ plasmid DNA and treated with (A and C) electric pulses of 100 V or (B and D) not treated with electric pulses. Five days later, the muscle was excised and stained for β -galactosidase activity. (A and B) Whole muscles. (C and D) Transverse sections of the muscle samples stained for β -galactosidase activity, and counterstained with eosin. Scale bar equals 1 mm.

muscle fibers and the density of staining (Fig. 3A). Transverse sections showed a wide distribution of these densely stained myofibers (Fig. 3C); in contrast, only a localized distribution of lacZ-positive myofibers was observed in the control muscle (Fig. 3D). These results demonstrate that in vivo electroporation increases the number of muscle fibers that take up plasmid DNA and probably also increases the copy number of plasmids introduced into individual muscle cells.

Discussion

These results demonstrate that in vivo electroporation provides an efficient approach for muscle-targeted gene expression. We tested this method by applying it to the transfer of an IL-5 expression plasmid. The serum IL-5 levels increased nearly in proportion to the voltage up to 100 V (Fig. 1), peaking at 25 ng/ml. This value was 100-fold higher than that obtained by simple DNA injection into regenerating muscle. Histochemical analysis of muscles injected with a lacZ expression plasmid showed that in vivo electroporation increases the number of muscle fibers that take up plasmid DNA and probably also increases the copy number of plasmids introduced into each muscle cell. Electroporated lacZ-expressing cells were broadly distributed in muscle. In contrast to simple DNA injection, electroporation was equally efficient at transferring genes to regenerating and normal muscle. These results suggest that the mechanism by which muscle cells take up DNA following simple injection is different from that occurring with electroporation.

There were no significant differences in the efficiency of gene transfer between longitudinal and transverse electric field directions relative to muscle fibers; however, the following issues must

be considered. Because muscle cells are oblong in shape, the number of cells between electrodes would be much larger in a transverse orientation than in a longitudinal orientation. Therefore, more cells are likely to be transfected with a transverse orientation. Higher voltage might be required for efficient electroporation in this orientation, as there are more cell membranes to be permeabilized between the electrodes. Further studies are required to determine how the direction of electric field relative to that of muscle fibers affects the efficiency of gene transfer.

We examined the effect of different electrode voltages on the efficiency of gene transfer by electroporation, but fixed other parameters, such as pulse length, number of pulses, DNA concentration, volume of injection fluid, and solution type²³. By optimizing these parameters, the efficiency of gene transfer might be improved further. This procedure will have to be tested in larger animals to assess the usefulness and safety of electroporation in vivo for the future application to humans. Gene expression by intramuscular DNA injection is less efficient in primate muscles than in mouse muscles²⁴. Although the precise reason for this difference is not known, electroporation in vivo may

improve the expression of transferred genes in primate muscles.

Gene transfer by electroporation, which uses plasmid DNA as the vector, has several advantages over transfer using viral vectors. A large quantity of highly purified plasmid DNA is easily and inexpensively obtained. Gene transfer can be repeated without apparent immunologic responses to the DNA vector. There is less likelihood of recombination events with the cellular genome, eliminating the risk of the insertional mutagenesis that is associated with the use of viral vectors. Because there are fewer size constraints than with current viral vectors, plasmid vectors can carry larger genes. It may also be possible to transfer a mixture of two or more different plasmid constructs into muscle by electroporation. Finally, new plasmid constructs can be made rapidly and tested. Further improvements to this method may provide a new approach to gene therapy for human diseases.

Experimental protocol

Mice. Eight-week-old female C57BL/6J mice purchased from Clea Japan (Osaka, Japan) were used throughout this study. Mice were maintained under specific pathogen-free conditions in the animal facility at the Osaka University Medical School.

Plasmid DNA. Plasmid pCAGGS-IL-5 (ref. 12) was constructed by inserting mouse IL-5 cDNA (ref. 21) into the unique EcoRI site between the CAG promoter and a 3'-flanking sequence of the rabbit β -globin gene of the pCAGGS expression vector²². Similarly, a pCAGGS-lacZ plasmid was constructed by inserting the *Escherichia coli* lacZ gene into the EcoRI site of the pCAGGS expression vector. Plasmids were grown in *E. coli* HB101 cells, extracted by the alkaline lysis method, and purified by two cycles of ethidium bromide-CsCl equilibrium density gradient ultracentrifugation. Plasmid DNA was further purified by isopropanol precipitation, phenol and phenol/chloroform extraction, and ethanol precipitation. DNA was then dis-

solved in saline (0.85% NaCl), and its quantity and quality were assessed by optical density at 260 and 280 nm.

Intramuscular DNA injection and electroporation. Mice were anesthetized with pentobarbital sodium. Sixty microliters of 0.5% bupivacaine were injected into the bilateral tibialis anterior muscles using a disposable insulin syringe with a 27-gauge needle. Three days later, the mice were anesthetized, and the bupivacaine-treated portions of the muscles were injected with 50 µg each of closed circular plasmid DNA (pCAGGS-IL-5, control pCAGGS, or pCAGGS-lacZ) at 1.5 µg/µl in saline using an insulin syringe with a 27-gauge needle. A pair of electrode needles was inserted into the muscle to a depth of 5 mm to encompass the DNA injection sites, and electric pulses were delivered (see below). In some experiments, bupivacaine treatment was omitted.

Electric pulse delivery and electrodes. Electric pulses were delivered using an electric pulse generator (Electro Square Porator T820M; BTX, San Diego, CA) connected to a switch box (MBX-4; BTX), and monitored using a graphic pulse analyzer (Optimizor 500; BTX). The shape of the pulse was a square wave; i.e., the voltage remained constant during the pulse duration. Electrodes consisted of a pair of stainless steel needles of 5 mm in length and 0.4 mm in diameter, fixed with a distance (gap) between them of 3 or 5 mm. Three pulses of the indicated voltage followed by three more pulses of the opposite polarity were administered to each injection site at a rate of one pulse/s, with each pulse being 50 ms in duration.

ELISA of IL-5. Serum samples obtained from the tail vein of mice subjected to DNA injection were assayed for IL-5 using an ELISA kit (Endogen, Woburn, MA), according to the supplier's instructions.

Histochemical staining. The bupivacaine-treated portions of the bilateral tibialis anterior muscles were injected with 50 µg pCAGGS-lacZ plasmid DNA at a concentration of 1.5 µg/µl in saline, and treated with electric pulses at 100 V. Five days after injection, mice were sacrificed by cervical dislocation. The tibialis anterior muscles were fixed in cold 4% paraformaldehyde in phosphate-buffered saline (PBS) for 3 h, then washed in PBS for 1 h, and stained at 37°C for 18 h in the presence of 1 mM X-gal (5-bromo-4-chloro-3-indolyl-β-D-galactopyranoside) to detect *E. coli* β-galactosidase activity. For transverse sections, muscles were embedded in optimal cutting temperature compound (Miles, Elkhart, IL) and frozen in dry ice-acetone. Serial sections (15 µm thick) were sliced with a cryostat and placed on slide glasses coated with 3-amino-propyltriethoxysilane. The slices were fixed in 1.5% glutaraldehyde for 10 min at room temperature and then washed three times in PBS. Samples were then incubated at 37°C for 3 h in the presence of 1 mM X-gal. The muscle sections were counterstained with eosin.

Statistical analysis. Statistical evaluations of the differences in serum IL-5 levels in two groups were performed using the Mann-Whitney's U-test. *p* values of <0.05 were considered to be of statistical significance.

Acknowledgments

The authors are grateful to H. Nakamura of Tohoku University for helpful advice, and to M. Yamamoto for animal care.

- Wolff, J.A., Malone, R.W., Williams, P., Chong, W., Acsadi, G., Jani, A. et al. 1990. Direct gene transfer into mouse muscle in vivo. *Science* **247**:1465-1468.
- Wolff, J.A., Ludtke, J.J., Acsadi, G., Williams, P., and Jani, A. 1992. Long-term persistence of plasmid DNA and foreign gene expression in mouse muscle. *Hum. Mol. Genet.* **1**:363-369.
- Davis, H.L., Demeneix, B.A., Quantin, B., Coulombe, J., and Whalen, R.G. 1993. Plasmid DNA is superior to viral vectors for direct gene transfer into adult mouse skeletal muscle. *Hum. Gene Ther.* **4**:733-740.
- Davis, H.L., Whalen, R.G., and Demeneix, B.A. 1993. Direct gene transfer into skeletal muscle in vivo: factors affecting efficiency of transfer and stability of expression. *Hum. Gene Ther.* **4**:151-159.
- Ulmer, J.B., Donnelly, J.J., Parker, S.E., Rhodes, G.H., Felgner, P.L., Dworki, V.J. et al. 1993. Heterologous protection against influenza by injection of DNA encoding a viral protein. *Science* **259**:1745-1749.
- Schofield, J.P. and Caskey, C.T. 1995. Non-viral approaches to gene therapy. *Br. Med. Bull.* **51**:56-71.
- Davis, H.L., Michel, M.-L., and Whalen, R.G. 1995. Use of plasmid DNA for direct gene transfer and immunization. *Ann. N.Y. Acad. Sci.* **772**:21-29.
- Wolff, J.A., Williams, P., Acsadi, G., Jiao, S., Jani, A., and Chong, W. 1991. Conditions affecting direct gene transfer into rodent muscle in vivo. *Biotechniques* **11**:474-485.
- Wells, D.J. and Goldspink, G. 1992. Age and sex influence expression of plasmid DNA directly injected into mouse skeletal muscle. *FEBS Lett.* **306**:203-205.
- Vitadello, M., Schiaffino, M.V., Picard, A., Scarpa, M., and Schiaffino, S. 1994. Gene transfer in regenerating muscle. *Hum. Gene Ther.* **5**:11-18.
- Wells, D.J. 1993. Improved gene transfer by direct plasmid injection associated with regeneration in mouse skeletal muscle. *FEBS Lett.* **332**:179-182.
- Tokui, M., Takei, I., Tashiro, F., Shimada, A., Kasuga, A., Ishii, M. et al. 1997. Intramuscular injection of expression plasmid DNA is an effective means of long-term systemic delivery of interleukin-5. *Biochem. Biophys. Res. Commun.* **233**:527-531.
- Tripathy, S.K., Svensson, E.C., Black, H.B., Goldwasser, E., Margalith, M., Hobart, P.M. et al. 1996. Long-term expression of erythropoietin in the systemic circulation of mice after intramuscular injection of a plasmid DNA vector. *Proc. Natl. Acad. Sci. USA* **93**:10876-10880.
- Titomirov, A.V., Sukharev, S., and Kistanova, E. 1991. In vivo electroporation and stable transformation of skin cells of newborn mice by plasmid DNA. *Biochim. Biophys. Acta.* **1088**:131-134.
- Muramatsu, T., Mizutani, Y., Ohmori, Y., and Okumura, J. 1997. Comparison of three nonviral transfection methods for foreign gene expression in early chicken embryos in ovo. *Biochem. Biophys. Res. Commun.* **230**:376-380.
- Heller, R., Jaroszeski, M., Atkin, A., Moradpour, D., Gilbert, R., Wands, J. et al. 1996. In vivo electroinjection and expression in rat liver. *FEBS Lett.* **389**:225-228.
- Rols, M.-P., Delteil, C., Golzio, M., Dumond, P., Cros, S., and Teissie, J. 1998. In vivo electrically mediated protein and gene transfer in murine melanoma. *Nat. Biotechnol.* **16**:168-171.
- Sanderson, C.J. 1992. Interleukin-5, eosinophils, and disease. *Blood* **79**:3101-3109.
- Takatsu, K. 1992. Interleukin-5. *Curr. Opin. Immunol.* **4**:299-306.
- Okabe, M., Ikawa, M., Kominami, K., Nakanishi, T., and Nishimune, Y. 1997. "Green mice" as a source of ubiquitous green cells. *FEBS Lett.* **407**:313-319.
- Miyazaki, J., Takaki, S., Araki, K., Tashiro, F., Tominaga, A., Takatsu, K. et al. 1989. Expression vector system based on the chicken β-actin promoter directs efficient production of interleukin-5. *Gene* **79**:269-277.
- Niwa, H., Yamamura, K., and Miyazaki, J. 1991. Efficient selection for high-expression transfectants with a novel eukaryotic vector. *Gene* **108**:193-199.
- Wolf, H., Rols, M.P., Boldt, E., Neumann, E., and Teissie, J. 1994. Control by pulse parameters of electric field-mediated gene transfer in mammalian cells. *Biophys. J.* **66**:524-531.
- Jiao, S., Williams, P., Berg, R.K., Hodgeman, B.A., Liu, L., Repetto, G. et al. 1992. Direct gene transfer into nonhuman primate myofibers in vivo. *Hum. Gene Ther.* **3**:21-33.

Electroporation with rat' s limb



1. Inject a pair of needle electrodes into muscle



2. Inject DNA into the place between electrodes

Toll-Like Receptor Adaptor Molecules Enhance DNA-Raised Adaptive Immune Responses against Influenza and Tumors through Activation of Innate Immunity

Fumihiko Takeshita,^{1*} Toshiyuki Tanaka,¹ Tomoko Matsuda,¹ Miyuki Tozuka,¹ Kouji Kobiyama,¹ Sukumar Saha,¹ Kiyohiko Matsui,¹ Ken J. Ishii,² Cevayir Coban,² Shizuo Akira,² Norihisa Ishii,³ Koichi Suzuki,³ Dennis M. Klinman,⁴ Kenji Okuda,¹ and Shin Sasaki¹

Department of Molecular Biodefense Research, Yokohama City University Graduate School of Medicine, Yokohama 236-0004, Japan¹; ERATO, Akira Innate Immunity Program, Japan Science and Technology Agency, Osaka 565-0871, Japan²; Department of Bioregulation, Leprosy Research Center, National Institute of Infectious Diseases, Tokyo 189-0002, Japan³; and Section of Retroviral Immunology, Center for Biologics Evaluation and Research, Food and Drug Administration, Bethesda, Maryland 20892⁴

Received 18 January 2006/Accepted 12 April 2006

Toll-like receptors (TLRs) recognize microbial components and trigger the signaling cascade that activates the innate and adaptive immunity. TLR adaptor molecules play a central role in this cascade; thus, we hypothesized that overexpression of TLR adaptor molecules could mimic infection without any microbial components. Dual-promoter plasmids that carry an antigen and a TLR adaptor molecule such as the Toll-interleukin-1 receptor domain-containing adaptor-inducing beta interferon (TRIF) or myeloid differentiation factor 88 (MyD88) were constructed and administered to mice to determine if these molecules can act as an adjuvant. A DNA vaccine incorporated with the MyD88 genetic adjuvant enhanced antigen-specific humoral immune responses, whereas that with the TRIF genetic adjuvant enhanced cellular immune responses. Incorporating the TRIF genetic adjuvant in a DNA vaccine targeting the influenza HA antigen or the tumor-associated antigen E7 conferred superior protection. These results indicate that TLR adaptor molecules can bridge innate and adaptive immunity and potentiate the effects of DNA vaccines against virus infection and tumors.

Vaccines have played a substantial role in controlling epidemic diseases since Jenner's innovation. However, despite the competency of current biomedical sciences, some pathogens remain in place and pose a serious threat. Although DNA vaccines have been highlighted for their potential to conquer such uncontrolled pathogens, the magnitude of the immune response elicited by DNA vaccines in larger animals, including humans, has been disappointing (3). Numerous strategies have been explored to improve their immunogenicity, ranging from the use of gene guns and electroporation to improve vaccine uptake, to the coadministration of cytokines and chemokines to boost local immunity, to the use of "combination" vaccines that boost immunity with protein- or vector-based components (13). One promising strategy is the use of adjuvants that enhance DNA-raised immune responses (17).

One important class of immune adjuvants triggers the innate immune system via Toll-like receptors (TLRs) (10, 19). These agents mimic infection by microbes, thereby eliciting the innate immune responses required for subsequent acquired immune activation against immunogens. However, the strong immunostimulatory properties of TLR ligands may induce unwanted side effects, ranging from local irritation to systemic shock (2). TLR ligands may also exacerbate preexisting neuronal or autoimmune diseases (7, 14, 16). To circumvent these complica-

tions, we examined whether TLR adaptor molecules in cells transfected together with DNA vaccines augment adaptive immune responses while avoiding adverse reactions.

TLR-mediated cell activation proceeds through two distinct pathways. The first pathway depends on an adaptor molecule, myeloid differentiation factor 88 (MyD88), that transduces downstream events leading to nuclear factor κ B (NF- κ B) activation (27). MyD88 associates with the proximal TIR domains of TLRs, initiating a signaling cascade that involves activation of interleukin-1 (IL-1) receptor-associated kinase (IRAK) family members and tumor necrosis factor (TNF) receptor-associated factor 6 (TRAF6) (28). This pathway is triggered by TLR2, TLR4, TLR5, TLR7, TLR8, and TLR9 (26). In the case of TLR7 and TLR9, the MyD88-dependent pathway also triggers phosphorylation of interferon regulatory factor 7 (IRF-7) by IRAK1, which leads to alpha interferon (IFN- α) production (35). Toll-IL-1 receptor domain-containing adaptor-inducing IFN- β (TRIF) and the TRIF-related adaptor molecule (TRAM) mediate a MyD88-independent alternative pathway. Once TRIF binds to activated TLR3 or TLR4, it interacts with TRAF6, inducible IKK, and TANK-binding kinase 1, mediating the induction of IFN- β through the activation of NF- κ B and IRF-3 (8). Overexpression of these adaptor molecules is proven to turn on downstream cellular signaling in the absence of TLRs or TLR ligands (11, 29); thus, we intended to use TLR-adaptor molecules as genetic adjuvants.

The present study shows that DNA vaccine immunogenicity is enhanced by cotransfection of MyD88 and TRIF. The TRIF genetic adjuvant improved the protective effect of DNA vaccines against lethal influenza virus challenge and tumor out-

* Corresponding author. Mailing address: Department of Molecular Biodefense Research, Yokohama City University Graduate School of Medicine, 3-9 Fukuura, Kanazawaku, Yokohama 236-0004, Japan. Phone: 81-45-787-2602. Fax: 81-45-787-2851. E-mail: takesita@yokohama-cu.ac.jp.

growth, a result that may have an impact on current vaccine development targeting emerging viral infections and tumors.

MATERIALS AND METHODS

Expression plasmids. cDNA fragments encoding immunogens and TLR adaptor molecules were amplified from parental plasmids by PCR and subcloned into the pGA vector. The FLAG-tagged expression plasmids CMV4-MyD88, CMV4-TRIF, CMV4-TIRAP, CMV4-TOLLIP, CMV4-IRAK1, and CMV4-TRAF6 have been described previously (29). LacZ or EGFP cDNA was amplified from pSV-β-Galactosidase (Promega, Madison, WI) or pEGFP-N1 (BD Biosciences, San Jose, CA), respectively. Influenza virus A/PR/8/34 (H1N1) HA (amino acids 18 to 566) was amplified from pJW4303/H1 and introduced into the pFLAG-CMV9 vector (Sigma, St Louis, MO). cDNA encoding E7₄₉ attached to the carboxy terminus of EGFP was cloned into pGA vector (4). Sequences of cloned PCR products were confirmed with an ABI PRISM Genetic Analyzer (PE Applied Biosystems, Foster City, CA).

Cell transfection and reporter gene assay. Transient transfections were conducted with FuGene 6 (Roche Diagnostics, Indianapolis, IN) according to the manufacturer's protocol. HEK293 cells (3×10^4) were cotransfected with each expression plasmid (CMV4, CMV4-MyD88, CMV4-TRIF, CMV4-TIRAP, CMV4-TOLLIP, CMV4-IRAK1, CMV4-TRAF6, pGA-LacZ, pGA-LacZ-MyD88, or pGA-LacZ-TRIF [200 ng]), the reporter plasmid (p5xNF-κB-luc or pGL3 hIFNβ [25 ng]), and the control *Renilla* luciferase (LUC) plasmid (pTK-RL [25 ng]; Promega, Madison, WI). Cells were incubated for 48 h after transfection, and LUC activity was measured with the Dual Luciferase Reporter Assay System (Promega) according to the manufacturer's protocol. Alternatively, LacZ activity was measured with a β-Gal Reporter Gene Assay kit (Roche Diagnostics). Finally, firefly LUC activity or LacZ activity of individual cell lysates was normalized to *Renilla* LUC activity.

Immunization schedule. Eight-week-old female BALB/c and C57BL/6 mice were purchased from SLC (Shizuoka, Japan) and housed in an animal facility under specific-pathogen-free conditions. After anesthetizing with a ketamine/xylazine mixture, the mice (eight mice/group) were injected in the quadriceps muscles with a plasmid solution (1 μg/μl saline, 50 μl/muscle) containing either pGA-LacZ, pGA-LacZ-MyD88, pGA-LacZ-TRIF, pGA-GFP, pGA-GFP-MyD88, pGA-GFP-TRIF, CMV9-HA, CMV9-HA-TRIF, pGA-GFP-E7, or pGA-GFP-E7-TRIF. The injection site was electroporated with a field strength of 30 V/cm (constant) and three pulses of 50 ms each, by using CUY21EDIT (NepaGene, Tokyo, Japan). The booster immunization was given 2 or 4 weeks after the primary immunization. The institutional animal care and welfare committee approved all of the animal experiments, and the mice were treated in accordance with NIH animal care guidelines.

ELISA. Serum antibody (Ab) titers were measured by enzyme-linked immunosorbent assay (ELISA), as described previously (30).

RT-PCR. Splenocytes were harvested 2 weeks after the final immunization. The cells were incubated with 1 μg/ml of H-2^d-restricted LacZ class I peptide (TPHPARIGL), E7 peptide (RAHYNIVTF), or NP peptide (ASNENMDAM) for 24 h at 37°C. Alternatively, inguinal lymph node (LN) cells were harvested 24 or 72 h after the final immunization. Total RNA was isolated as described previously (31). Real-time PCR (RT-PCR) was performed with TaqMan probes (Applied Biosystems, Foster City, CA) specific for IFN-γ, IL-12 p40, IL-18, IL-4, IL-6, IFN-β, TNF-α, IP-10, JE/MCP-1, major histocompatibility complex class I (MHC-I) (D1), MHC-II (Ea), CD40, CD80, CD86, or 18S rRNA and an ABI PRISM 7700 sequence detection system (Applied Biosystems). The relative mRNA expression levels of IFN-γ, IL-12 p40, IL-18, IL-4, IL-6, IFN-β, TNF-α, IP-10, JE/MCP-1, MHC-I (D1), MHC-II (Ea), CD40, CD80, and CD86 in the individual samples were normalized to 18S rRNA levels.

CTL assay. Splenocytes were harvested 2 weeks after the final immunization. The cytotoxic T-lymphocyte (CTL) isolates (effector cells) were prepared after incubation with 1 μg/ml of H-2^d-restricted LacZ class I peptide and 20 U/ml of IL-2 (Sigma) for 4 days at 37°C. P815 cells pulsed with 1 μg/ml of H-2^b-restricted LacZ class I peptide (DAPIYTNV [control peptide]) or H-2^d-restricted LacZ class I peptide were used as the target cells. The target cells (1×10^4) were cultured with increasing numbers of the effector cells for 4 h. The amount of lactate dehydrogenase released from target cells was measured by the Cytotox 96 (Promega) system, and the percentage of specific lysis was calculated according to the manufacturer's protocol.

Influenza challenge. Two weeks after the booster immunization with pGA-GFP, CMV9-HA, or CMV9-HA-TRIF, the mice were challenged intranasally with 1×10^4 PFU (4 50% lethal doses [LD₅₀]) or 5×10^4 PFU (20 LD₅₀) of influenza virus A/PR/8/34 (21). The body weight and the mortality of the challenged mice were monitored for the next 10 days.

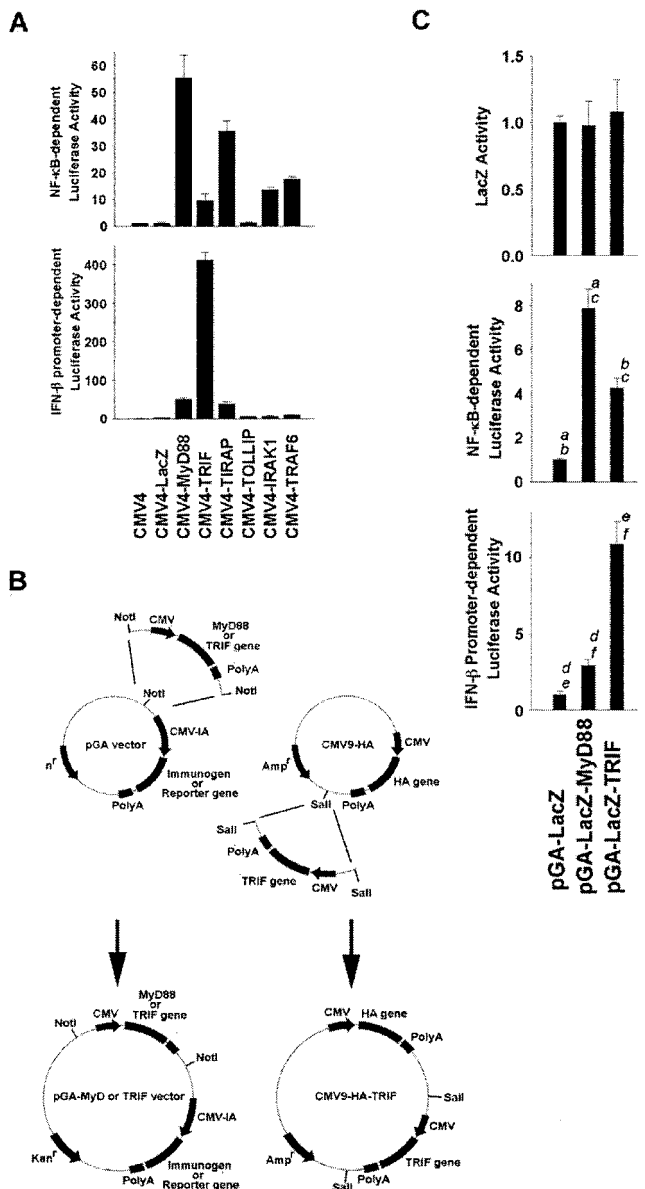


FIG. 1. Characterization of TLR adaptor molecules as activators of the NF-κB and IFN-β promoters. (A) HEK293 cells (4×10^5) were cotransfected with 25 ng of pTK-RL and 25 ng of 5x NF-κB-luc or pGLhIFNβ-luc, plus 250 ng of each indicated expression plasmid for TLR adaptor molecules. Firefly LUC activity was assayed 48 h after transfection and normalized to *Renilla* LUC activity. Values are means ± standard deviations for three independent experiments. The relative LUC activity of cells transfected with 5x NF-κB-luc plus CMV4-MyD88 was significantly higher than that with 5x NF-κB-luc plus any other plasmid ($P < 0.0001$). The relative LUC activity of cells transfected with pGLhIFNβ-luc plus CMV4-TRIF was significantly higher than that with pGLhIFNβ-luc plus any other plasmid ($P < 0.0001$). (B) Schematic diagram of a DNA vaccine expressing a single antigen alone (pGA-LacZ, pGA-GFP, CMV9-HA, and pGA-GFP-E7) or both antigen and adjuvant molecules (pGA-LacZ-MyD88, pGA-GFP-MyD88, pGA-LacZ-TRIF, pGA-GFP-TRIF, CMV9-HA-TRIF, and pGA-GFP-E7-TRIF). (C) HEK293 cells (4×10^5) were transfected as described above. Values are means ± standard deviations for three independent experiments. Significances of differences are as follows: c and d, $P < 0.01$; e and f, $P < 0.001$; a and b, $P < 0.0001$.

HI assay. Sera were collected 2 weeks after the booster immunization with pGA-GFP, CMV9-HA, or CMV9-HA-TRIF. Hemagglutinin inhibition (HI) titers were determined by using influenza virus A/PR/8/34, as described previously (4).

Tumor transplantation. Three days before the primary immunization with pGA-GFP, pGA-GFP-E7, or pGA-GFP-E7-TRIF, the mice were administered subcutaneously 2.5×10^4 cells of TC-1, a mouse lung carcinoma expressing E7 antigen. The size of the local tumor mass was monitored for the next 4 weeks.

Statistical analysis. All experiments were repeated at least twice. Statistical significance was evaluated by Student's *t* test, a one-way analysis of variance using the Bonferroni method, or nonparametric survival analysis using the Kaplan-Meier method, with a *P* value of <0.05 considered statistically significant.

RESULTS

Activation of NF- κ B and IFN- β promoters by overexpression of TLR adaptor molecules. To identify candidate molecules that might serve as adjuvants for DNA vaccines, a variety of TLR adaptor molecules, including MyD88, TRIF, TIR domain-containing adaptor protein/MyD88 adaptor-like protein (TIRAP/Mal), Toll-interacting protein (TOLLIP), IRAK1, and TRAF6, were tested for the ability to activate the NF- κ B and IFN- β promoters of HEK293 cells. NF- κ B up-regulates the expression of cytokine, chemokine, and costimulatory molecules central to activation of the innate immune system. Type I IFNs, such as IFN- α and IFN- β , play critical roles in the innate immune response. As shown in Fig. 1A, MyD88 was the most potent inducer of NF- κ B activation, while TRIF induced the strongest activation of the IFN- β promoter ($P < 0.0001$). Thus, these two molecules were selected for further evaluation as candidate genetic adjuvants.

Activity of dual-promoter plasmids encoding antigen plus MyD88 or TRIF. To optimize analysis of their adjuvant activity, dual-promoter plasmids were constructed to coexpress LacZ (a surrogate antigen) plus MyD88 or TRIF (Fig. 1B) in a single backbone. Our dual-promoter strategy ensures that the TLR adaptor molecules and an antigen are simultaneously present in the same cells. The ability of these combination plasmids to promote antigen expression was examined in HEK293 cells. Transfection with pGA-LacZ-MyD88 resulted in a 7.8-fold increase in NF- κ B-dependent LUC activity compared to control plasmid (pGA-LacZ) (Fig. 1C) ($P < 0.0001$). Transfection with pGA-LacZ-TRIF resulted in an 11.7-fold increase in IFN- β promoter-dependent LUC activity compared with the control plasmid (Fig. 1C) ($P < 0.001$). The levels of LacZ expression were similar in all groups (Fig. 1C). These data demonstrate that antigen expression is comparable among the groups, but innate cell signaling is activated in cells transfected with the combination plasmids of LacZ and a TLR adaptor molecule.

The MyD88-expressing DNA vaccine enhances humoral immunity. Mice were immunized and boosted 4 weeks later by intramuscular electroporation (imePT) with the pGA-LacZ, pGA-LacZ-MyD88, or pGA-LacZ-TRIF DNA vaccine. Four weeks after primary immunization, all three groups developed similarly low immunoglobulin G (IgG) anti-LacZ Ab responses (Fig. 2A). By comparison, animals immunized and boosted with pGA-LacZ-MyD88 generated sevenfold-higher serum IgG anti-LacZ titers at week 6 than did recipients of the control pGA-LacZ or pGA-LacZ-TRIF plasmid (Fig. 2A) ($P < 0.01$). This improved humoral response was primarily due to the 15-fold-higher IgG2a anti-LacZ response elicited by pGA-

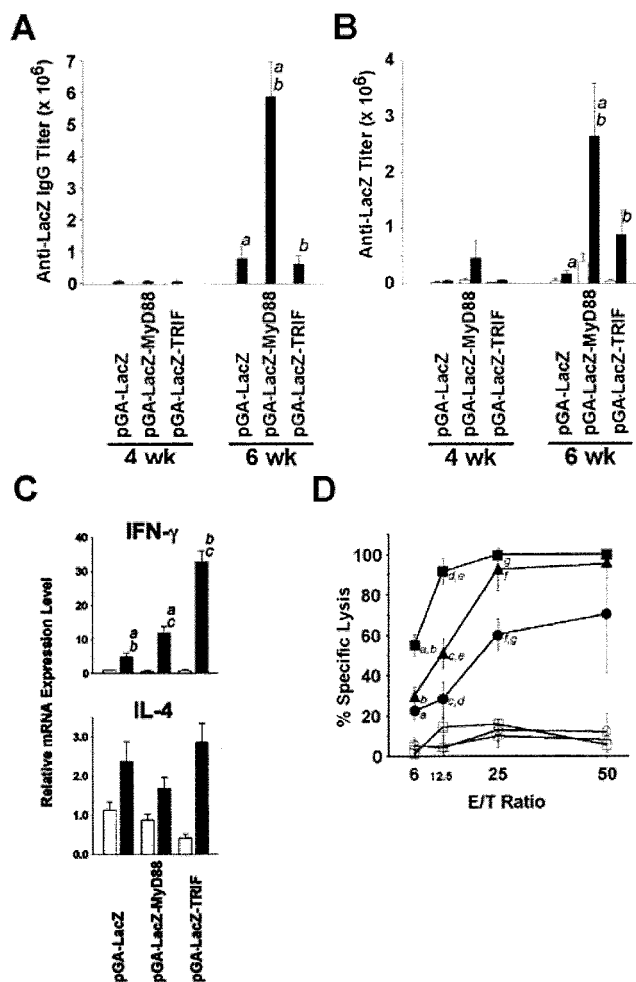


FIG. 2. MyD88 enhances humoral immunity, whereas TRIF enhances cellular immunity. (A and B) Five mice/group were immunized at 0 and 4 weeks with pGA-LacZ, pGA-LacZ-MyD88, or pGA-LacZ-TRIF by imePT. Blood was drawn at 4 and 6 weeks, and serum anti-LacZ Ab titers were monitored by ELISA. IgG (panel A, open bars), IgG1 (panel B, open bars), and IgG2a (panel B, filled bars) titers were examined by ELISA. (C) Splenocytes were prepared from individual mice and stimulated *in vitro* with 1 μ g/ml of class I (H-2^d) peptide (filled bars) or class I (H-2^b) peptide (open bars) for 24 h. mRNA was extracted and reverse transcribed. Aliquots of the reaction were examined for IFN- γ , IL-4, and 18S rRNA levels. The levels of IFN- γ and IL-4 mRNA expression were normalized to the levels of 18S rRNA and described as relative levels of mRNA expression. The graphs present means \pm standard deviations. (D) Effector CTL isolates were prepared as described in Materials and Methods. MHC haplotype-matched (H-2K^d) P815 cells were pulsed with 1 μ g/ml of class I (H-2^d) peptide (filled symbols) or class I (H-2^b) peptide (empty symbols) for 1 h and used as target cells. The effector and target cells were mixed at effector-to-target ratios of 6 to 50 and cultured for 4 h, and the lactate dehydrogenase activity of the culture supernatants was assayed. The graph shows the mean percent specific lysis \pm standard deviation calculated as described in Materials and Methods. ● and ○, pGA-LacZ; ▲ and △, pGA-LacZ-MyD88; ■ and □, pGA-LacZ-TRIF. Significances of differences are as follows: a (B), b (B), a (C), and c (C), $P < 0.05$; a (A), b (A), b (C), c (D), and f (D), $P < 0.01$; b (D) and e (D), $P < 0.001$; a (D), d (D), and g (D), $P < 0.0001$.

TABLE 1. Characterization of draining LN cells present after vaccine administration

Cell type	No. of cells (mean ± SD) after indicated treatment ^a		
	None	pGA-GFP	pGA-GFP-TRIF
CD11c ⁺	1.01 ± 0.21*†	2.60 ± 0.41*	3.36 ± 0.50†
CD40 ⁺	12.68 ± 2.66§	16.58 ± 4.62¶	36.49 ± 4.41§¶

^a Significances of differences are as follows: *, §, and ¶, *P* < 0.01; †, *P* < 0.001.

LacZ-MyD88 (Fig. 2B) (*P* < 0.05). These results suggest that overexpression of MyD88 improves induction of Th1-dependent antigen-specific humoral immunity to an antigen coexpressed by the same DNA vaccine.

Cellular immune responses modulated by the MyD88 and TRIF genetic adjuvants. The antigen-specific cytokine production by bulk splenocytes from mice 2 weeks post-boost was analyzed. Splenocytes were restimulated in vitro with a LacZ-derived H-2^d-restricted MHC-I peptide, and mRNA levels for IFN-γ and IL-4 were quantified by RT-PCR. Splenocytes from the pGA-LacZ-MyD88- and pGA-LacZ-TRIF-treated groups produced 2.4- and 6.6-fold more IFN-γ mRNA than cells from the control group (Fig. 2C) (*P*, <0.05 and <0.01, respectively). There was no difference between groups with respect to IL-4 mRNA expression (Fig. 2C). Finally, CTL activity was examined by the lysis of P815 (H-2K^d) cells pulsed with a class I LacZ peptide. CTL isolates from pGA-LacZ-TRIF-vaccinated

animals showed the strongest lytic activity (Fig. 2E) (*P*, <0.001 at all effector-to-target ratios), although those from pGA-LacZ-MyD88-vaccinated mice also exceeded the response of controls (Fig. 2D) (*P* < 0.01). These results indicate that MyD88 and TRIF can act as genetic adjuvants to enhance the induction of a Th1-dominated cellular immune response to a coexpressed antigen encoded by a DNA vaccine.

TRIF genetic adjuvant increases the number of CD11c⁺ and CD40⁺ cells in draining LNs. The immune response induced by DNA vaccines is dependent on transfected antigen-presenting cells (APCs) reaching the draining LNs (1, 5, 20). A single-cell suspension was prepared from inguinal LNs 3 days after boosting, and cell frequencies were determined by surface staining. Compared with resting LNs, the number of CD11c⁺ dendritic cells (DCs) increased significantly within 72 h of imEPT delivery of plasmid (Table 1) (*P* < 0.01). The pGA-GFP-TRIF plasmids significantly increased the number of CD40⁺ cells present in draining LNs compared with control plasmid, suggesting that these genetic adjuvants might increase the number of mature B lymphocytes, activated T lymphocytes, and CD40⁺ DCs at that site (Table 1) (*P* < 0.05).

Effect of TRIF genetic adjuvant on cytokine, chemokine, and cell surface molecule expression in draining LNs. Inguinal LNs were removed 24 and 72 h after booster immunization, and changes in mRNA expression for various cytokines, chemokines, and cell surface molecules were quantified by RT-PCR. The levels of IFN-γ and Th1 cell-promoting cytokines,

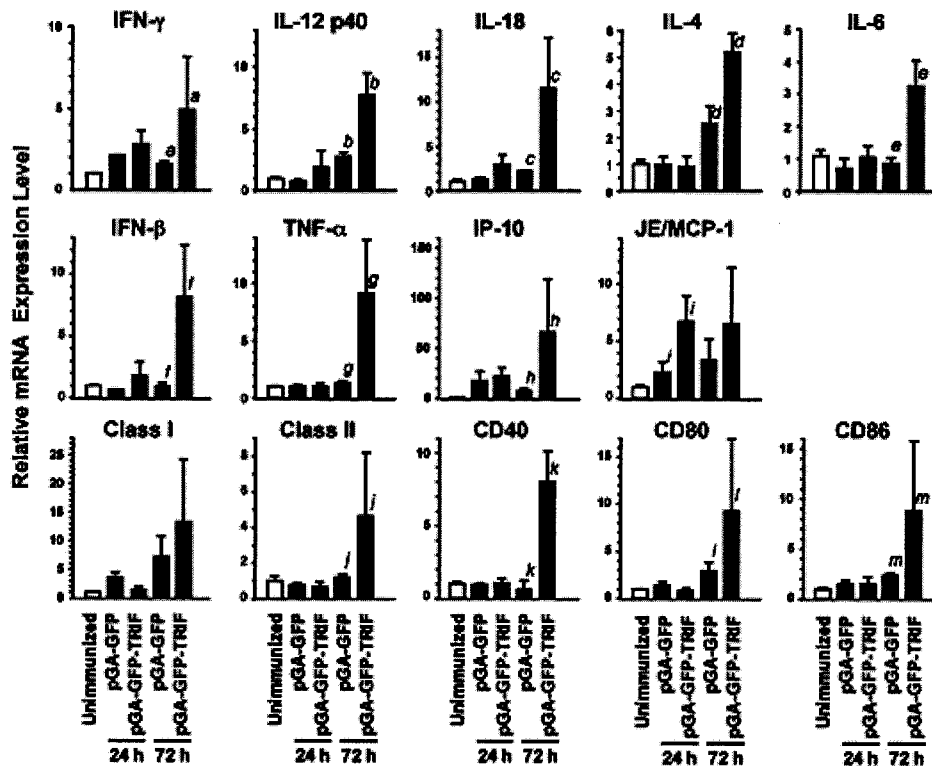


FIG. 3. Activation of cells present in draining LNs after imEPT with the MyD88 or TRIF genetic adjuvant. Twenty-four or 72 h after booster immunization with 50 μg of pGA-GFP or pGA-GFP-TRIF by imEPT, draining LNs (inguinal LNs, 10/group) were removed. Sample mRNA was extracted and reverse transcribed, and then the cDNA aliquots were assessed for expression of IFN-γ, IL-12 p40, IL-18, IL-4, IL-6, IFN-β, TNF-α, IP-10, JE/MCP-1, MHC-I, MHC-II, CD40, CD80, and CD86 by RT-PCR. The graph shows means ± standard deviations for samples prepared from 10 individual LNs. Significances of differences are as follows: a, d, i, j, l, and m, *P* < 0.05; b, c, e, f, g, h, and k, *P* < 0.01.

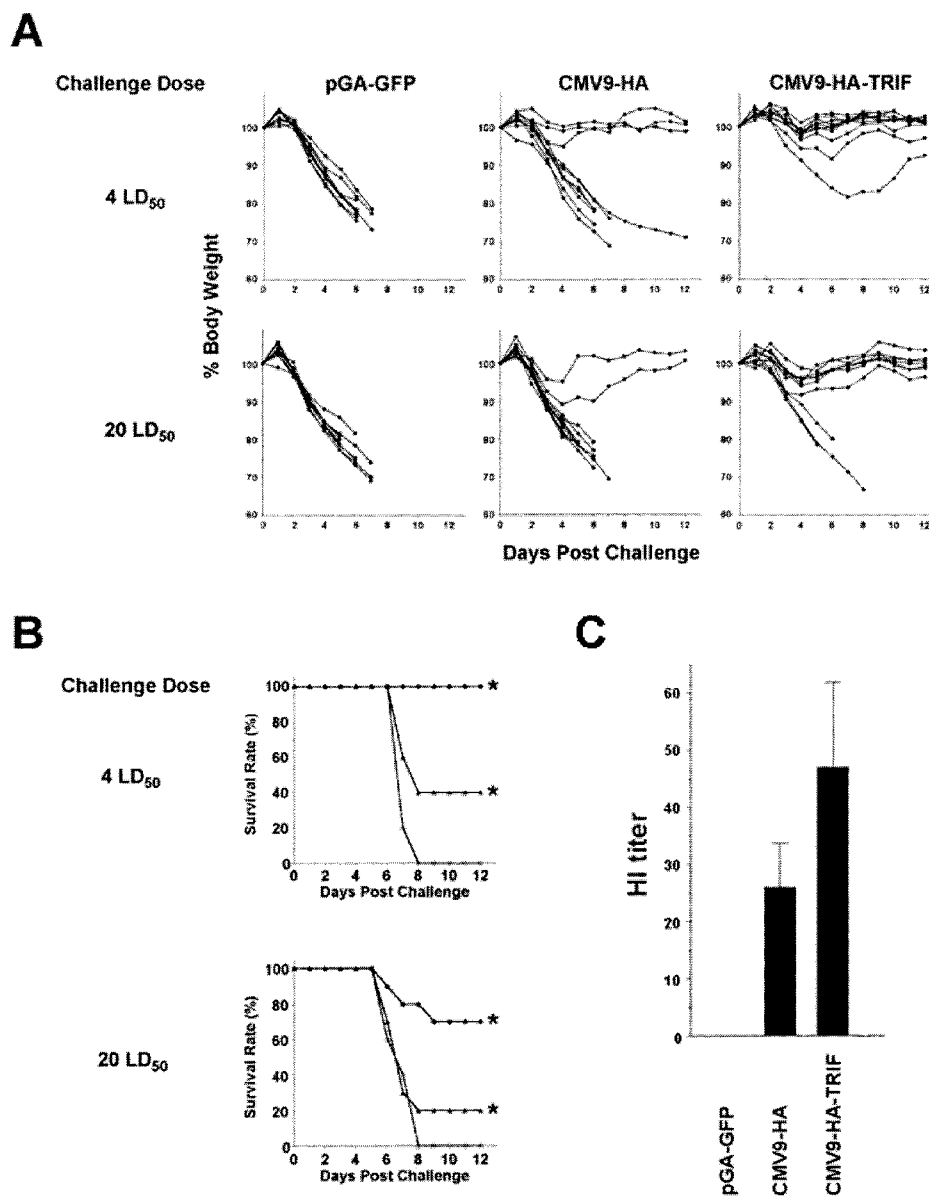


FIG. 4. TRIF increases the protective activity of an influenza HA-encoding DNA vaccine. Ten mice/group were immunized at 0 and 4 weeks with 2 μ g of pGA-GFP, CMV9-HA, or CMV9-HA-TRIF by imEPT. Two weeks later, they were challenged with 4 or 20 LD₅₀ of influenza virus A/PR/8/34. (A) Percent change in body weight compared to day zero. (B) Survival rates monitored for the following 12 days. \circ , pGA-GFP; \blacktriangle , CMV9-HA; \bullet , CMV9-HA-TRIF. *, $P < 0.01$. (C) HI titers measured with sera obtained 2 weeks after booster immunizations.

including IL-12 p40 and IL-18, were significantly up-regulated 72 h after immunization with pGA-GFP-TRIF compared to control groups (Fig. 3) ($P < 0.05$). Th2 cytokine mRNAs, including IL-4 and IL-6, were also up-regulated at 72 h ($P < 0.05$). Factors regulating APC function (i.e., IFN- β , TNF- α , IP-10, and JE/MCP-1) and elements associated with APC function (i.e., MHC-II, CD40, CD80, and CD86) were consistently increased 72 h after immunization with pGA-GFP-TRIF compared to control plasmid (Fig. 3) ($P < 0.05$).

Incorporation of TRIF genetic adjuvant into DNA vaccines targeting influenza and tumors. To explore whether TRIF could contribute to improving the protective effect of a DNA vaccine, vectors targeting the influenza HA antigen and the

tumor-associated antigen E7 were constructed (Fig. 1B). Mice primed and boosted with each HA-encoding vaccine were challenged intranasally 2 weeks later with 4 to 20 LD₅₀ of live influenza virus A/PR/8/34. Two outcomes of disease were monitored: weight loss and mortality. Animals immunized with the irrelevant pGA-GFP plasmid uniformly demonstrated severe weight loss and subsequently died (Fig. 4A and B). Vaccination with CVM9-HA protected approximately half of the mice from low-dose challenge but <20% of animals from higher-dose challenge. In contrast, the CMV9-HA-TRIF vaccine protected all mice from low-dose challenge and 70% of mice from high-dose influenza virus challenge ($P < 0.05$). The HI titer was determined as shown in Fig. 4C. CMV9-HA-TRIF and

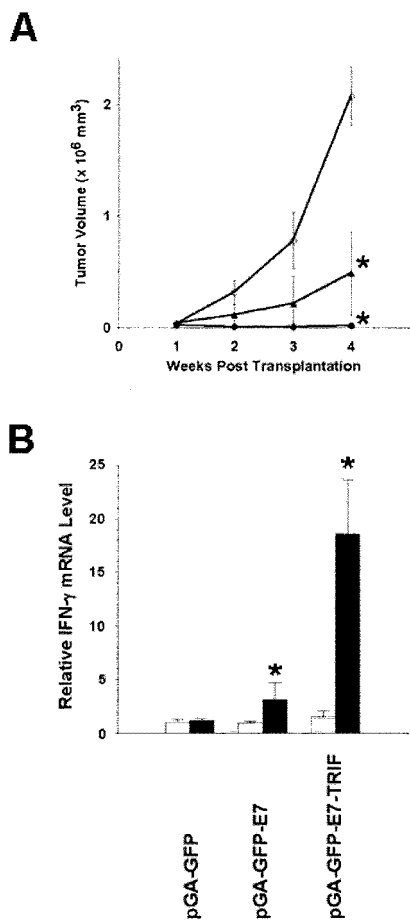


FIG. 5. TRIF increases the protective activity of a tumor-associated antigen E7-encoding DNA vaccine. (A) Three days before vaccination, mice were challenged with 2.5×10^4 TC-1 cells. Ten mice/group were immunized at 0 and 2 weeks with 20 μ g of pGA-GFP, pGA-GFP-E7, or pGA-GFP-E7-TRIF by imEPT. Tumor outgrowth was monitored for the following 4 weeks. ○, pGA-GFP; ▲, pGA-GFP-E7; ●, pGA-GFP-E7-TRIF. *, $P < 0.05$. (B) Splenocytes were prepared 2 weeks after the booster immunization and stimulated in vitro with 1 μ g/ml of E7 peptide (filled bars) or NP peptide (open bars) for 24 h. The relative IFN- γ mRNA expression levels were measured as described in the legend to Fig. 2. *, $P < 0.01$. The graphs present means \pm standard deviations.

CMV9-HA raised comparable levels of HI activity, suggesting that the TRIF genetic adjuvant raised a stronger innate and/or cellular immune response, which may confer superior protection in combination with the humoral immune response (Fig. 4C). Mice that had been established with subcutaneous tumors were primed and boosted with each E7-expressing vaccine. Tumor masses grew steadily in mice vaccinated with the irrelevant pGA-GFP plasmid (Fig. 5A). pGA-GFP-E7 treatment partially protected against tumor outgrowth, while pGA-GFP-E7-TRIF progressively protected (Fig. 5A). This observation was in accordance with the levels of E7-specific IFN- γ production from splenocytes of immunized mice (Fig. 5B). These results clearly indicate that the TRIF genetic adjuvant can improve the protective effect of DNA vaccines in infectious

and neoplastic disease models, both major targets of current vaccine development.

DISCUSSION

There is an urgent need to develop effective vaccines against emerging infectious diseases and biothreat pathogens (12, 13). DNA vaccines represent a promising strategy for accomplishing this goal, but their success has been limited due to poor immunogenicity in large animals. We postulated that TLR adaptor molecules might be used as genetic adjuvants to promote immunity against DNA vaccine-encoded antigens by their nature as activators of innate immune responses. To minimize potential side effects, these agents were incorporated into the antigen-encoding plasmid, thereby insuring their targeting to cells contributing to the induction of protective immunity. Initial results demonstrated that both MyD88 and TRIF were functionally active, enhancing antigen-specific humoral and/or cell-mediated immune responses in vivo. Of greater importance, the addition of TRIF significantly improved the protective activity of an HA-encoding DNA vaccine in mice challenged with influenza virus and the therapeutic activity of an E7-encoding DNA vaccine in mice transplanted with lung carcinoma cells.

Incorporating cassettes expressing the MyD88 or TRIF gene into DNA vaccine vectors increased the size of the DNA by 2.1 and 3.7 kb, respectively. Since the size of the DNA vaccine generally affects in vivo transfection efficiency (6, 15), plasmids containing the genetic adjuvant cassettes were less-effective inducers of target molecule expression (data not shown). Since IFNs and proinflammatory cytokines have the ability to suppress virus promoters, such factors induced by genetic adjuvants might inhibit the levels of antigen expression. However, DNA vaccine immunogenicity was improved by increasing the expression of MyD88 or TRIF in transfected cells. MyD88 plays an essential role in DC maturation, thereby improving CD8⁺ T-lymphocyte priming via cross-presentation (18). MyD88-deficient mice have a profound defect in the activation of antigen-specific Th1 immune responses (23). TLR3-deficient mice exhibit impaired CTL cross-priming of antigens associated with virus-infected cells, indicating that TLR3-mediated TRIF-dependent signaling provides an important link between innate and acquired immunity following virus infection (24). Type I IFNs play a key role in maintaining innate and acquired immunity. Mice lacking type I IFN receptors or signaling molecules exhibit defective immune responses to eliminate cancer cells and cells infected by viruses (32). Recent studies have demonstrated that TLR-mediated cellular signaling is also mediated by IRF-3 or IRF-7, which serves as a crucial transcription factor regulating the production of IFN- β or IFN- α , respectively (9). In this regard, we demonstrated previously that IRF-3 and IRF-7 genetic adjuvants are both effective at amplifying DNA vaccine-raised immune responses (22).

A numbers of cytokines, hematopoietic factors, and costimulatory molecules have been tested for the ability to act as genetic adjuvants (25, 33, 34). However, the immunological processes associated with stimulation through these molecules are downstream of the activation of the innate immune system mediated by MyD88 and TRIF following TLR ligation. We therefore hypothesized that increasing expression of these molecules would im-

prove the signaling cascade required for activation of both innate and subsequent adaptive immune responses.

In conclusion, the present study demonstrates that TLR adaptor molecules, particularly TRIF, can improve the immunogenicity and protective and therapeutic effects of DNA vaccines. These findings may open a new avenue for designing vaccines that elicit both innate and adaptive immunity, mimicking the effects of live pathogen exposure. Following up the present study with further vaccination studies that involve TRIF genetic adjuvant targeting of a variety of microbial and tumor antigens is necessary to realize the value of this novel approach.

ACKNOWLEDGMENTS

We thank A. de la Fuente for secretarial assistance and K. Takase for technical assistance.

This work was supported in part by a Grant-In-Aid from the National Institute of Biomedical Innovation, a Grant-In-Aid for the Advancement of Medical Science from the Yokohama Foundation, and a Grant-In-Aid for Young Fellows in Scientific Research from the Ministry of Education, Culture, Sports, Science, and Technology of Japan.

REFERENCES

- Akbari, O., N. Panjwani, S. Garcia, R. Tascon, D. Lowrie, and B. Stockinger. 1999. DNA vaccination: transfection and activation of dendritic cells as key events for immunity. *J. Exp. Med.* **189**:169–178.
- Alexander, C., and E. T. Rietschel. 2001. Bacterial lipopolysaccharides and innate immunity. *J. Endotoxin Res.* **7**:167–202.
- Babiuk, L. A., R. Pontarollo, S. Babiuk, B. Loehr, and S. van Drunen Littel-van den Hurk. 2003. Induction of immune responses by DNA vaccines in large animals. *Vaccine* **21**:649–658.
- Bins, A. D., A. Jorritsma, M. C. Wolkers, C. F. Hung, T. C. Wu, T. N. Schumacher, and J. B. Haanen. 2005. A rapid and potent DNA vaccination strategy defined by in vivo monitoring of antigen expression. *Nat. Med.* **11**:899–904.
- Casares, S., K. Inaba, T. D. Brumeanu, R. M. Steinman, and C. A. Bona. 1997. Antigen presentation by dendritic cells after immunization with DNA encoding a major histocompatibility complex class II-restricted viral epitope. *J. Exp. Med.* **186**:1481–1486.
- Darquet, A. M., R. Rangara, P. Kreiss, B. Schwartz, S. Naimi, P. Delaere, J. Crouzet, and D. Scherman. 1999. Minicircle: an improved DNA molecule for in vitro and in vivo gene transfer. *Gene Ther.* **6**:209–218.
- Deng, G. M., I. M. Nilsson, M. Verdrengh, L. V. Collins, and A. Tarkowski. 1999. Intra-articularly localized bacterial DNA containing CpG motifs induces arthritis. *Nat. Med.* **5**:702–705.
- Fitzgerald, K. A., D. C. Rowe, B. J. Barnes, D. R. Caffrey, A. Visintin, E. Latz, B. Monks, P. M. Pitha, and D. T. Golenbock. 2003. LPS-TLR4 signaling to IRF-3/7 and NF- κ B involves the Toll adapters TRAM and TRIF. *J. Exp. Med.* **198**:1043–1055. (First published 29 September 2003; doi:10.1084/jem.20031023.)
- Honda, K., H. Yanai, H. Negishi, M. Asagiri, M. Sato, T. Mizutani, N. Shimada, Y. Ohba, A. Takaoka, N. Yoshida, and T. Taniguchi. 2005. IRF-7 is the master regulator of type-I interferon-dependent immune responses. *Nature* **434**:772–777.
- Kaisho, T., and S. Akira. 2002. Toll-like receptors as adjuvant receptors. *Biochim. Biophys. Acta* **1589**:1–13.
- Kawai, T., K. Takahashi, S. Sato, C. Coban, H. Kumar, H. Kato, K. J. Ishii, O. Takeuchi, and S. Akira. 2005. IPS-1, an adaptor triggering RIG-I- and Mda5-mediated type I interferon induction. *Nat. Immunol.* **28**:28.
- Klinman, D. M., D. Verthelyi, F. Takeshita, and K. J. Ishii. 1999. Immune recognition of foreign DNA: a cure for bioterrorism? *Immunity* **11**:123–129.
- Levine, M. M., and M. B. Szein. 2004. Vaccine development strategies for improving immunization: the role of modern immunology. *Nat. Immunol.* **5**:460–464.
- Lodes, M. J., Y. Cong, C. O. Elson, R. Mohamath, C. J. Landers, S. R. Targan, M. Fort, and R. M. Hershberg. 2004. Bacterial flagellin is a dominant antigen in Crohn disease. *J. Clin. Investig.* **113**:1296–1306.
- McMahon, J. M., and D. J. Wells. 2004. Electroporation for gene transfer to skeletal muscles: current status. *BioDrugs* **18**:155–165.
- Nguyen, M. D., T. D'Aigle, G. Gowing, J. P. Julien, and S. Rivest. 2004. Exacerbation of motor neuron disease by chronic stimulation of innate immunity in a mouse model of amyotrophic lateral sclerosis. *J. Neurosci.* **24**:1340–1349.
- O'Hagan, D. T., and N. M. Valiante. 2003. Recent advances in the discovery and delivery of vaccine adjuvants. *Nat. Rev. Drug Discov.* **2**:727–735.
- Palliser, D., H. Ploegh, and M. Boes. 2004. Myeloid differentiation factor 88 is required for cross-priming in vivo. *J. Immunol.* **172**:3415–3421.
- Pashine, A., N. M. Valiante, and J. B. Ulmer. 2005. Targeting the innate immune response with improved vaccine adjuvants. *Nat. Med.* **11**:S63–S68.
- Porgador, A., K. R. Irvine, A. Iwasaki, B. H. Barber, N. P. Restifo, and R. N. Germain. 1998. Predominant role for directly transfected dendritic cells in antigen presentation to CD8⁺ T cells after gene gun immunization. *J. Exp. Med.* **188**:1075–1082.
- Sasaki, S., R. R. Amara, A. E. Oran, J. M. Smith, and H. L. Robinson. 2001. Apoptosis-mediated enhancement of DNA-raised immune responses by mutant caspases. *Nat. Biotechnol.* **19**:543–547.
- Sasaki, S., K. Q. Xin, K. Okudela, K. Okuda, and N. Ishii. 2002. Immunomodulation by apoptosis-inducing caspases for an influenza DNA vaccine delivered by gene gun. *Gene Ther.* **9**:828–831.
- Schnare, M., G. M. Barton, A. C. Holt, K. Takeda, S. Akira, and R. Medzhitov. 2001. Toll-like receptors control activation of adaptive immune responses. *Nat. Immunol.* **2**:947–950.
- Schulz, O., S. S. Diebold, M. Chen, T. I. Naslund, M. A. Nolte, L. Alexopoulos, Y. T. Azuma, R. A. Flavell, P. Liljestrom, and C. Reis e Sousa. 2005. Toll-like receptor 3 promotes cross-priming to virus-infected cells. *Nature* **433**:887–892. (First published 13 February 2005; doi:10.1038/nature03326.)
- Sumida, S. M., P. F. McKay, D. M. Truitt, M. G. Kishko, J. C. Arthur, M. S. Seaman, S. S. Jackson, D. A. Gorgone, M. A. Lifton, N. L. Letvin, and D. H. Barouch. 2004. Recruitment and expansion of dendritic cells in vivo potentiate the immunogenicity of plasmid DNA vaccines. *J. Clin. Investig.* **114**:1334–1342.
- Takeda, K., and S. Akira. 2005. Toll-like receptors in innate immunity. *Int. Immunol.* **17**:1–14.
- Takeda, K., T. Kaisho, and S. Akira. 2003. Toll-like receptors. *Annu. Rev. Immunol.* **21**:335–376.
- Takeshita, F., I. Gursel, K. J. Ishii, K. Suzuki, M. Gursel, and D. M. Klinman. 2004. Signal transduction pathways mediated by the interaction of CpG DNA with Toll-like receptor 9. *Semin. Immunol.* **16**:17–22.
- Takeshita, F., K. J. Ishii, K. Kobiyama, Y. Kojima, C. Coban, S. Sasaki, N. Ishii, D. M. Klinman, K. Okuda, S. Akira, and K. Suzuki. 2005. TRAF4 acts as a silencer in TLR-mediated signaling through the association with TRAF6 and TRIF. *Eur. J. Immunol.* **35**:2477–2485.
- Takeshita, F., K. J. Ishii, A. Ueda, Y. Ishigatsubo, and D. M. Klinman. 2000. Positive and negative regulatory elements contribute to CpG oligonucleotide-mediated regulation of human IL-6 gene expression. *Eur. J. Immunol.* **30**:108–116.
- Takeshita, F., K. Suzuki, S. Sasaki, N. Ishii, D. M. Klinman, and K. J. Ishii. 2004. Transcriptional regulation of the human TLR9 gene. *J. Immunol.* **173**:2552–2561.
- Theofilopoulos, A. N., R. Baccala, B. Beutler, and D. H. Kono. 2005. Type I interferons α/β in immunity and autoimmunity. *Annu. Rev. Immunol.* **23**:307–336.
- Tsuji, T., K. Hamajima, J. Fukushima, K. Q. Xin, N. Ishii, I. Aoki, Y. Ishigatsubo, K. Tani, S. Kawamoto, Y. Nitta, J. Miyazaki, W. C. Koff, T. Okubo, and K. Okuda. 1997. Enhancement of cell-mediated immunity against HIV-1 induced by coinoculation of plasmid-encoded HIV-1 antigen with plasmid expressing IL-12. *J. Immunol.* **158**:4008–4013.
- Tsuji, T., K. Hamajima, N. Ishii, I. Aoki, J. Fukushima, K. Q. Xin, S. Kawamoto, S. Sasaki, K. Matsunaga, Y. Ishigatsubo, K. Tani, T. Okubo, and K. Okuda. 1997. Immunomodulatory effects of a plasmid expressing B7-2 on human immunodeficiency virus-1-specific cell-mediated immunity induced by a plasmid encoding the viral antigen. *Eur. J. Immunol.* **27**:782–787.
- Uematsu, S., S. Sato, M. Yamamoto, T. Hirotani, H. Kato, F. Takeshita, M. Matsuda, C. Coban, K. J. Ishii, T. Kawai, O. Takeuchi, and S. Akira. 2005. Interleukin-1 receptor-associated kinase-1 plays an essential role for Toll-like receptor (TLR)-7- and TLR9-mediated interferon- α induction. *J. Exp. Med.* **201**:915–923.

EP protocol of gene delivery into mouse's leg at Yokohama City University

Target	Impedance (Ω)	Voltage (V)	Pulse length (msec)	Pulse interval (msec)	No. of pulses	Measured Current (A)
Right leg	240	30	50	100	3	0.18
					3*	0.21
Left leg	222	30	50	100	3	0.18
					3*	0.20
Right leg	218	30	50	100	3	0.19
					3*	0.21
Left leg	277	30	50	100	3	0.15
					3*	0.16
Right leg	294	30	50	100	3	0.14
					3*	0.17
Left leg	277	30	50	100	3	0.12
					3*	0.12
Right leg	264	30	50	100	3	0.15
					3*	0.17
Left leg	298	30	50	100	3	0.12
					3*	0.13

*Reverse polarity